Dissertation

Processing of APP in cerebrovascular endothelial cells - regulation by LXR agonists and altered cholesterol homeostasis

submitted by

Mag.rer.nat.

Cornelia Katrin Schweinzer

for the Academic Degree of

Doctor of Philosophy

(Ph.D.)

at the

Medical University of Graz

Institute of Pathophysiology and Immunology

under Supervision of

Ass. Prof. Dr. Ute Panzenboeck

2011

Acknowledgements

Zahlreiche Persönlichkeiten begleiteten mich während meiner Zeit als PhD Student und einigen möchte ich hiermit besonders danken:

Meiner Betreuerin Prof. Dr. Ute Panzenböck, die mir all die Jahre hilfreich zur Seite stand und mir die Möglichkeit gab, „meine wissenschaftliche Seite zu entfalten".
Prof. Dr. Wolfgang Sattler, der stets Zeit und Rat für mich und meine Anliegen bereitstellte.
Meinen Kollegen Alex, Anil, Carmen, Karo und Moni für die wissenschaftliche, soziale, mentale und kulinarische Unterstützung.
Der DSA Runde Babsi, David, Manu, Norbert Sabine und Sandra, mit denen ich zahlreiche Abenteuer bestreiten durfte und mich somit für einige Stunden der Realität lossagte.
Der größte Dank jedoch gilt meiner Familie, meinen Großeltern und Manuel, die mich all die Jahre bedingungslos unterstützt, aufgebaut, motiviert aber auch angespornt haben. Von ganzem Herzen möchte ich meiner Mutter Anita und meinem Vater Johann danken, für die ich immer das „Sonntagskind" bleiben werde und die mir gezeigt haben, dass man alles im Leben schaffen kann, wenn man es nur wirklich will und daran glaubt. Meiner Schwester Nicole danke ich dafür, dass sie mir immer wieder das Gefühl gegeben hat eine „spezielle" kleine Schwester zu sein und für die allererste Starthilfe, mein erstes Semestergeld. Die gemeinsamen, leider oft zu seltenen Stunden im Kreise der Familie Musal, Paps, Nici, Dominik, Laura, Seppi, Oma und Opa, gaben mir stets das Gefühl von Geborgenheit, Kraft und Zuversicht – DANKE!
Besonders danken möchte ich Manuel, der mich all die Jahre begleitet hat, mir die schönen Stunden versüßt hat und die schlimmen schneller verstreichen ließ. Er war mir Stütze und Kraft, sowie Vorbild an Herzlichkeit und Wärme, aber auch in wissenschaftlicher Hinsicht und ich möchte keine Sekunde missen – DANKE!

Carpe Diem

Declaration

I hereby declare that this thesis is my own original work and that I have fully acknowledged by name all of those individuals and organisations that have contributed to the research for this thesis. Due acknowledgement has been made in the text to all other materials used. Throughout this thesis and in all related publications I followed the guidelines of “Good Scientific Practice”.

31.08.2011, Cornelia Schweinzer

Table of Contents

Abbreviations used

A

Aβ, amyloid beta; ABCA1, ABCG1, and ABCG4, ATP-binding cassette transporter A1, G1, and G4; ACAT-1/2, acyl-coenzyme A: cholesterol acyltransferase 1/2; AD, Alzheimer's disease; ADAM, a disintegrin- and metalloproteinase domain; APH1a, anterior pharynx defective 1 homolog A; apoA-I, A-IV, D, E H, J, apolipoprotein A-I, A-IV, D, E, H, J; APP, Amyloid Precursor Protein;

B

BBB, blood-brain barrier; BACE1, Beta-site APP-cleaving enzyme 1; BEC, brain endothelial cells, BCEC, brain capillary endothelial cells;

C

CAA, cerebral amyloid angiopathy; CNS, central nervous system; COX2, cytochrome c oxidase subunit II; CSF, cerebrospinal fluid; CTF, C-terminal fragment; CYP27A1, cytochrome P450, family 27, subfamily A, polypeptide 1; CYP46A1, cytochrome P450, family 46, subfamily A, polypeptide 1;

D

E

ER, endoplasmatic reticulum

F

G

H

HDL, high density lipoprotein; HMGCR, HMG-CoA reductase, hydroxymethylglytaryl-CoA reductase; HPRT1, hypoxanthine phosphoribosyltransferase 1;

I

ISF, interstitial fluid;

J

K

KPI, Kunitz Protease Inhibitor;

L

LRP1, low-density lipoprotein receptor-related protein 1; LXRs, liver-X receptors;

M

N

NCSTN, nicastrin; ND, neurodegenerative diseases; NFT, neurofibrillary tangles;

O

P

(p)BCEC, (porcine) brain capillary endothelial cells; PS1&2, presenilin 1&2; PSENEN, presenilin enhancer 2 homolog;

Q

R

RAGE, receptor of advanced glycation end products; RPII, RNA Polymerase II;

S

SR-AI, macrophage scavenger receptor 1; Scavenger receptor class B, type 1, SR-BI; Scavenger receptor expressed on endothelial cells, SREC-I; SREBP-2, sterol regulatory element binding protein 2;

T

TJ, tight junctions; TNFα, tumor necrosis factor alpha; TO, TO-901317,

U

V

W

w/v, weight per volume

X

Y

Z

24OH-C, 24(S)-hydroxycholesterol; 27OH-C, 27-hydroxycholesterol;

Summary

Impaired clearance of cerebral amyloid beta peptide (Aβ) across the blood-brain barrier (BBB) may facilitate the onset and progression of Alzheimer's disease (AD). Additionally, experimental evidence suggests a central role for cellular cholesterol in amyloid protein precursor (APP) processing. The present study aimed to investigate whether brain capillary endothelial cells (BCEC; the anatomical basis of the BBB) are capable of endogenous APP synthesis and whether and to what extent APP synthesis and processing is under control of cellular cholesterol homeostasis. Intracellular cholesterol metabolism was pharmacologically manipulated by using natural and synthetic liver-X receptor (LXR) agonists. Using an *in vitro* model of the BBB consisting of primary porcine BCEC (pBCEC), we demonstrate that endogenous full-length APP synthesis by pBCEC is significantly increased while the amount of cell-associated, amyloidogenic Aβ oligomers is decreased in response to 24*(S)*-hydroxycholesterol (24OH-C) or 27OH-C, TO901317, cholesterol, or simvastatin treatment. Oxysterols as well as simvastatin enhanced the secretion of non-amyloidogenic sAPPα up to 2.5-fold. In parallel, LXR agonists reduced cholesterol biosynthesis by 30-80% while stimulating esterification (up to 2.5-fold) and efflux (up to 2.5-fold) of cellular cholesterol by modifying HMG-CoA reductase (HMGCR), sterol regulatory element-binding protein (SREBP-2), acyl-coenzyme A:cholesterol acyltransferase (ACAT-2), and ATP binding cassette transporter A1 (ABCA1) expression levels. In a polarized *in vitro* model mimicking the BBB, pBCEC secreted sAPPα preferentially to the basolateral compartment. In summary, endothelial cells of the BBB actively synthesize APP, Aβ oligomers, and secrete APPα in a polarized manner. APP processing by pBCEC is regulated by LXR agonists, which have been proven beneficial in experimental AD models.

Characterization of the (apo)lipoprotein profile in pBCEC supernatants revealed that these cells secrete apoA-I and/or apoJ, major protein components of HDL-like particles formed at the BBB. Interestingly, both apolipoproteins were found in the same lipoprotein density fractions as sAPPα, suggesting that apoA-I and apoJ may interact with sAPPα, and the addition of apoA-I to pBCEC culture medium enhanced sAPPα

production. Altogether our findings highlight the importance of gaining knowledge of the interplay between cholesterol, lipoprotein and APP/Aβ metabolism at the blood-brain barrier.

The major part of the work presented in this thesis has been published in the manuscript “Processing of Endogenous AβPP in Blood-Brain Barrier Endothelial Cells is Modulated by Liver-X Receptor Agonists and Altered Cellular Cholesterol Homeostasis” by Schweinzer et al., Journal of Alzheimer’s disease 2011 Aug 2. [Epub ahead of print]

Zusammenfassung

Ein verringerter Efflux von zerebralen Amyloid Beta Peptiden (Aβ) über die Blut-Hirn-Schranke (BHS) könnte ein Auslöser oder stimulierender Faktor für die Entstehung von Morbus Alzheimer sein. Zahlreiche Experimente belegen die zentrale Rolle von zellulärem Cholesterin bei der Spaltung des Amyloid Precursor Proteins (APP).

Diese Arbeit beschäftigte sich mit der Frage ob Gehirnendothelzellen (die anatomische Basis der BHS) selbst APP produzieren und ob und in welchem Ausmaß die APP Synthese und Prozessierung vom zellulären Cholesterin-Stoffwechsel beeinflusst wird. Natürliche und synthetische Leber-X Rezeptor (LXR) Agonisten wurden verwendet, um den intrazellulären Cholesterinstoffwechsel pharmakologisch zu manipulieren. Wir konnten zeigen, dass sich die Synthese von endogenem APP in einem *in vitro* Modell der BHS, bestehend aus primären Schweinehirnendothelzellen (pBCEC), nach Stimulation mit 24*(S)*-Hydroxycholesterin (24OH-C) oder 27OH-C, TO901317, Cholesterin, oder Simvastatin, signifikant erhöhte. Parallel dazu verringerte sich die Menge an zell-assoziierten Aβ Oligomeren. Weiters erhöhten beide Oxysterole (24OH-C und 27OH-C) und Simvastatin die Sekretion von nicht-amyloidogenem sAPPα bis zu 2,5-fach. Alle LXR Agonisten inhibierten die Cholesterinbiosynthese zu 30-80% und stimulierten die Cholesterinester-Bildung und den Cholesterin-Efflux bis zu 2,5-fach, indem sie die Level von HMG-CoA reductase, sterol regulatory element-binding protein, acyl-coenzyme A:cholesterol acyltransferase, and ATP binding cassette transporter A1 regulierten. In einem polarisierten *in vitro* Modell, das die BHS simuliert, sekretierten pBCEC sAPPα verstärkt in das basolaterale Kompartiment. Zusammenfassend synthetisieren Endothelzellen der BHS aktiv APP, Aβ Oligomere und sekretieren sAPPα auf eine polarisierte Art und Weise. Die Prozessierung von APP in pBCEC wird durch LXR Agonisten reguliert, die in experimentellen Alzheimer Modellen eine begünstigende Wirkung gezeigt haben.

Die Charakterisierung von (Apo)Lipoproteinen in pBCEC Zellüberständen zeigte, dass dieser Zelltyp apoA-I und/oder apoJ sekretiert, Hauptbestandteile von HDL-ähnlichen Partikeln, die an der BHS entstehen können. Interessanterweise fanden sich beide Apolipoproteine in derselben Lipoprotein-Dichtefraktion wie sAPPα. Somit könnten

apoA-I und apoJ mit sAPPα interagieren. Die Zugabe von exogenem apoA-I stimulierte zudem die sAPPα Produktion in pBCEC.

Diese Studie gewährt erste Einblicke in das Zusammenspiel von Cholesterin, Lipoprotein und APP/Aβ Stoffwechsel an der Blut-Hirn Schranke.

1. Introduction

1.1. Alzheimer's Disease

Currently, estimated 35.6 millions of people suffer from dementia worldwide, increasing to 65.7 million by 2030 (Alzheimer's Disease International). Alzheimer's disease (AD) is the most common cause of dementia (50-70%) with rising occurrence [1] and a higher incidence in women than in men [2]. Until so far, most therapies are merely able to slow the progress of the disease – a common therapy does not exist.

Beside the most abundant sporadic late-onset form of AD that occurs in patients after the age of 65, a minor fraction (<10% of all cases), suffers from the familial early-onset AD. It affects patients after the age of 40 and is a consequence of inherited autosomal dominant gene mutation, i.e. in the genes for amyloid precursor protein (APP) and presenilin (PS1 and PS2) [3-5]. Carriers of the apolipoprotein E4 allele (apoE4) face a greater risk of developing sporadic late-onset AD [6-8] as carriers of the E3 allele or the E2 allele (represents a protecting factor, [9]).

AD patients display various symptoms: i) cognitive decline: memory loss (amnesia), disorientation, loss of language skills (aphasia), loss of motor activity (apraxia) and the inability to recognize (agnosia); ii) psychiatric symptoms: personality changes, depression, hallucinations, delusions and misidentification; iii) impaired handling of daily routine: money-handling, telephone-use, driving ,dressing and feeding [1, 10]. The diagnosis of AD in living patients is a challenging task [11] and a histological confirmation via post-mortem detection of neuropathological hallmarks in AD brains, is crucial.

Already in 1907, Alois Alzheimer (Figure 1A) recovered these neuropathological alterations in the brain of Auguste Deter (Figure 1B), including extracellular deposits of a 'peculiar substance' in the brain parenchyma as well as in the cerebrovasculature, and intraneuronal neurofibrillary tangles (NFT, Figure 1C) [12]. 80 years later the extracellular accumulating substance was identified as amyloid β peptide (Aβ) and its

deposits named Aβ plaques [13, 14]. Only a few years later the secret component of NFT was identified as hyperphosphorylated tau protein [15-18]. As a consequence of Aβ plaques and NFT, dystrophic neuritis and cerebral amyloid angiopathy (CAA) manifest in AD brains [19].

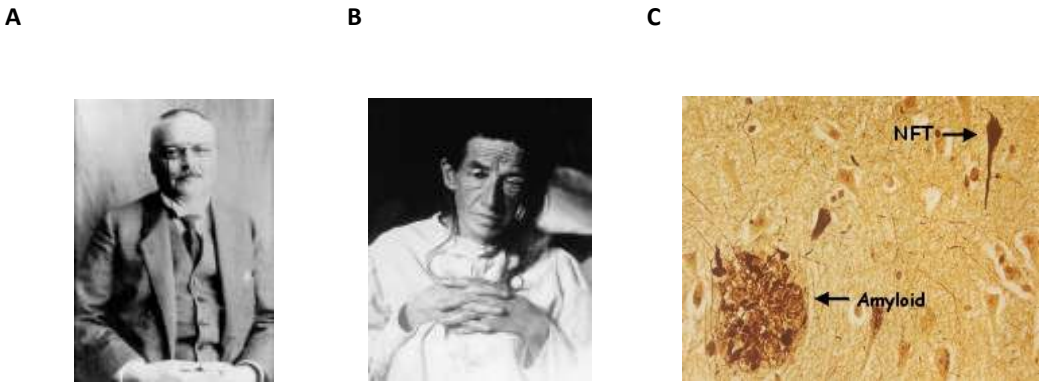

Figure 1: History of AD. (A) Alois Alzheimer. **(B)** Alzheimer's first patient, Auguste D. (modified from Burns et al. [1]) **(C)** Characteristic AD hallmarks in diseased brains: neurofibrillary tangles (NFT) and amyloid beta (Aβ) plaques (modified from medkuleuven.be)

1.2. The blood-brain barrier and transfer of Aβ peptide

In 1904, Paul Ehrlich discovered the blood-brain barrier (BBB). He injected dyes into the circulation and realised that most other organs, but not the brain was stained [20]. Further studies performed by one of his students revealed that the injection of the dye directly into the central nervous system (CNS) stained all cerebral cell types, but not peripheral organs [21]. Their findings suggested that the BBB separates CNS and periphery and prevents exchange between cerebral and peripheral molecules (unless lipid-soluble ones). Nowadays it is known that the BBB acts a physical and metabolic barrier which allows selective exchange between substances that leave or enter the brain [22].

The BBB consists of highly specialized brain capillary endothelial cells (BCEC), connected via typical tight junctions (TJ) which are responsible for the selective passage of molecules across the BBB [23] and peg and socket junctions to pericytes [24, 25]. The pericytes are surrounded by a vascular basement membrane which is in contact with the astrocytic end-feet processes of the glia limitans (Figure 2) [26]. Neurons, microglia and the BBB together form the neurovascular unit [27].

In contrast to peripheral endothelial cells, BCEC lack fenestrations [28], possess a higher number of mitochondria [29] and show less pinocytotic activity [30]. For instance, the BBB constrains hydrophilic macromolecules to pass through BCEC, instead of entering the CNS via passive diffusion through the paracellular space [31].

Aβ peptides are polar molecules and therefore unable to pass BCEC [32]. Thus, specific transporter molecules expressed at the BBB allow Aβ peptides to leave or enter the brain. For instance, Aβ clearance from brain to blood across the BBB is facilitated by low-density lipoprotein receptor-related protein 1 (LRP1) [33]. LRP1-mediated Aβ transport across the BBB starts abluminally (the brain-facing side of BCEC) and directly eliminates Aβ from brain interstitial fluid (ISF) into the peripheral blood [34]. Reduced expression of LRP1 in BCEC correlates with enhanced cerebral Aβ load in AD brains [33]. Aβ uptake across the BBB into the CNS is facilitated by the receptor of advanced glycation end products (RAGE) and can lead to pathophysiological Aβ concentrations in

the brain. Deletion of the RAGE gene in animal models protects the cerebral Aβ pool via inhibiting the uptake of peripheral Aβ [35].

Inflammatory mediators present in the blood stream, such as tumor necrosis factor-alpha (TNFα), are increased in neurodegenerative diseases (ND) and are known to destabilize TJ and therefore to disrupt BBB integrity [36]. Dysfunction of the BBB is believed to play an important role in AD development [22, 37].

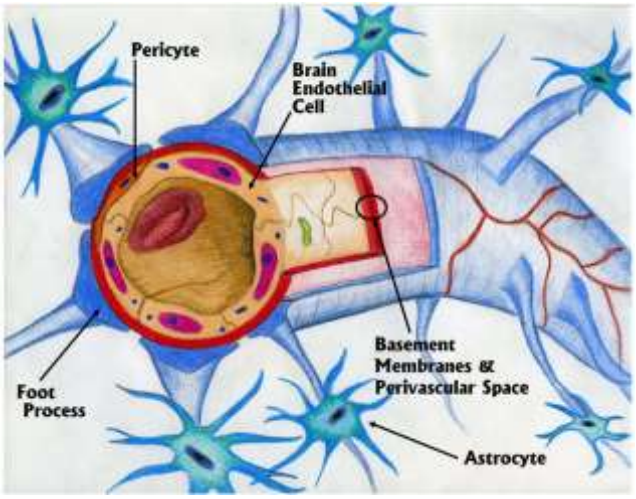

Figure 2. Structure of the blood-brain barrier. (modified from Carvey et al. [22])

1.3. Cellular APP processing and Aβ peptide formation

The precursor of Aβ, amyloid precursor protein (APP) is a glycosylated, single-pass type I membrane protein, containing a large extracellular domain and a short cytoplasmatic region [19, 38]. Although APP belongs to a large protein family, the Aβ domain is an unrivaled feature of APP. Innumerable studies examined the roles of APP with some promising results: involvement of APP in neurite outgrowth and synaptogenesis, in neuronal protein trafficking along the axon, in transmembrane signal transduction, in cell adhesion, and in calcium- and lipid metabolism has been reported [39, 40]. However, the physiological function of APP remains further unknown.

The genetic information for human APP resides within chromosome 21 and alternative splicing leads to formation of the isoforms APP695, 751 and 770 [3]. In contrast to APP751 and 770 that are expressed in most tissues and contain the Kunitz Protease Inhibitor (KPI) ectodomain, APP695 is preponderantly expressed in neurons and does not possess a KPI domain [41, 42]. The presence of elevated protein and mRNA levels of KPI-containing APP isoforms in AD brains correlates with an increase in Aβ plaques [43], supporting the hypothesis that disturbed splicing of APP RNA participates in AD pathogenesis [44].

APP can be processed via enzymes called secretases by two alternative pathways - the most prevalent, non-amyloidogenic pathway and the amyloidogenic pathway (Figure 3 and Figure 4) [10, 45, 46]. The non-amyloidogenic pathway includes cleavage of α-secretase within the Aβ domain of APP and the release of a soluble, secreted form of APP (sAPPα) [47]. After the action of α-secretase, a 83 amino acid (aa) large C-terminal fragment (CTF83) remains in the membrane which is further processed to fragment p3 (via γ-secretase) [48]. Since α-secretase cleaves within the Aβ domain, Aβ peptide formation is impossible. The amyloidogenic pathway is triggered by the action of β-secretase and results in the release of sAPPβ and the remaining 99 aa large C-terminal fragment (CTF99). Subsequent cleavage of CTF99 by γ-secretase leads to Aβ generation [49]. Since γ-secretase can occur between residues 38 and 43 of the CTF99 fragment, the resulting Aβ peptide length can vary from 38 to 43 aa. The most

prevalent form of Aβ species is $A\beta_{40}$. Only a minor fraction (~10% of total Aβ) counts for $A\beta_{42}$ which is more hydrophobic and tends to form fibrils quicker than $A\beta_{40}$ [49]. It is also $A\beta_{42}$ that is more abundant in cerebral plaques [50]. Until so far the origin (neurons, periphery or cerebral vasculature) of Aβ plaques found in the brain parenchyma and cerebrovasculature remains unclear [51].

While several proteins belonging to the ADAM family (a disintegrin- and metalloproteinase-family enzyme) have been shown to possess α-secretase activity (ADAM 9, 10 and 17) [52], only one protein seems to display β-secretase activity: β-site APP-cleaving enzyme 1 (BACE1). BACE1 is a type I integral membrane protein and a member of the pepsin family of aspartyl proteases [53-55]. γ-secretase is an enzyme complex composed of PS1 or PS2, nicastrin, anterior-pharynx defective and presenilin enhancer 2 [56-60]. Although the molecular pathways of APP processing are largely explored, the regulation of these remains unclear.

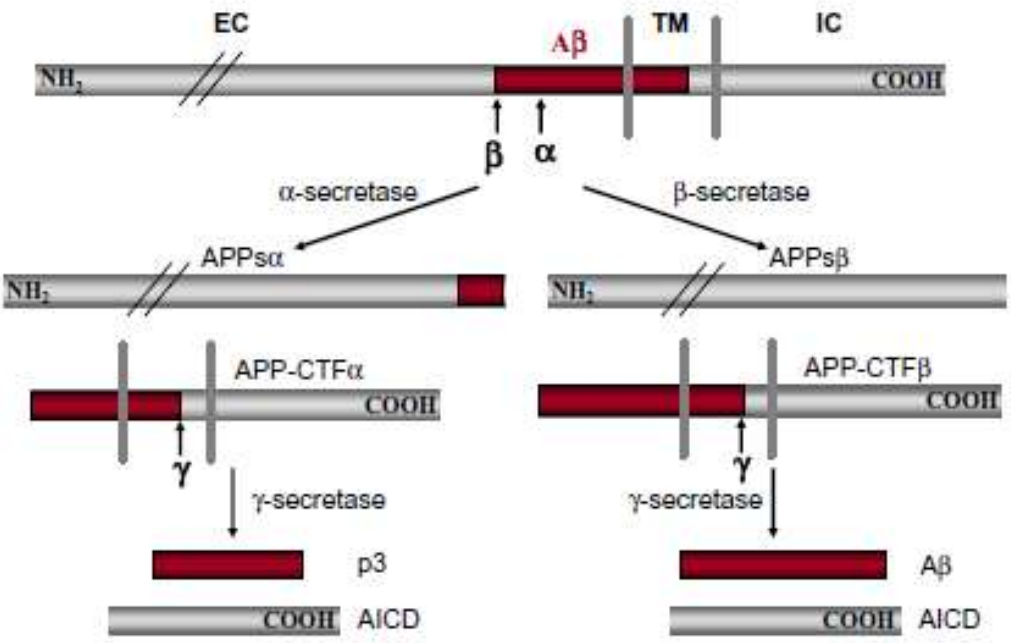

Figure 3: Overview of amyloid precursor protein (APP) processing (from Zheng et al. [40]). APP contains cleavage sites for α-, β- and γ-secretases. Non-amyloidogenic processing includes α-secretase action and precludes Aβ formation. Amyloidogenic processing via β- and γ-secretases leads to Aβ generation.

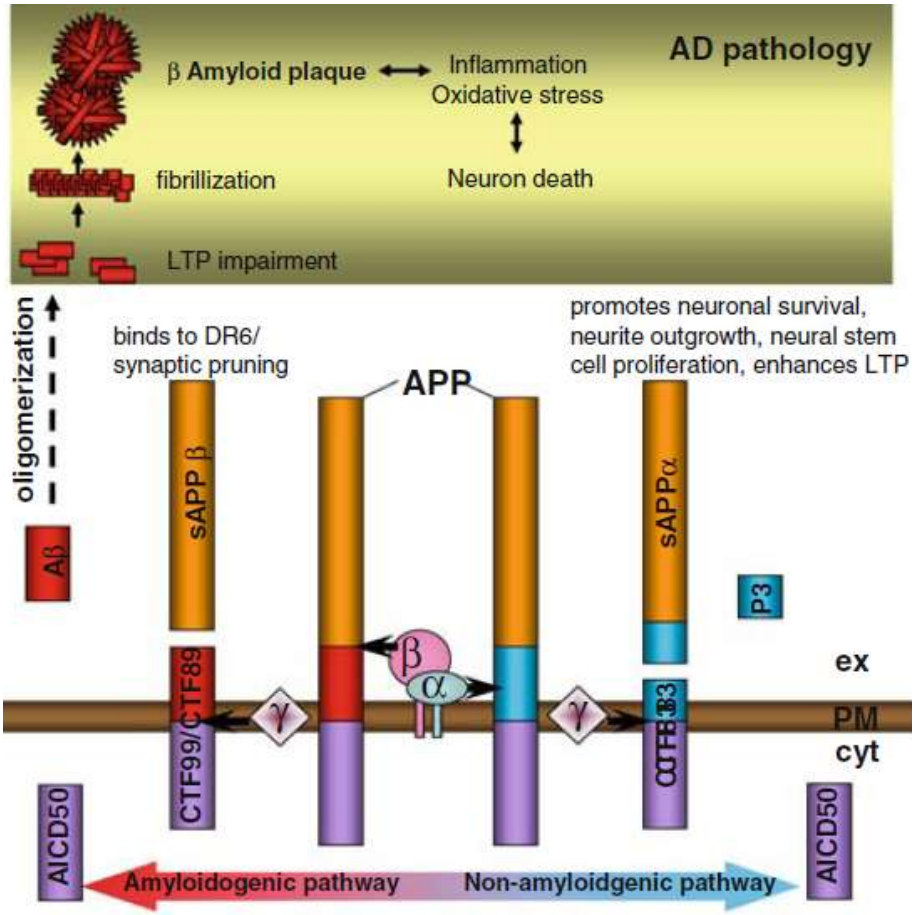

Figure 4: APP processing and cleavage products (modified from Chow et al. [45]). The non-amyloidogenic pathway (right) involves α- and γ-secretase cleavage and results in secretion of sAPPα, CTF83 and p3. The amyloidogenic pathway (left) involves β- and γ-secretase cleavage resulting in secretion of sAPPβ, CTF99 and Aβ. Aβ fragments oligomerize and fibrillize leading to AD pathology (left and upper panel). Ex, extracellular; PM, plasma membrane; cyt, cytosol; DR6, death receptor 6.

1.4. Cholesterol metabolism and lipoproteins in the central nervous system

The brain is the most cholesterol-rich organ in the body. Up to 25% of total body's unesterified cholesterol is located in the CNS within two different pools: plasma membranes of glial and neuronal cells [61] and myelin sheets [62, 63]. Various studies reported that the BBB hinders the exchange of cerebral and peripheral lipoproteins [64-67]. Thus, cholesterol in the CNS is synthesized *de novo* by astrocytes, oligodendrocytes and to a lesser extent by neurons [68, 69]. While cholesterol synthesis in the evolving CNS is high, it drastically decreases in adult brains [65]. This is due to the efficient recycling of cerebral cholesterol and its resulting long half-life (5 years in humans) [70].

To abide cholesterol homeostasis, excess cholesterol has to be excreted from the brain. Since cholesterol is incapable of traversing the BBB, it must be further processed via the enzyme cytochrome P450, family 46, subfamily A, polypeptide 1 (CYP46A1, [71]) to 24(S)-hydroxycholesterol (24OH-C) which is more polar and secreted readily across the BBB into the circulation and eliminated by the liver [65]. This brain-specific oxysterol is a potent ligand of liver X receptors (LXRs), members of the nuclear hormone receptor family [72].

Both LXR isoforms (α and β) are expressed in the brain [73], form heterodimers with the retinoid X receptor (RXR) and regulate genes containing LXR-response elements (LXREs, Figure 5) [74]. LXRs regulate various cholesterol metabolism genes and therefore are powerful modulators of cholesterol homeostasis. For instance, they activate cholesterol efflux via ATP-binding cassette transporter A1 (ABCA1) and apolipoprotein E (apoE) in astrocytes [75], via ABCA1 and apoA-I in pBCEC [76, 77], respectively, and regulate cholesterol biosynthesis by inhibiting its key-enzyme 3-hydroxy-3-methylglutaryl-CoA reductase (HMGCR) [78].

27-hydroxycholesterol (27OH-C) formed by the enzyme cytochrome P450, family 27, subfamily A, polypeptide 1 (CYP27A1, mainly in the periphery) is another oxysterol

that can pass the BBB [79] and activate LXRs. Net flux of 27-OH-C into the brain may be an important link between intra- and extracerebral cholesterol homeostasis [79]. Beside oxysterols, representing natural agonists of LXRs, synthetic ligands (e.g., TO901317) are widely used to study LXR action [74].

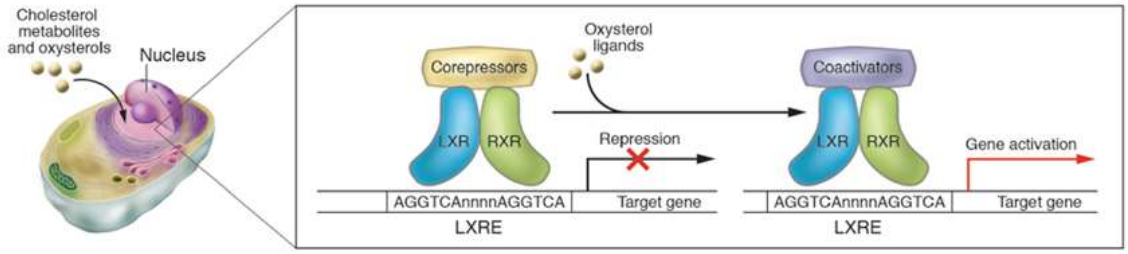

Figure 5: LXRs are ligand-activated nuclear transcription factors. (modified from Zelcer et al. [80])

High density lipoprotein (HDL)-like particles circulating in the cerebrospinal fluid (CSF) are responsible for cerebral lipid transport [81]. Compared to peripheral HDL (mainly containing apoA-I), CNS-derived HDL is mainly composed of apoE, apoA-I, apoA-IV, apoD, apoH and apoJ [82, 83]. CSF lipoproteins can be grouped into four classes (depending on size and apolipoprotein content) and are crucial for the redistribution of cerebral lipids [81]. ApoE-containing HDL is a major ligand to LRP1 and stimulates neurite growth [84, 85].

ApoE is a 35 kDa glycoprotein produced and secreted by astrocytes and microglia and the major apolipoprotein in the CNS [86, 87]. Nascent, apoE-containing lipoprotein particles secreted from glia are discoidal (because they lack cholesteryl esters and triglycerides) [87]. Incorporation of cholesterol (effluxed by neurons and glia) into these nascent particles is facilitated first by ABCA1, followed by ATP-binding cassette transporter G member 1 (ABCG1) [88, 89]. The presence of low density lipoprotein receptors (LDLR) on neuronal and glial cells allows intermediate apoE-containing lipoproteins to re-distribute their contents (Figure 6) [90].

ApoA-I is a 28 kDa apolipoprotein expressed and secreted by pBCEC [76, 91]. Previous results of our group show that LXR activation stimulates ABCA1-mediated cholesterol efflux from pBCEC to apoA-I and results in the enhanced formation of HDL-like particles at the BBB *in vitro* [76].

ApoJ, also known as clusterin is a multifunctional disulfide-linked glycoprotein produced by astrocytes [92] that contains two ~40 kDa subunits (α and β chain) [93]. Despite functioning as a complement inhibitor, apoJ is present in lipoprotein particles and involved in cholesterol/lipid trafficking in the brain [94], it is believed to play a role in cholesterol efflux [95] and is known to be rapidly cleared across the BBB via LRP2 [96].

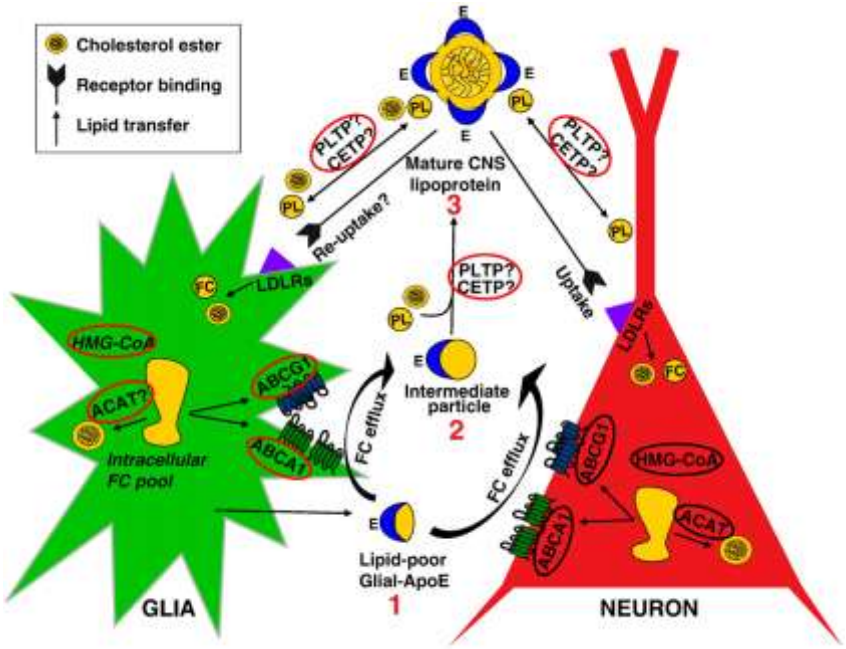

Figure 6: Hypothesis for lipoprotein remodelling in the parenchyma of the brain. 1) Nascent apoE-containing particles are secreted by glial cells. 2) ABCA1 in glia and neurons promotes FC efflux to the nascent particles, followed by additional FC efflux by ABCG1. The result is an intermediate particle(s). 3) Intermediate particle(s) become mature CNS lipoproteins by a poorly understood process that includes acquiring a CE core and additional PL (modified from Yu et al. [87]).

1.5. Role of cholesterol and lipoproteins in AD

There is striking evidence that dysregulated cholesterol and lipoprotein metabolism play a decisive role in the pathogenesis of AD [97-101]. Several studies have reported a link between cholesterol homeostasis, APP processing, Aβ peptide formation, and the development of AD. First, high peripheral cholesterol and LDL levels are a reported risk factor for AD [102-104]. Reduced plasma levels of HDL and its major apolipoprotein apoA-I are common in AD patients [105105]. Individuals with high serum apoA-I levels are supposed to have a significantly lower risk of dementia [106]. In contrast to elevated peripheral cholesterol levels, total cholesterol levels in AD brains are low compared to healthy-matched controls [107]. AD brain regions with unbalanced cholesterol homeostasis show a gradual deterioration and loss of nerve synapses [104]. Statins - potent inhibitors of hydroxymethylglytaryl-CoA (HMG-CoA reductase), the rate-limiting enzyme in cholesterol metabolism - decrease the risk to develop AD along with reduced plasma cholesterol levels (although studies on their effects in AD have produced inconsistent data) [108]. A reduction in Aβ peptide formation upon statin treatment of neuronal cells was reported [109, 110], while hypercholesterolemic animals established increased intraneuronal and extracellular Aβ deposits and a reduced non-amyloidogenic processing of APP in the hippocampus and frontal cortex [98]. Treatment of high-cholesterol fed animals with statins was reported to decrease the cholesterol-induced cerebral Aβ burden [111-113]. Obviously statin effects depend on the disease-state of AD patients: cognitive impairment in individuals with mild to moderate AD was reduced by statin usage, whereas advanced AD patient's symptoms did not improve [114-116]. Furthermore, simvastatin in contrast to atorvastatin delivers promising data on a reduced incidence of dementia [117]. One possible explanation could be that simvastatin is more hydrophobic and thus easier crosses the BBB and/or the fact that it enhances HDL levels more effectively than atorvastatin [46].

Second, intracellular cholesterol levels and its distribution affect APP processing. Thus, a reduction in sAPPα due to high levels of intracellular cholesterol was observed in APP

stably transfected HEK293 cells [118]. There is increasing evidence for amyloidogenic events occurring within membrane lipid rafts, detergent-resistant membrane microdomains rich in cholesterol and sphingolipid, in the trans-Golgi network and in endosomes. In contrast, the non-amyloidogenic processes are believed to occur outside of lipid rafts at sites of low cholesterol concentrations in the plasma membrane [119-121]. Statins are believed to modulate lipid rafts [122] which harbor BACE1 and Y-secretase [121]. A decrease in membrane cholesterol reduces activity of both secretases and leads to decreased Aβ formation *in vitro* [111, 118, 123]. Additional *in vitro* studies provided evidence that statins promote the non-amyloidogenic processing of APP via α–secretase [124-126].

Third, the fact that the inhibition of acyl-coenzyme A: cholesterol acyltransferase (ACAT) activity – the enzyme responsible for the esterification of cellular cholesterol – causes a reduction in Aβ production in various cell lines and in AD mice [127-129] is another strong indication for a relationship between cellular cholesterol turnover and Aβ metabolism.

Finally, cellular cholesterol efflux promoted by the apoA-I/ABCA1 pathway has been reported to relate to Aβ generation. Thus, increased ABCA1 expression suppressed Aβ levels in cultured cells [130]. Conversely, a deletion of ABCA1 in mouse models of AD considerably decreased apoE levels, correlating with increased cerebral Aβ deposits [131-133]. LXRs stimulate the expression of ABCA1 and G1, both genes believed to play important overlapping roles in maintaining cerebral lipid and lipoprotein homeostasis [86, 134]. ABCG1 is highly expressed in the brain and was detected close to amyloid plaques [135]. However, *in vitro* studies which examined a possible influence of ABC transporters on Aβ metabolism delivered conflicting results [136, 137].

Patients with dementing disorders display higher plasma 24OH-C to 27OH-C ratios than healthy subjects [138] and in AD patient's plasma 24OH-C to cholesterol ratios are reduced [79, 139] whereas 24OH-C levels in CSF of AD patients are elevated [140-145]. The fact that 27OH-C has a higher capacity to pass hydrophobic membranes

(such as the BBB) than 24OH-C, corroborate the theory of 27OH-C being the missing link between hypercholesterolemia and AD [146]. This oxysterol is metabolised within the CNS (mainly in neuronal cells) into more polar products that are transported across the BBB into the blood [147]. Neuronal loss would therefore reduce such mechanisms of cholesterol clearance and enhance neurodegeneration in AD [46].

Certain apolipoprotein levels (apoE, D and J) are elevated in AD brains [148-150] and some (apoE, A-I, B and J) are associated with amyloid plaques [151-155]. ApoE and apoJ were reported to bind/transport Aβ *in vivo* and *in vitro* [33, 96, 151, 156, 157]. Based on these results, increasing apoJ levels in the CSF are a suggested therapeutic agent to prevent AD [158]. In addition, apoJ has recently been identified as one of two novel AD susceptibility genes, independently, during two genome-wide association studies [159, 160].

HDL and Aβ metabolism appear to be linked since HDL is able to suppress Aβ production through the activation of reverse cholesterol transport mediated by ABC transporters [161], HDL can directly bind excess Aβ and inhibit its oligomerization [162], and HDL transports Aβ in both CSF and plasma [163].

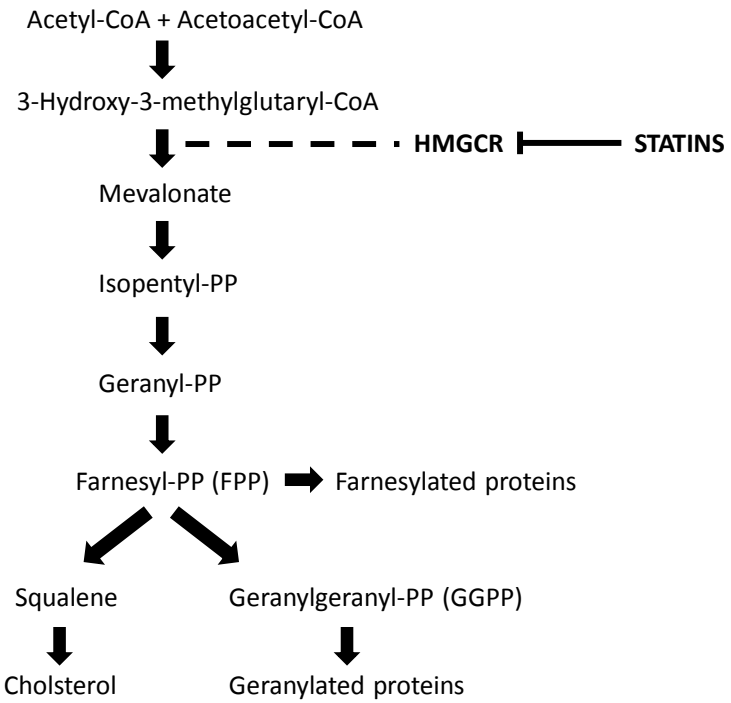

Figure 7: Scheme of cholesterol biosynthesis. Statins block HMGCR in the ER and therefore production of mevalonate and all down-stream products i.e. cholesterol and non-sterol isoprenoids such as FPP. (modified from [124])

2. Aims

Disturbed cholesterol and lipoprotein metabolism are widely accepted to influence AD etiopathology. Brain capillary endothelial cells (BCEC), the key components of the blood-brain barrier (BBB), hinder the exchange between brain and plasma lipoproteins. Therefore, exact mechanisms by which (peripheral) cholesterol and lipoproteins influence AD pathogenesis are still unknown. Further insights are vital to close the existing gaps of knowledge and to develop novel and effective strategies of therapy. To further clarify the mechanisms that link AD pathogenesis and lipoprotein/cholesterol metabolism we addressed the following aims:

2.1. To characterize APP/Aβ- and cholesterol metabolism at the BBB *in vitro*

Experimental evidence suggests a central role for cellular cholesterol in APP processing. During the major part of this study we examined if processing of endogenous APP in cerebrovascular endothelial cells is modulated by LXR agonists (24*(S)*-hydroxycholesterol and 27-hydroxycholesterol and the non-steroidal ligand TO901317) and altered cellular cholesterol homeostasis (cholesterol or simvastatin treatment). Studies were carried out at the BBB *in vitro* by using a well-established model consisting of primary, porcine brain capillary endothelial cells (pBCEC).

2.2. To investigate BBB-derived (apo)lipoproteins and Aβ turnover at the BBB

The fact that BCEC synthesize both apoA-I containing HDL-like particles and Aβ peptide, but the precise mechanisms underlying these processes as well as the functions of BBB lipoproteins are incompletely understood, encouraged us to investigate potential interactions between BBB-derived apo- and lipoproteins and

BCEC Aβ metabolism. Using the established *in vitro* model of the BBB will further enable us to find novel binding partners for Aβ peptide in BCEC.

3. Materials and Methods

3.1. Materials

3.1.1. Chemicals and solutions used for cell culture experiments

Purchased chemicals and solutions are listed in Table 1. Recipes for self-made solutions and buffers are listed below. Transwell multiwell plates were obtained from Sigma Aldrich. FlexiPerms and all other cell culture plastic ware were obtained from Greiner Bio-One. Oak-Ridge tubes, 50 ml PC (Cat. Nr. 3118-0050) were from Fisher Scientific. Evohm ohmmeter was from World Precision Instruments.

Table 1: Chemicals and solutions used for cell culture experiments

Product name	Company
Medium 199 (1x)	Invitrogen
Minimum Essential Medium (MEM, 10 x)	Invitrogen
MCDB 131 Medium (1x)	Invitrogen
Collagenase/Dispase	Roche
Dispase	Invitrogen
Penicillin/Streptomycin/Gentamycin	PAA Laboratories
Trypsin-EDTA	PAA Laboratories
Ox Serum	PAA Laboratories
L-Glutamine	PAA Laboratories
Accutase™	Sigma Aldrich
Percoll® pH 8.5-9.5	Sigma Aldrich
Collagen G from bovine calf skin	M&B Stricker
Dextran	VWR
24(*S*) -hydroxycholesterol	Medical Isotopes
27-hydroxycholesterol	Avanti Polar Lipids
TO 901317	Cayman Chemicals
Simvastatin	Sigma Aldrich
Cholesterol	Sigma Aldrich
Hydrocortisone	Sigma Aldrich

1x PBS, pH 7.38-7.42, 5 liter

40 g NaCl

1.5 g KCl

0.1 g KH_2PO_4

0.457 g Na_2HPO_4 + 2 H_2O

10 g Glucose or Dextrose

Fill up to 5 liters with d_2H_2O, filter the solution and autoclave it.

Preparation Medium

500 ml Medium M199 (1x)

1% Penicillin/Streptomycin

1% Gentamycine

1 mM L-Glutamine

Plating Medium A

500 ml Medium M199 (1x)

1% Penicillin/Streptomycin

1% Gentamycin

1 mM L-Glutamine

10% Ox Serum

Plating Medium B

500 ml Medium M199 (1x)

1% Penicillin/Streptomycin

1 mM L-Glutamine

10% Ox Serum

Collagenase/Dispase solution

100 mg enzyme

10 ml Plating medium A

Transfer solution trough a sterile-filter (0.2 µm pore size), prepare 350 µl aliquots and store them at -20°C.

Dextran solution

200 g Dextran (Lot D-4568A)

2.4 g $NaHCO_3$

109.1 ml MEM (10x)

Fill up to 1.2 liter, stir solution overnight at 4°C, determine density and adjust with d_2H_2O until the density is 1.0612 (4°C). Mark liquid level, autoclave solution and add sterile d_2H_2O water up to the mark.

Percoll® biphase

1.03 density (50 ml)

40 ml 1x PBS

9 ml Percoll

1 ml MEM (10x)

1.07 density (50 ml)

20 ml 1x PBS

27 ml Percoll

3 ml MEM (10x)

Hydrocortisone solution (50 µg/ml)

Add 1 ml ethanol and 19 ml medium to 1 mg hydrocortisone. Prepare 2 ml aliquots and store them at –20°C. (For 500 ml medium take 2 ml hydrocortisone).

MCDB 131 Medium

500 ml MCDB 131 Medium (1x)

2% FCS

1% Penicillin/Streptomycin

1 mM L-Glutamine

TO 903017 stock

Add 1 ml ethanol (absolute) to 50 mg TO901317, then dilute further (1:10) with ethanol to obtain a 10 mM stock. Prepare aliquots and store them at -20°C.

24(*S*)/27 –hydroxycholesterol stock

Add 621 µl ethanol (absolute) to 5 mg of the oxysterol obtain a 20 mM stock. Prepare aliquots and store them at -20°C.

Cholesterol stock

Add 1 ml ethanol (absolute) to 7.74 mg cholesterol to obtain a 20 mM stock. Store the stock at – 20°C.

Simvastatin stock

Add 100 µl ethanol (absolute) to 1 mg simvastatin. Then add 150 µl of 0.1 N NaOH to the solution and incubate at 50 °C for 2 hours. Adjust pH to 7.0 with HCl, and the final concentration of the stock solution to 4 mg/ml. Store aliquots at – 20°C.

3.1.2. Materials used for RNA isolation, cDNA synthesis and quantitative real-time PCR

All purchased products are listed in Table 2. Primers for quantitative real-time PCR were self-designed (Primer 3 software), obtained from Invitrogen and are listed in Table 3-Table 5. Self-made solutions and buffers are listed below.

Table 2: Materials used for RNA isolation, cDNA synthesis and quantitative real-time PCR

Product name	Company
RNeasy® Plus Kit	Qiagen
iScript™ cDNA Synthesis Kit	Biorad
iQ™ SYBR® Green Supermix	Biorad
ß-mercaptoethanol	Sigma Aldrich
Nuclease-free water	Carl Roth
2-Log DNA ladder	New England Laboratories
Gel Loading Dye, Blue (6x)	New England Laboratories
Biozym LE Agarose	Biozym
Ethidiumbromide (10 mg/ml)	Invitrogen
Wizard® SV Gel and PCR Clean-Up System	Promega
Microseal 'B' Adhesive Seals for PCR Plates	Biorad
NanoDrop® ND-1000 UV-Vis Spectrophotometer	Peqlab
C-1000™ Thermal Cycler	Biorad
iCycler iQ™, Real-Time PCR Detection System	Biorad
0.2 ml PCR Tube Strips	Biorad
OneTouch Filter-Tips, 10 µl	Biozym
HE 33 Mini Submarine Electrophoresis Units	Hoefer® Inc.
Molecular Imager ChemiDoc XRS System	Biorad
Power Pac HC, Power supply	Biorad
ELMA Transsonic 460, ultrasonic unit	Carl Roth

TAE buffer (50x)

2 M Tris

0.05 M EDTA

57.1 ml glacial acid

Adjust the pH to 8.5 and fill it up to 1 liter with d_2H_20, filter the solution and store at 4°C in the dark.

MOPS buffer (10x)

200 mM MOPS

50 mM Na-acetate

5 mM EDTA

Adjust the pH to 7.0, fill it up to 1 liter with d_2H_20, filter the solution and store at 4°C in the dark.

Table 3: Primers used for quantitative real-time PCR of amyloid metabolism genes.

Gene name	Forward primer 5'-3' Reverse primer 5'-3'	Product size in bp
APP	GTGAAGATGGATGCGGAGTT GTGATGACAATCACGGTTGC	152
ADAM10	AGCAACATCTGGGGACAAAC CTTCCCTCTGGTTGATTTGC	219
BACE1	ACAGTGGCACCACCAACCTT GCCAGAAACCATCAGGGAAC	105
PS-1	CATGACTATTCTCCTGGTGG GCAATCATTCCTACCACACC	201
PS-2	CCTCCTCAACTCCGTGCTCA GGTAGTCCATGGCCACGTTG	203
NCSTN	GGTCTCCTTCGCCTTCTGTC GCTCTCCAGCAGAACCATGT	255
PSENEN	ATGAACCTGGAGCGAGTGTC CTCTGTTCTGTGTAGGCTGG	152
APH-1a	GCCTCTGTGGTCTGGTTCAT ATCTTCCGTCCTCACTCAGC	184
HPRT1	AGGACCTCTCGAAGTGTTGG CAGATGGCCACAGGACTAGA	247

Table 4: Primers used for quantitative real-time PCR of amyloid-transporter genes.

Gene name	Forward primer 5'-3' Reverse primer 5'-3'	Product size in bp
RAGE	GGTGCTGGTCCTCAGTCTGT TCCAAGCTTCTGTCCGGCCT	155
LRP-1	ATCACCCCTGCAAAGTCAAC ACACAAACTGGCTTGCTGTG	149
SREC-1	CTGGAGGCAGAAGGATCAAG CAGGCTTGCATCGACAGAG	107
SR-A1	TCCTCCGGGTCTTAAAGGTG CCCTTTCTGGCCTTTTGGT	110

Table 5: Primers used for quantitative real-time PCR of lipid metabolism genes.

Gene name	Forward primer 5'-3' Reverse primer 5'-3'	Product size in bp
ACAT-1	GCCACTAAGCTTGGTTCCAT GCTTGTCCTTCACCTCCTTG	118
ACAT-2	CATAGAAGCCATGTCCAAGC ACATCTTCCAGTGACCAACC	264
SREBP-2	GCTTCTCCCCCTACTCCATC GAGAGGCACAGGAAGGTGAG	151
HMGCR	CTTGTTCACGCGCACAGTCG GACAGCCAGAAGGAGAGCCA	207
APOJ	CCTTCTTCGACATGATCCAC TCTTCGACATGATCCACCAG	
ABCA1	GCCATTCTCCGGGCCAAC GGCTTCACGCCGCTGAT	252

Table 6: Murine primers used for quantitative real-time PCR

Gene name	Forward primer 5'-3' Reverse primer 5'-3'	Product size in bp
APP	TCCGAGAGGTGTGCTCTGAA CCACATCCGCCGTAAAAGAATG	115
ß-actin	TCCCTGGAGAAGAGCTACG GTAGTTTCGTGGATGCCACA	247
RPII	CTGGACCTACCGGCATGTTC GTCATCCCGCTCCCAACAC	133

3.1.3. Materials used for protein isolation-, determination, immunoprecipitation, SDS PAGE and immunoblotting

Table 7 and Table 8 display all purchased products used for protein isolation, -quantification, SDS PAGE, and immunoblotting. Self-made solutions and buffers are listed below.

Table 7: Purchased products for protein isolation, precipitation and determination.

Product name	Company
Protease inhibitor cocktail	Sigma Aldrich
NP-40	Sigma Aldrich
Chemicals (e.g. Tris)	Carl Roth or Sigma Aldrich
Pierce® BCA Protein Assay Kit	Thermo Scientific
Quant-iT™ Protein Assay Kits	Invitrogen
Qubit® Fluorometer	Invitrogen
Sunrise photometer with Magellan software	Tecan
Bovine Serum Albumine, 2 mg/ml	Thermo Scientific
Centrifuge Sigma 3K15 with angle rotor 12154-H	Sigma
Concentrator Plus	Eppendorf
IKA® Model MS 1 minishaker	Carl Roth
Combi-Shaker KL 2	Carl Roth
Centriprep® Centrifugal Filter Devices	Millipore
Thermomixer comfort 1.5 ml	Eppendorf
Microcentrifuge, Qualitron DW-41	Carl Roth
Magnetic stirrer with heating, MR 3001, Heidolph	VWR
WTW Handheld meter pH 330i	WTW
Beckman GS-6R Centrifuge with swinging bucket rotor GH3.8	Beckman Coulter
Ratek RSM7, Rotary Suspension Mixer	VWR
Julabo SW 21 Shaking Water Bath	Julabo
Dynabeads® Protein A	Invitrogen
Dimetyl pimelimidate dihydrochloride (DMP)	Sigma Aldrich
Triethanolamine	Sigma Aldrich
Glycine	Sigma Aldrich
Bradford Reagent	Sigma Aldrich

Table 8: Purchased products for SDS PAGE and immunoblotting.

Product name	Company
Protran BA Nictrocellulose membrane	VWR
Hybond-P PVDF membrane	VWR
Precision Plus Protein™ Western C™ Pack	Biorad
Immun-Star™ WesternC™ Chemiluminescent Kit	Biorad
CL-XPosure Film (12,5 x 17,5 cm)	Thermo Scientific
XT sample buffer (4x)	Biorad
XT sample reducing agent (20x)	Biorad
NuPAGE Antioxidant	Invitrogen
NuPAGE® Novex 4-12% Bis-Tris Midi Gel	Invitrogen
Criterion XT™ Bis-Tris Gel	Biorad
Criterion XT™ Tris Acetate Gel	Biorad
Perfect-Block	VWR
Bovine Serum Albumin, Fraction V	Sigma Aldrich
Blotting-Grade blocker, nonfat dry milk	Biorad
Precision Protein™ StrepTactin-HRP Conjugate	Biorad
NuPAGE® MES SDS Running Buffer (20x)	Invitrogen
Blotting Filter Papers, 2.5 mm thickness, 8.6 cm x 13.5 cm	Invitrogen
Criterion™ Blotter Filter Paper	Biorad
SuperSignal® West Pico Chemiluminescent Substrate	Thermo Scientific
Criterion™ Cell	Biorad
Criterion™ Blotter	Biorad
Tween-20	Sigma Aldrich
Triton-X	Sigma Aldrich
Acrylamid solution	Sigma Aldrich

Protein lysis buffer (pH 7.4)

50 mM Tris

10 mM EDTA

1% v/v NP-40

0.1 v/v protease inhibitor cocktail

Fill up to 5 liter with d_2H_20.

TBS-TT (1x, 5 liter)

100 ml Tris, 1M, pH 7.5

250 ml NaCl, 5 M

10 ml Triton-X

2.5 ml Tween-20

Fill up to 5 liter with d_2H_20.

Blocking solution

Dissolve 1% w/v casein (Perfect Block) in

1x TBS-TT.

Towbin buffer (10x)

30.3 g Tris

144 g Glycine

10 g SDS

Fill up to 1 liter with d_2H_20. Do not adjust the pH it should be 8.3.

SDS running buffer (1x)

100 ml Towbin buffer (10x)

Fill up to 1 liter with d_2H_2O.

Transfer buffer (1x)

100 ml Towbin buffer (10x)

200 ml methanol

Fill up to 1 liter with d_2H_2O.

SDS separating gel (10%), 1.5 mm, 1 gel

5.9 ml d_2H_2O

5 ml acrylamide

3.8 ml separating Gel Buffer, (Tris, pH 8.8)

150 µl SDS, 10% w/v

155 µl APS, 10% w/v
15 µl TEMED

SDS stacking gel (4%), 2 gels

3.6 ml d_2H_2O

800 µl acrylamide

1.5 ml stacking Gel Buffer, (Tris, pH 6.8)

60 µl SDS, 10% w/v

60 µl APS, 10% w/v

6 µl TEMED

Sodium phosphate buffer (10 ml pH 8.0)

Stock A:

0.2 M $NaH_2PO_4*H_2O$ (1.38 g/50ml d_2H_2O)

Stock B:

0.2 M $Na_2HPO_4*7H_2O$ (2.68g/50 ml d_2H_2O)

Mix:
265 µl stock A + 4.74 ml stock B; adjust volume to 10 ml with d_2H_2O

Mild elution buffer for immunoprecipitation

50 mM Glycine, pH 2.8

Cross-linker for immunoprecipitation
20 mM DMP in 0.2M Triethanolamine, pH 8.2 (5.4 mg DMP/ml buffer) **Always prepare the solution fresh!**

3.1.4. Antibodies

Primary and secondary antibodies used for immunoblotting, immunhistochemistry, and immunofluorescence are listed in Table 9.

Table 9: Primary and secondary antibodies used for immunoblotting, immunohistochemistry and immunofluorescence.

Protein name	Company	Working dilution	Used for detecting
Primary antibodies:			
rabbit-anti-b-Actin	Sigma Aldrich	1: 5000	
rabbit-anti-APP	Invitrogen	1:1500	full-length APP
rabbit-anti-Ab	Sigma Aldrich	1:200	APP/Aβ via IHC
A11 rabbit-anti-amyloid oligomer	Millipore	1:10,000	Aβ oligomers
Bam-10 mouse-anti-b-amyloid	Sigma Aldrich	1:1500	sAPPα
rabbit-anti-sAPPb	Covance/Anopoli	1:1000	sAPPβ
rabbit-anti-HMGCR	Abcam	1:1000	
rabbit-anti-SREBP-2	Abcam	1:1000	
rabbit-anti-Apo J	Santa Cruz	1:1000	
rabbit-anti-Apo A-I	Dr. Ernst Malle	1:2000	
rabbit-anti-ABCA1	Abcam	1:1000	
rabbit-anti-von Willebrand Factor	DAKO*	1:10,000	pBCEC via IHC
Secondary antibodies:			
goat-anti-Rabbit-HRP	Abcam	1:6000	
goat-anti-Mouse-HRP	Sigma Aldrich	1:5000	
goat-anti-Rabbit-Cy™3	Dianova#	1:200	

*provided by Dr. Ingrid Lang, Institute of Cell Biology, Histology & Embryology,
#provided by Dr. Eva Bernhart, Institute of Molecular Biology and Biochemistry

3.1.5. Materials used for immunohistochemistry and immunocytochemistry

All products used for immunohistochemistry and immunocytochemistry are listed in Table 10.

Table 10: Materials used for immunohistochemistry

Product name	Company
HM560 Cryo Star, Cryostat	Microm International
Tissue-Tek®, O.C.T.™ Compound	Sakura Finetek
Microscope slides, Super Frost®	Carl Roth, Assistant, Karl Hecht AG
Microtome blades, C53 Type	MPOE GesmbH
UltraVisionLP Detection System	Thermo Scientific
Antibody diluent	DAKO
Normal rabbit immunoglobulin fraction	DAKO
AEC	Thermo Scientific
Mayer's hemalum	Merck
Kaiser's glycerol gelatine	Merck
Vectashield® Mounting Medium with DAPI	Vector Laboratories
Leica DM 4000B fluorescence microscope with DFC300FX digital colour camera	Leica
Motic BA310 light microscope	Motic Deutschland GmbH

3.1.6. Materials used for cholesterol assay and radiometric assays for cholesterol biosynthesis, esterification and cholesterol efflux

[1,^{14}C]-acetic acid sodium salt ([^{14}C]-acetate), [1,2-^{3}H(N)]-cholesterol ([^{3}H]-cholesterol), scintillation vials and Ultima Gold scintillation cocktail were from New England Nuclear was from NEN (Vienna, Austria). Enzymatic kits for determining total cholesterol were from Greiner Bio-One. TLC silica plates were from Merck (Vienna, Austria).

3.1.7. Materials used for Aβ/apo A-I labeling, Aβ/apo A-I transport, binding and uptake assay

Aβ(1-40) was from Sigma Aldrich (Vienna, Austria). Alexa Fluor® 488 5-tetrafluorophenyl esters (TFP) was from Invitrogen (Vienna, Austria). Apo A-I was a gift from Dr. Ernst Malle (Institute of Molecular Biology and Biochemistry, Medical University of Graz). [125-I] was from New England Nuclear. PD-10 size-exclusion columns were from GE Healthcare (Vienna, Austria). All solvents were from Sigma Aldrich (Vienna, Austria) or Lactan (Graz, Austria).

Carbonatebicarbonate (CBC) buffer, pH 9.0
0.5 M Na_2CO_3
0.5 M $NaHCO_3$

3.2. Methods

3.2.1. Isolation and culture of porcine brain capillary endothelial cells (pBCEC)

For isolation of pBCEC [76], porcine brains were obtained from freshly slaughtered pigs (6 months on average) from the local abattoir. After removal of the meninges and secretory areas, the gray and white matter of the brain cortex was minced. Capillaries

were isolated by enzymatic digestion with dispase (70 mg/brain) and gentle stirring in a water bath at 37°C for 1 h. After mixing with dextran solution (10% w/v) and centrifugation (6800 g, 10 min, 4°C), the pellets were resuspended in serum-free 'preparation medium' (M199, containing 1% P/S, 1% gentamycine, and 1mM L-glutamine). The size of capillary fragments was checked by light microscopy and the cell suspension was carefully transferred on top of a Percoll gradient (15 mL of 1.07 g/mL; 20 mL of 1.03 g/mL), and centrifuged at 1300 g for 10 min in a swinging bucket rotor. Endothelial cells were recovered from the interphase of the gradient and washed in serum-free medium to remove Percoll. Cells were plated on collagen-coated (60 µg/ml) 75 cm^2 flasks in 'plating medium' (M199, containing 1% gentamycine, 1% P/S, and 1mM L-glutamine and 10% ox serum) at 37°C in humidified air containing 5% CO_2. After 24 h cells were washed twice with PBS and cultured in fresh 'medium B' (M199 containing 1% P/S, 1mM L-glutamine and 10% ox serum) until confluence. Confluent cells were trypsinised and split onto collagen-coated multiwell plates (60 µg/ml collagen) or Transwell filters (120 µg/ml collagen) and grown until confluence in 'medium B' at 37°C in humidified air containing 5% CO_2.

3.2.2. Isolation of murine brain capillaries (MBEC)

Mice (C57BL/6J) were killed by cervical dislocation. Brains were transferred into phosphate-buffered saline (PBS; containing 1% P/S) on ice and dissected mechanically. After addition of dispase, brains in a final volume of 5 mL serum-free M199 medium were stirred in a water bath at 37°C for 45 min to 1 h. The digestion was controlled microscopically to obtain intact capillaries. Then, 5 mL dextran was added and the solution was centrifuged at 10 000 g for 10 min (4°C). After microscopic control, the pellet was re-suspended in 2 mL serum-free preparation medium and transferred to a Percoll gradient consisting of 4 mL of 1.03 g/mL density and 3 mL of 1.07 g/mL density Percoll solution. Following a centrifugation step at 2400 rpm (10 min at 22°C without brake), the interphase was transferred into a fresh tube, washed in serum-free medium, and either seeded on collagen-coated (60 µg/ml) flasks (25 cm^2 area) lysed in

RLT Plus buffer with β-mercaptoethanol for RNA isolation or lysed in protein lysis buffer for protein isolation.

3.2.3. Transwell experiments

To induce tight junction formation - pBCEC grown on 12-well Transwell filters for usually 3 days were exposed (over night) to DMEM/Ham's F12 medium containing 500 nM hydrocortisone (Sigma Aldrich), 1% P/S and 0.25% glutamine. Rising transendothelial electrical resistance (TEERs) of pBCEC - measured by using an Endohm tissue resistance chamber and the Evohm ohmmeter (World Precision Instruments) - indicated formation of intact tight junctions in the *in vitro* BBB model system [76].

3.2.4. Quantitative real-time PCR

pBCEC were exposed to vehicle (ethanol), 10 µM 24OH-C, 10 µM 27OH-C, 5 µM simvastatin, 2 µM TO, or 100 µM cholesterol in serum-free medium for 24 h. Total RNA was isolated (Rneasy Plus Kit, Qiagen) and 1 µg was used for cDNA synthesis (iScript cDNA synthesis Kit, Biorad). Quantitative PCR was performed by using cDNA, sequence specific primer pairs and the fluorescent dye SYBR Green (Biorad) on an iCycler iQ Real-time PCR Detection System (Biorad), following the manufacturer's protocol. Briefly, each reaction (20 µl) contained 1x SYBR Green supermix, 0.2 µM primers, and 20 ng template. Amplification was carried out for each sample in triplicate, with 40 cylces at 95°C for 20 s, at 60°C for 40 s and at 72°C for 40 s. Melting curve analysis confirmed the specificity and purity of each PCR product. Sequence analysis on a CEQ 8000 (Beckman Coulter) instrument was performed to confirm the identity of PCR products. Expression levels of genes of interest (hypoxanthine phosphoribosyltransferase 1, HPRT1; sterol regulatory element binding protein 2, SREBP-2; presenilin 1 and 2, PSEN1 and PSEN2; nicastrin, NCSTN; presenilin enhancer 2 homolog, PSENEN; anterior pharynx defective 1 homolog A, APH1A; ADAM metallopeptidase domain 10; ADAM10; beta-site APP-cleaving enzyme 1, BACE1;

mitochondrially encoded cytochrome c oxidase II, COX2; tumor necrosis factor, TNFα) were normalized to HPRT-1. Data were analysed using a standard curve method [164]. The primer sequences are listed in Table 3-Table 5.

3.2.5. Immunoprecipitation of proteins from cell culture supernatants

Immunoprecipitation of secreted proteins was performed following a modified version of the manufacturer's protocol. In brief, 50 µl Dynabeads® were transferred to a microcentrifuge tube and washed once by the addition of 0.5 ml 0.1 M sodium phosphate buffer pH 8.0. The tube was placed onto the magnet (DynaMag™-Spin Invitrogen) for 1 min and the supernatant was removed. The washing step was repeated once.

The antibody (0.5-10 µg) diluted in 200 µl PBS-T (1x PBS pH 7.4 containing 0.02% w/v Tween 20) was added to the beads, the suspension was mixed and put on a rotating wheel for 10 min at room temperature. The tube was placed on the magnet for 2 min and the supernatant was removed and 1 mL 0.2 M triethanolamine (pH 8.2) was used to wash the beads twice (as described in the first paragraph).

The beads-antibody complex was resuspended in 1 ml of 20 mM DMP in 0.2 M triethanolamine (pH 8.2; 5.4 mg DMP/ml buffer) and put on the rotating wheel for 30 min at room temperature. The tube was placed on the magnet for 2 min, supernatant was removed and the reaction was stopped by resuspending the beads with 1 mL 50 mM Tris, pH 7.5 and incubation for 15 min with rotational mixing.

The tube was placed on the magnet for 2 min, supernatant was removed and the beads were washed 3 times with 1 mL PBS pH 7.4 for 1 min. Antigen-containing solution was added to the beads and the mixture was incubated O.N. at 4°C on the rotating wheel. The tube was placed on the magnet for 2 min, supernatant was removed and beads were washed 3 times with 0.2 ml 1x PBS for 1 min.

Beads were resuspended in 100 µl 1x PBS and transferred to a clean tube that was placed for 2 min on the magnet. The supernatant was removed and 40 µl mild elution

buffer was added and beads were gentle resuspended. The mixture was incubated with rotation for 2 min at room temperature to dissociate the complex. The tube was placed on the magnet for 2 min, supernatant (eluate) was transferred to a clean tube and stored at -20°C for further analyses.

3.2.6. SDS-PAGE and immunoblotting

Cells grown in 6-well plates or 12-well Transwell filters were incubated in serum-free medium containing 10 µM 24OH-C, 10 µM 27OH-C, 5 µM simvastatin, 2 µM TO, 100 µM cholesterol, or equal volumes of ethanol (control) for 24 h. The medium was collected, centrifuged (10,000 g, 10 min, 4°C) and proteins were precipitated with 3% (v/v) trichloroacetic acid from the obtained supernatants, and pellets were dissolved in 1x sample buffer (Biorad). After removal of the cell culture medium, cells were washed twice with PBS and lysed in protein lysis buffer (50 mM Tris, 10 mM EDTA, 1% v/v NP-40, 0.1 v/v protease inhibitor cocktail, pH 7.4), or NaOH (0.3 N; for cells grown on Transwell filters). Cell lysates were sonicated, centrifuged (10,000 g, 10 min, 4°C), and protein content was determined using the BCA assay (Thermo Scientific). Aliquots containing 10 µg of cellular protein or equal amounts of secreted proteins (normalized to the cell protein content of each sample), were mixed with 4x loading buffer, 20x reducing agent (Biorad) and heated for 2 min at 95°C. Samples were loaded onto 4-12% Bis-Tris gels (Biorad) in 2-(N-morpholino)ethanesulfonic acid buffer (MES) (Invitrogen), proteins were separated by SDS-PAGE and transferred onto 0.45 µm PVDF membranes (GE Healthcare) at 50 V for 60 min. Membranes were blocked with 10% non-fat dry milk (Biorad) in TBS containing 0.5% Tween 20 for 1 h at room temperature. The membranes were then probed with primary antibodies for 1.5 h at room temperature (please refer to section “Antibodies” under ‘Material and Methods’). After three washing steps (using TBS containing 0.05% Tween 20 and 0.2% Triton X 100 for 10 min), membranes were incubated with polyclonal horseradish peroxidase conjugated secondary antibodies (please refer to section “Antibodies”) for 45 min at room temperature. After three washing steps signals were detected on X-ray

films using enhanced chemiluminescence (Western C Immunstar Kit, Biorad). Blots were incubated with polyclonal goat-anti rabbit anti-β-actin antibody (Sigma, 1:5000 in TBS containing 0.5% Tween 20) as loading control; washing steps and incubation with secondary ab were carried out as described above for primary ab. Films were scanned and bands densitometrically analysed using Image J software (version 1.42q).

3.2.7. Immunhistochemistry

Cryosections (6 µm) of porcine brain samples were mounted on microslides (Assistent, Karl Hecht AG, Sondheim, Germany), air-dried over night and stored frozen. Prior to immunostaining, tissue sections were fixed in acetone for 4 min and subsequently immunolabeled using the UltraVision LP Detection System (Thermo Scientific, Fremont, CA, USA) according to the manufacturer's instructions. The following antibodies were diluted in antibody diluent (Dako) and applied for 30 min at room temperature: von Willebrand factor antibody (vWF, Dako, 0.725 µg/ml, immunoglobulin fraction, rabbit anti-human), APP (Sigma, 1 µg/ml, rabbit anti-human). Normal rabbit immunoglobulin fraction (Dako, 1µg/ml) was used as control. After washing in PBS, slides were incubated with primary antibody enhancer for 10 min, followed by HRP-polymer for 15 min. The slides were washed and immunolabeling was visualized by a 5 min exposure to 3-amino-9-ethylcarbacole (AEC, all from UltraVision kit, Thermo Scientific). The slides were counterstained with Mayer's hemalum (Merck, Darmstadt, Germany), washed in distilled water and mounted with Kaiser's glycerol gelatin (Merck).

3.2.8. Immunocytochemistry

pBCEC were grown on collagen-coated FlexiPerm cell culture chambers (0.9 cm^2) in medium B until 70-80% confluence. Cells were washed twice with PBS and incubated in the presence of ethanol (0.5%; vehicle control) or 10 µM 24OH-C, 10 µM 27OH-C, 5 µM simvastatin, 2 µM TO or 100 µM cholesterol in serum-free medium for 24 h. Cells

were fixed with acetone (5 min), permeabilized with PBS containing 0.1% Tween 20, and blocked with goat serum (2.5% in PBS containing 0.1% Tween 20) for 45 min at room temperature. Incubation with polyclonal rabbit anti human Aβ antibody (Sigma, 1:200 in PBS containing 0.5% Tween 20) was carried out for 1 h at room temperature, followed by two washing steps (10 min and 5 min in PBS containing 0.5% Tween 20) and incubation with polyclonal goat anti-rabbit antibody conjugated to Cy3 (Dianova, kindly provided by Eva Bernhart, 1:100). After two washing steps (10 min and 5 min in PBS containing 0.5% Tween 20 in the dark), slides were mounted (Vectashield medium containing Dapi, Vector laboratories), and cells and fluorescent signals were analysed with a Leica DFC 300 FX fluorescence microscope.

3.2.9. Quantification of cellular cholesterol levels

Cells grown in 6-well plates were incubated in serum-free medium containing 10 µM 24OH-C, 10 µM 27OH-C, 5 µM simvastatin, 2 µM TO, 100 µM cholesterol, or equal volumes of ethanol (control) for 24 h. Cells were washed twice with PBS, and incubated for 30 min under gentle agitation with cholesterol reagent (Greiner Bio-One) in the presence of 5 mg/mL enhancer sodium 3,5–dichloro-2-hydroxybenzenesulfonate (DHB; Sigma Aldrich). Absorbance (at 562 nm) was measured on a Sunrise photometer with Magellan software (Tecan) and values obtained were normalized to intracellular protein content.

To analyze unesterified and esterified cellular cholesterol, cells were treated as described above and cellular lipids subsequently extracted twice with 500 µl of hexane/2-propanol (3:2, v/v). After centrifugation at 14000 g, 500 µl of the organic phase was removed and hydrolysed in KOH. The neutral lipids were extracted into hexane, dried and converted into the corresponding trimethylsilyl ether derivatives (80 µl of acetone/20 µl bis(trimethylsilyl)trifluoroacetamide containing 1% trimethylchlorosilane; 15 min at 50°C). Lipid extracts without prior hydrolysis were processed as described above to determine the intracellular unesterified cholesterol content. The difference between the cholesterol contents of hydrolysed versus non-

hydrolysed samples should reflect the contribution of esterified cholesterol to the total cellular cholesterol content. The trimethyl-silyl-ether derivatives were analysed by GC and quantified with 5α-cholestane as an internal standard [165].

3.2.10. Radiometric assays for cholesterol biosynthesis and esterification

PBCEC were incubated with [^{14}C]-acetate (10 µCi/mL) in the presence of 10 µM 24OH-C, 27OH-C, 2 µM TO, 100 µM cholesterol, 5 µM simvastatin, or ethanol vehicle (control) in serum-free medium for 24 h. Cells were rinsed twice in PBS and cellular lipids were extracted by incubation in n-hexane:isopropanol (3:2 v/v) (2x 1 mL for 30 min, gently agitating at room temperature). Lipid extracts were dried under a nitrogen stream and resuspended in 50 µl of chloroform:methanol (2:1 v/v). Aliquots of the samples were counted on a beta counter to obtain total counts/well. Lipid extracts were loaded onto Silica gel thin layer chromatography (TLC) plastic plates (Merck). For separating cholesterol (C) and cholesterol esters (CE), n-hexane:diethylether:acetic acid (79:29:1, v/v) was used as the mobile phase. Standards (Sigma Aldrich) for all lipid classes (1 mg/mL) were run in parallel to the samples. Lipid class spots were stained with iodine vapour, cut out, and radioactivity was determined by beta counting (Liquid Scintillation Analyzer, Packard). Total counts per sample were normalized to intracellular protein content (determined using the Qubit® fluorometer and the Qubit® Protein Assay Kit, Invitrogen).

3.2.11. Radiometric assay for cholesterol efflux

pBCEC were grown on collagen-coated 12-well plates in medium B until confluence and cholesterol efflux was assayed essentially as previously described [76]. In brief, cellular cholesterol pools were labeled with 1 µCi/ml [^{3}H]-cholesterol in medium B for 24 h. On the next day, the cholesterol pools were briefly equilibrated by incubating the cells in 1 ml serum-free medium for 2 h. After two washing steps (1x PBS) pBCEC were incubated in the absence or presence of apoA-I (20 µg/ml) and the presence of 10 µM

24OH-C, 27OH-C, 2 µM TO, 100 µM cholesterol, 5 µM simvastatin, or ethanol vehicle (control) in serum-free medium for 24 h. After centrifugation (10,000 rpm, 5 min) aliquots of cell supernatants were counted on a β-counter to obtain total counts/supernatant. Cells were carefully washed with 1x PBS and lysed in 0.2 ml 0.3N NaOH. Aliquots of cell lysates were counted on a β-counter to obtain total counts/cell lysates. Total cellular protein content was determined (using the Qubit® fluorometer and the Qubit® Protein Assay Kit, Invitrogen) and [^{3}H]-cholesterol efflux was calculated in cpm/mg cell protein.

3.2.12. Oil Red O (ORO) staining of neutral lipids

pBCEC were grown on collagen-coated FlexiPerm cell culture chambers (0.9 cm^2) in medium B until 70-80% confluence. Differentiated human Simpson-Golabi-Behmel syndrome (SGSBS) adipocytes (grown on FlexiPerm chambers and obtained from the group of Dr. Rudolf Zechner) were used as positive control. Cells were washed twice with PBS and incubated in the presence of ethanol (0.5%; vehicle control) or 100 µM cholesterol in serum-free medium for 24 h. Slides were stained with 0.5% ORO in 60% isopropanol for 30 min. Counter-stained slides (hematoxylin, 10 min) were mounted with Kaiser's Gelatine (both from VWR, Vienna, Austria).

3.2.13. Labeling and transport studies of radiolabeled $A\beta_{1-40}$ peptide and apoA-I

Proteins/peptides were iodinated using N-Br-succinimide as the oxidizing agent [166]. Routinely, 100 µCi [^{125}I]-Na was used to label 1 mg of protein. This procedure resulted in specific activities of between 50 and 100 cpm per ng protein.

pBCEC were grown on collagen-coated 12-well Transwell plates in medium 'B' until confluence. Tight junction formation was induced as described in Material and Methods 'Transwell experiments' and monitored at the start and end of the experiments. For Aβ transport studies cells were incubated with 0.5 µg/ml [^{125}I]-$A\beta_{1-40}$ added either to the basolateral or apical compartment for up to 60 min. After 3 time

points (10, 30 and 60 min) aliquots of media were taken (100 µl from the apical, 400 µl from the basolateral side) and radioactivity was measured on a gamma-counter. The aliquots were replaced by fresh medium. After a final washing step with 1x PBS, cells were lysed in 300 µl 0.3N NaOH, cell-associated radioactivity was counted from an aliquot (100 µl)and protein content was determined using the Bradford Reagent (Sigma Aldrich) according to the manufacturer's protocol [167].

For apoA-I transport studies, cells were incubated with 2, 5 or 10 (± HDL_3) µg/ml [^{125}I]-apoA-I added to the apical compartment for up to 3 h. After several time points (0.5, 1, 2 and 3 h), aliquots were taken (400 µl) from the basolateral compartment and measured on a gamma-counter. The aliquots were replaced by fresh medium. After a final washing step with 1x PBS, cells were lysed in 300 µl 0.3N NaOH, cell-associated radioactivity was counted from an aliquot (100 µl) and protein content was determined using the Bradford Reagent (Sigma Aldrich) according to the manufacturer's protocol [167].

3.2.14. Fluorescent labelling of $A\beta_{1-40}$

$A\beta_{1-40}$ peptide was labeled with Alexa Fluor 488 5-TFP during incubation at 37°C for 1 h in carbonatebicarbonate (CBC) buffer (Table 11). Unbound fluorescent dye was removed via size-exclusion on a PD-10 column. Elution was performed with 1 ml PBS and the final concentration of the fluorescent Aβ (Alexa-Aβ) peptide was 150 µg/ml.

Table 11: Labeling of amyloid beta$_{1-40}$ peptide

component	amount
$A\beta_{1-40}$ (5 mg/ml)	**30 µl**
CBC buffer pH 9.0	**6 µl**
Alexa Fluor 488 5-TFP	**1 µl**

3.2.15. Flow-cytometric Alexa-Aβ_{1-40} peptide binding and uptake assay

BW transductants were counted using a Nucleocounter (Chemometec A/S) and 100,000 cells per 96 well were prepared in 100 µl RPMI 1640 (without FBS+1 mg/ml BSA), transferred into FACS tubes where incubation with Alexa-Aβ_{1-40} peptide (20 µg/ml) was carried out for 45 min at 4°C. After centrifugation at 500 g for 5 min, cells were washed once with PBS and then resuspended in 100 µl FACS FIX solution. Samples were analysed using a BD FACSCalibur Flowcytometer (experiments were conducted by Michael Holzer, Institute of Experimental Pharmacology, Medical University Graz).

pBCEC were cultured on collagen-coated (60 µg/ml) 48 well plates (Greiner) in serum-free medium containing Alexa- Aβ_{1-40} peptide (0-50 µg/ml) in the absence or presence of fucoidan (Sigma Aldrich, 50 µg/ml, pre-incubation of cells for 30 min) for 2 h at either 37°C or 4°C. Cells were then washed with PBS and detached from the culture ware using accutase (Sigma Aldrich). After centrifugation (900 rpm, 5 min) cells were resuspended in 100 µl FACS Cellfix solution (BD Biosciences) and samples were analysed using a BD FACSScan Flowcytometer and CELLQuest software (Beckton Dickinson). Gates were set to exclude cell debris and Alexa fluorescence intensity was measured in FL1 channel (green, 488 nm). Fluorescence intensity of the gated events was quantified (10,000 events for each sample).

3.2.16. Fluorescence microscopy

pBCEC cultured on collagen-coated (60 µg/ml) self-made flexiPERM objective slides were incubated in serum-free medium containing Alexa- Aβ_{1-40} peptide (0-50 µg/ml) for 2 h at 37°C. Cells were then washed with 1x PBS, fixed with acetone for 5 min, shortly re-hydrated with PBS and mounted with Vectashield containing DAPI. Visualization of cells was performed using a Leica DM 4000B fluorescence microscope.

3.2.17. Lipoprotein profiling in pBCEC supernatants

pBCEC were grown on petri dishes (10 mm diameter) and treated with 10 µM 24OH-C 2 µM TO901317, 100 µM cholesterol or vehicle control (ethanol) for 24 h. Media were collected, centrifuged at 2400 rpm for 10 min at room temperature and concentrated (Eppendorf concentrator), the final volume was 2 ml. Supernatants were adjusted to a density of 1.24 g/ml by adding KBr, carefully layered underneath a KBr density solution (1.006 g/ml) and centrifuged at 100,000 rpm for 3 h at 15°C (TLA 100.4 rotor, Beckman Optima TLX ultracentrifuge). Human plasma and isolated human HDL were run in parallel as positive controls, lipoprotein fractions were stained with 1,1'-dioctadecyl-3,3,3',3'-tetramethylindocarbocyanine perchlorate (Invitrogen). Four lipoprotein fractions were recovered, their mean density was determined by weighing 2x100 µl and was: 1.00-1.04 g/ml for fraction 1, 1.05-1.12 g/ml for fraction 2, 1.13-1.20 g/m for fraction 3 and 1.21-1.24 g/ml for fraction 4. Fractions were used for proteomic analysis by tryptic digestion and liquid chromatography-mass spectrometry analysis (performed by Dr. Ruth Birner Gruenberger) and by immunoblotting/immunoprecipitation.

3.2.18. LC-MS

For tryptic digest, isolated lipoprotein fractions were reduced with 34 µl of 10 mM DTT for 20 min by shaking at 550 rpm at 56°C and alkylated with 8 µl of 55mM iodoacetamide by shaking at 550 rpm at room temperature for 15 min. Protein was digested by adding 1 µg of Promega modified trypsin and shaking over night at 550 rpm at 37°C. The resulting peptide solution was acidified by adding 1.6 µl of 5% formic acid and diluted in solvent A to a theoretical final concentration of 50 ng/µl. 40 µl were separated by nano-HPLC on an Agilent 1200 system equipped with a Zorbax 300SB-C18, 5µm, 5x0.3mm enrichment column and a Zorbax 300SB-C18, 3.5µm, 150x0.075mm nanocolumn. 40 µl samples were injected and concentrated on the enrichment column for 6 min using 0.1% formic acid as isocratic solvent at a flow rate of 20 µl/min. The column was then switched in the nanoflow circuit, and the sample

was loaded for 6 min on the nanocolumn at a flow rate of 300 nl/min and separated using the following gradient: solvent A: water, 0.3% formic acid; solvent B: acetonitril/water 80/20, 0.3% formic acid; 0-10 min: 90% A; after 120 min 60% B, after 2 min 95% B, then for 8 min 95% B, after 2 min 10% B, and 18 min reequilibration at 10% B. The sample was ionized in the nanospray source equipped with nanospray tips (PicoTipTM Stock# FS360-75-15-D-20, Coating: 1P-4P, 15+/- 1µm Emitter, New Objective) and analyzed in a Thermo LTQ-FT mass spectrometer in positive ion mode by alternating full scan MS (m/z 200 to 2000) in the ICR cell and MS/MS by CID of the 5 most intense peaks in the ion trap with dynamic exclusion enabled. The MS/MS data were analyzed by searching the NCBI nonredundant public database with Spectrum mill Rev. A.03.03.078 (Agilent) and Mascot 2.2 (MatrixScience). Detailed search criteria: enzyme: trypsin, max. missed cleavage sides: 2, N-terminus: hydrogen, C-terminus : free acid, Cys modification: carbamidomethylation, search mode: homology search, possible multiple oxidised methionine and carbamylated lysine, maximum precursor charge 3; precursor mass tolerance +/- 0.05 Da, product mass tolerance +/- 0.7 Da; acceptance parameters were 2 or more identified peptides after automatic validation (Mascot: $p<0.05$, FDR>0.05 using decoy database search; Spectrum Mill: for precursor charge of 2: score threshold is 6.0, %SPI threshold is 60.0, Fwd-Rev score threshold is 2.0 and rank 1-2 score threshold is 2.0, for precursor charge of 1: score threshold is 6.0, %SPI threshold is 70.0, Fwd-Rev score threshold is 2.0 and rank 1-2 score threshold is 2.0, for precursor charge of 3: score threshold is 8.0, %SPI threshold is 70.0, Fwd-Rev score threshold is 2.0 and rank 1-2 score threshold is 2.0).

4. Results

4.1. Characterization of APP and cholesterol metabolism in BCEC

4.1.1. Localization of APP in brain microvascular endothelial cells

It has been reported that Aβ is transported across the BBB in both directions and that in AD, Aβ may accumulate in cerebrovessels [33, 35, 168]. In our first series of experiments we addressed the question if APP is present in porcine and murine cerebrovessels (Figure 8). Immunostaining of APP and of endothelial cell specific marker von Willebrand factor was performed on serial coronal sections of porcine midbrain and murine midbrain. Non-immune rabbit IgG was used as negative control for the immunostaining. We detected pronounced APP staining in porcine cerebral vessels (Figure 8 A, [169]), and in murine cerebral vessels (Figure 8 E), indicating that APP is present at both the porcine and murine BBB under normal physiological conditions. In addition, porcine glial cells also positively stained for APP (Figure 8 A,

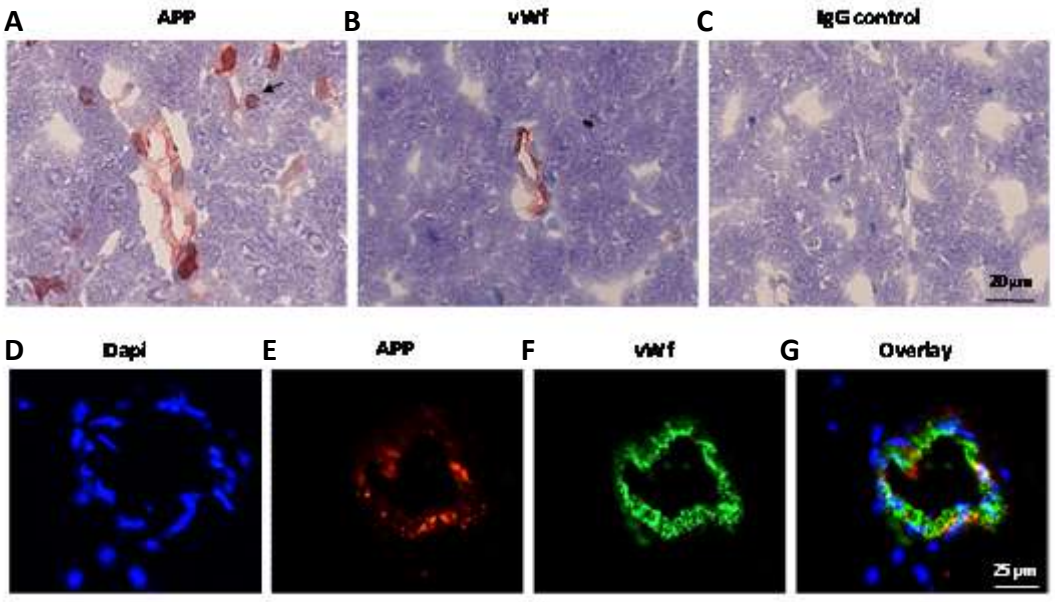

arrow, [169]).

Figure 8: Cerebral microvascular endothelial cells express APP. (A-C) Immunostaining of endothelial cells and APP in cerebral vessels in serial coronal thionine stained sections of porcine brain (**A**, pBCEC positive for APP; **B**, pBCEC positive for von Willebrand factor; **C,** non-immune rabbit IgG control; arrow, glial cells positive for APP). Scale bar = 20, [169]. **(D-G)** Immunofluorescence staining of endothelial cells and APP in serial coronal thionine stained sections of murine brain (blue, Dapi staining of cell nuclei; red: MBEC positive for APP; green: MBEC positive for von Willebrand factor; **G**: overlay of Dapi, APP and vWF signals). Scale bar = 25 µm.

4.1.2. APP is expressed and processed in cerebral microvascular endothelial cells

To investigate if the APP signal immunodetected in cerebrovessels was of exogenous or endogenous origin, we examined APP mRNA and protein expression in isolated, cultured pBCEC. Real-time PCR analysis (Figure 9, [169]) revealed the presence of APP mRNA in pBCEC. In addition, expression of a subset of mRNAs belonging to the proteolytic machinery necessary for APP processing was confirmed by qPCR. This set was composed of γ-secretase subunits presenilin 1 & 2 (PSEN1, PSEN2; Figure 9), Nicastrin (NCSTN), Presenilin enhancer homolog 2, (PSENEN), Anterior pharynx defective 1 homolog A (APH1A), alpha-site APP-cleaving enzyme (ADAM10) and beta-site APP-cleaving enzyme 1 (BACE1). These data demonstrate that pBCEC express the machinery for both non amyloidogenic (APPα production) and amyloidogenic processing of APP to amyloid peptide derivatives.

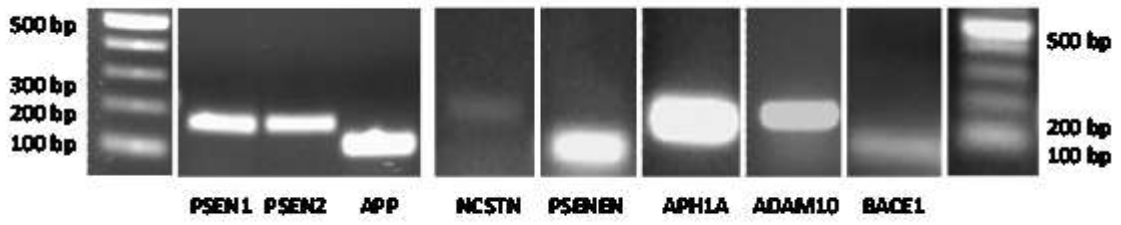

Figure 9: Porcine BCEC express APP-processing enzymes of the non-, and amyloidogenic pathway. Brain endothelial cells express mRNAs of APP, alpha-, beta-, and gamma-secretase. Cells were incubated for 24 h in serum-free medium. Quantitative real-time PCR was performed as described in Materials and Methods. One representative separation of PCR products on a 1% agarose gel is shown. Presenilin 1 and 2, PSEN1, PSEN2; Amyloid β precursor protein, APP; Nicastrin, NCSTN; Presenilin enhancer homolog 2, PSENEN; Anterior pharynx defective 1 homolog A, APH1A; ADAM metallopeptidase domain 10, ADAM10; beta-site APP-cleaving enzyme 1, BACE1, [169].

Immunoblotting experiments using antibodies specific for full-length APP, Aβ oligomers, APPα, or APPβ (for details refer to section '3.1.4 Antibodies' under 'Material and Methods'), confirmed the expression of endogenous intracellular APP on protein level, as well as its cleavage products soluble (s)APPα and sAPPβ, and the presence of Aβ oligomers in pBCEC (Figure 10, [169]). In detail, we detected immature ($_{im}$APP, ~105 kDa) and mature ($_{m}$APP, ~130 kDa) intracellular APP (Figure 10A). For intracellularly detected Aβ oligomers (Figure 10 A) the most prominent bands appeared at 16 kDa (tetramer) and 32 kDa (octamer). The analyses of pBCEC supernatants revealed secretion of sAPPα, sAPPβ and Aβ oligomers into the culture medium (Figure 10 B). For secreted Aβ oligomers (Figure 10 B), bands at ~16 kDa (tetramer), ~32 kDa (octamer) and ~48 kDa (dodecamer) were detected. Further immunoblot analyses of extracellular sAPPα and sAPPβ (both ~110 kDa, Figure 10 B) revealed sAPPα as the most prominent species of secreted APP in pBCEC. These findings highlight the α-secretase pathway as the major APP processing pathway in BCEC.

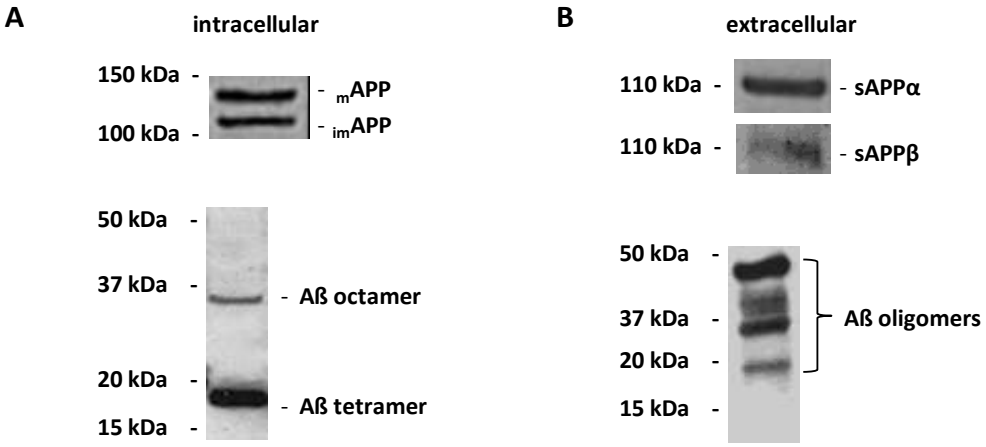

Figure 10: Processing of APP in pBCEC. Representative immunoblot analysis of intracellular **(A)** and secreted **(B)** APP and Aβ oligomers in pBCEC cultures. Cells were grown in serum-free medium for 24 h.

Cells were lysed and expression of mature ($_{m}$APP) and immature ($_{im}$APP), and intracellular Aβ oligomers were determined by immunoblotting. Secreted, soluble APPα (sAPPα), APPβ (sAPPβ; 6.8-fold amount loaded as compared to sAPPα) and immunoprecipitated Aβ oligomers (equal amounts of media as for sAPPβ immunoblots) were detected by immunoblotting of TCA-precipitated culture media as described in Materials and Methods section '3.2.6 SDS-PAGE and immunoblotting', [169].

4.1.3. APP processing in cerebral microvascular endothelial cells is affected by LXR activation and altered cholesterol levels

To scrutinize effects of LXR activation or cholesterol enrichment and/or depletion on cellular APP metabolism, pBCEC were incubated in the absence or presence of 10 µM 24OH-C, 10 µM 27OH-C, 2 µM TO, 100 µM cholesterol, or 5 µM simvastatin prior to analyses of APP mRNA and protein expression levels (Figure 11, [169]). During immunocytochemical detection and fluorescence microscopy using polyclonal antibody recognizing amino residues 693-706 of human APP, we observed a significant increase in intracellular fluorescent Cy3 signal for APP in pBCEC exposed to either 24OH-C, cholesterol, or TO (Figure 11 A). Similar microscopic pictures were obtained from simvastatin or 27OH-C treated cells. Consistent with these results, immunoblotting and densitometric evaluation revealed that all treatments increased intracellular APP protein levels (Figure 11 B): 27OH-C was most potent in stimulating APP protein expression (3.4-fold) during 24 h of incubation, followed by TO (2.6-fold), cholesterol (2.2-fold), and 24OH-C or simvastatin (both 1.4-fold). However, in contrast to APP protein expression levels, all of the compounds tested were without effect on APP mRNA expression levels (Figure 11 C), indicating that regulation of APP in pBCEC occurs at the post-translational level. Similar results were obtained for APP expression in MBEC (Figure 12): APP protein expression was significantly enhanced in the presence of 24OH-C and 27OH-C (Figure 12 A, 1.5-fold, 1.6-fold, respectively), whereas APP mRNA levels in oxysterol-treated MBEC did not change (Figure 12 B).

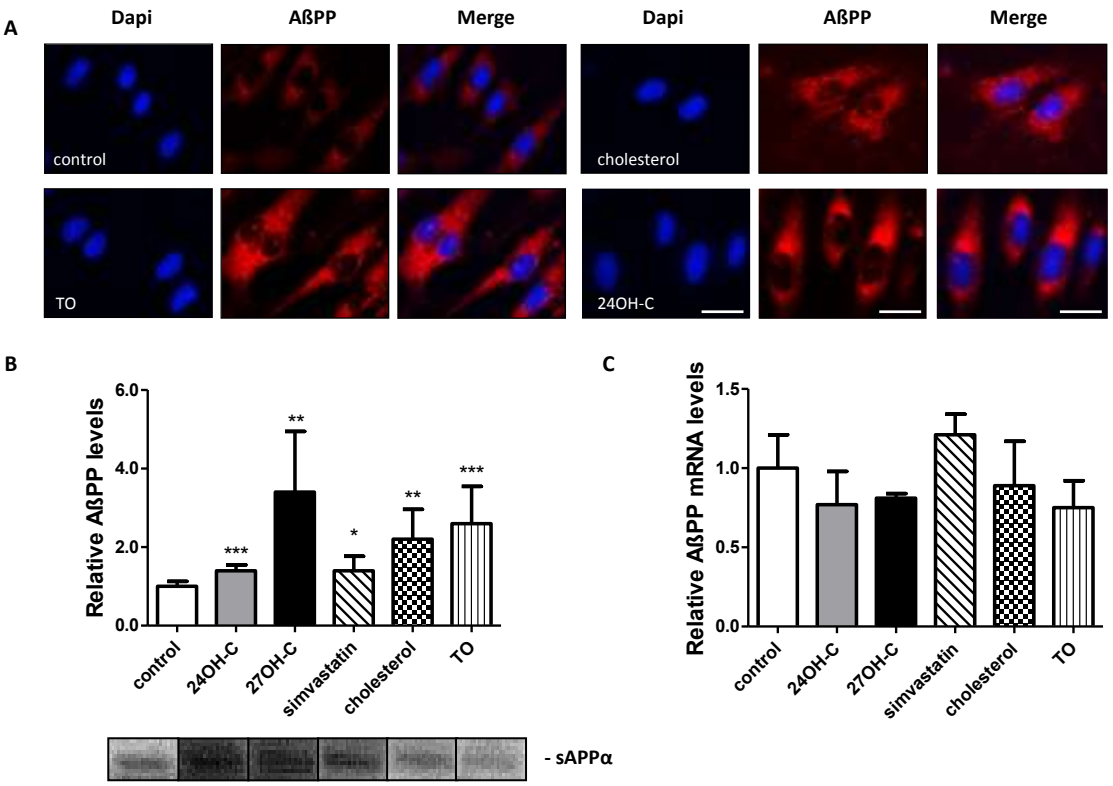

Figure 11: APP expression is influenced by LXR agonists and cholesterol and simvastatin. Cells were treated for 24 h with 10 µM 24(*S)*-hydroxycholesterol (24OH-C), 10 µM 27-hydroxycholesterol (27OH-C), 5 µM simvastatin, 100 µM cholesterol, or 2 µM TO901317 (TO) in serum-free medium. **(A)** Immunofluorescent detection of accumulated intracellular APP protein in pBCEC treated with LXR ligands or cholesterol. Cultured pBCEC were exposed to 100 µM cholesterol, 2 µM TO, or 10 µM 24OH-C for 24 h, fixed and immunolabeled for APP (Cy3, red) as described in Materials and Methods. Cells were stained with DAPI (blue) to visualize cell nuclei. Immunoreactivity for APP in control cells was less intense as compared to cells treated with cholesterol, TO or 24OH-C. Images are representative for at least three experiments. Scale bar = 20 µm. **(B)** Semi quantitative immunoblot analysis of cell associated full-length APP. Cells were lysed and intracellular APP expression was determined and normalized to the levels of β-actin expression (contr., control; 24OH, 24OH-C; 27OH, 27OH-C; simva, simvastatin; chol, cholesterol). Shown are representative immunoblots. Data represent mean ± SEM of eight independent experiments performed in triplicates. *P < 0.05; **P < 0.01; ***P < 0.001. **(C)** Quantification of APP mRNA expression in pBCEC. Quantitative real-time PCR was performed as described in Materials and Methods. HPRT1 mRNA was used for normalization. Data shown represent mean ± SEM of three independent experiments performed in triplicates, [169].

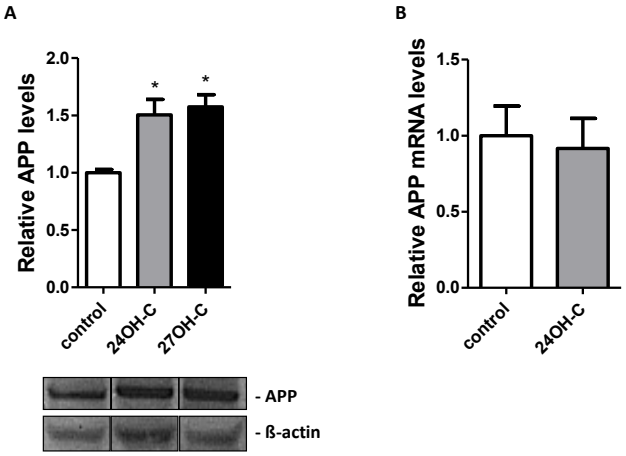

Figure 12: APP expression in MBEC is modulated by oxysterols. Cells were treated with oxysterols for 24 h in serum-free medium. (**A)** Immunoblot analysis for intracellular APP was performed and normalized to b-actin levels. Shown is one representative immunoblot. Data shown represent mean ± SD of one single experiment performed in triplicates. *P < 0.05. **(B)** Quantification of APP mRNA expression in MBEC. Quantitative real-time PCR was performed as described in Materials and Methods. Geometric means of RPII (qPCR) and b-actin (immunoblotting) were used for normalization. Data shown represent mean ± SD of two independent experiments performed in triplicates.

Secretion of sAPPα in pBCEC was increased 2.1-fold in the presence of 24OH-C, 1.9-fold in the presence of 27OH-C and at least (see below) 1.4-fold in the presence of simvastatin. (Of note, secreted sAPPα levels varied from 1.4-fold up to 14.2-fold up-regulation in response to simvastatin between different experiments/cell preparations used; n=6). In contrast, sAPPα expression levels remained unaltered in pBCEC incubated with cholesterol or TO (Figure 13 A, [169]). Interestingly, mRNA levels of ADAM10 (known for α-secretase activity) were 1.4-fold increased only in the presence of simvastatin whereas all other compounds tested did not show any effects (Figure 13 B, [169]).

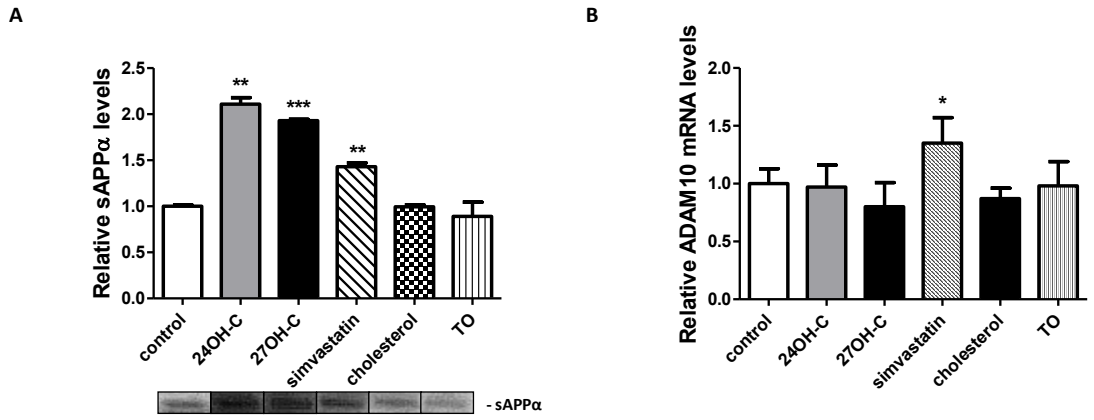

Figure 13: APPα expression is affected by oxysterols and modulators of cholesterol biosynthesis. (A) Semi quantitative immunoblot analysis of secreted sAPPα in pBCEC treated for 24 h with 10 µM 24OH-C, 10 µM 27OH-C, 5 µM simvastatin, 100 µM cholesterol, or 2 µM TO in serum-free medium. Secreted sAPPα was determined by immunoblotting of conditioned media as described in Materials and Methods. Shown is one representative immunoblot. Data shown represent mean ± SD of one representative of three independent experiments performed in triplicates. **P < 0.01; ***P < 0.001. **(B)** Quantification of ADAM10 mRNA levels analysed by real-time PCR. Cells were as indicated above and quantitative real-time PCR was performed as described in Materials and Methods. HPRT1 mRNA was used for normalization. Data represent mean ± SEM of three independent experiments performed in triplicates. *P < 0.05, [169].

Analyses of intracellular Aβ oligomers revealed a reduction of Aβ tetramers in pBCEC, by 35% with 24OH-C, by 71% with 27OH-C, by 48% with simvastatin and cholesterol, and by 26% with TO (Figure 14 A, [169]). Aβ octamers were decreased to similar extents (Figure 14 C, [169]). In parallel, mRNA levels of BACE1 (β-secretase) were significantly reduced in pBCEC, i.e. by 24% with 24OH-C, by 27% with 27OH-C, by 16% with simvastatin, and most pronounced (by 64%) with TO. There was a slight but non-significant trend towards reduced BACE1 mRNA levels in pBCEC treated with cholesterol (Figure 14 B, [169]).

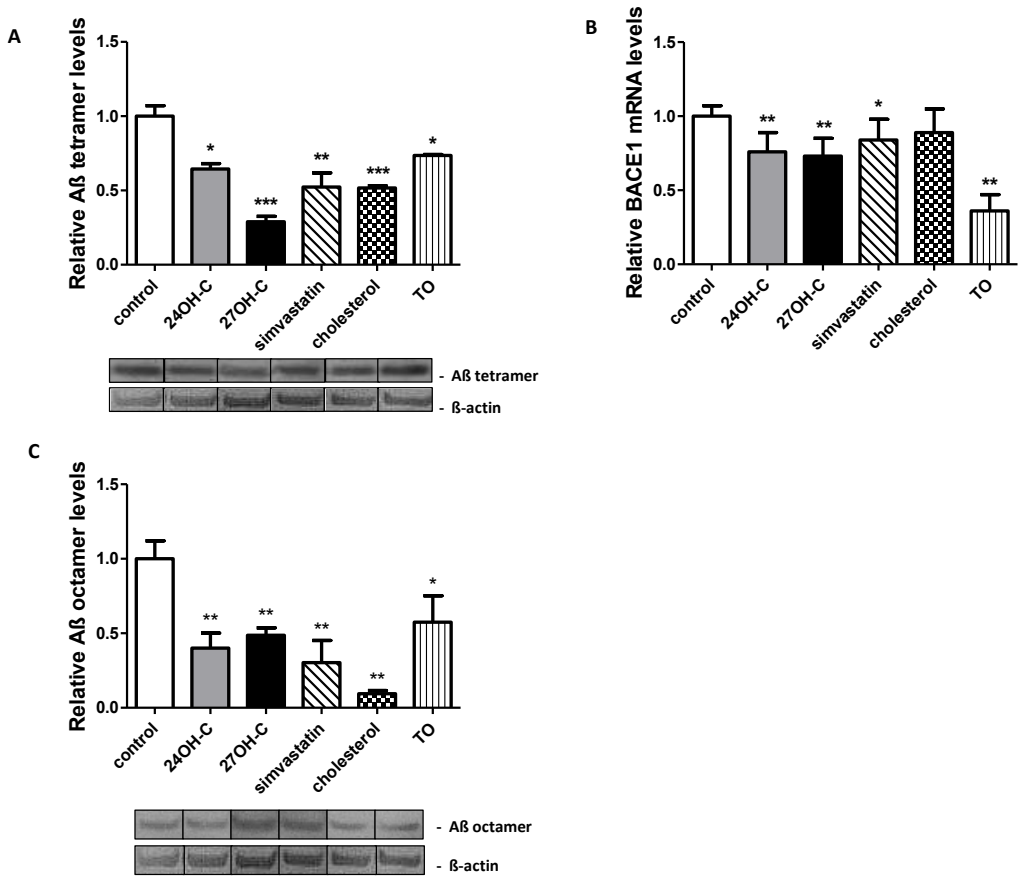

Figure 14: Decreased Aβ oligomerization in pBCEC treated with LXR ligands, cholesterol and simvastatin. (A) Quantification of cell-associated Aβ tetramer levels in pBCEC. After the respective treatments, cells were lysed and intracellular Aβ oligomer levels were analysed by immunoblotting. Data shown represent mean ± SD of one representative of three independent experiments performed in triplicates. *P < 0.05; **P < 0.01; ***P < 0.001. **(B)** Quantification of BACE1 mRNA levels analysed by real-time PCR. Cells were as indicated above and quantitative real-time PCR was performed as described in Materials and Methods. HPRT1 mRNA was used for normalization. Data represent mean ± SEM of three independent experiments performed in triplicates. *P < 0.05; **P < 0.01. **(C)** Quantification of cell-associated Aβ octamer levels in pBCEC. After the respective treatments, cells were lysed and intracellular Aβ oligomer levels were analysed by immunoblotting. Data shown represent mean ± SD of one representative of three independent experiments performed in triplicates. *P < 0.05; **P < 0.01, [169].

4.1.4. Cholesterol homeostasis of BCEC is regulated by LXR agonists and exogenously added cholesterol

Since we observed major effects of LXR agonists, cholesterol, and simvastatin on APP protein expression levels and processing/secretion, effects on cellular cholesterol homeostasis in pBCEC were analysed (Figure 15, [169]).

Total intracellular cholesterol levels were unaltered in pBCEC during 24 h of incubation with either of the oxysterols or the non-steroidal LXR ligand TO901317. In contrast, supplementation with 100 µM cholesterol resulted in 3-fold elevated cholesterol contents, whereas not surprisingly, simvastatin treatment significantly decreased total cellular cholesterol levels (by 33%) as compared to control conditions (Figure 15 A).

To get further insights into the effects on cholesterol biosynthesis and esterification in pBCEC, cells were incubated in the presence of [^{14}C]-acetate (used as metabolic precursor for newly synthesized cholesterol) during the incubation period with 24OH-C, 27OH-C, TO, cholesterol, or simvastatin. Cellular lipids were extracted and separated by TLC to quantify radioactivity incorporated in the cholesterol and the cholesterol ester fractions. Treatment with either of the oxysterols markedly reduced the synthesis of [^{14}C]-cholesterol from its precursor [^{14}C]-acetate in pBCEC as compared to vehicle treated controls (mean ± SEM, $1.02x10^6$ ± $4.2x10^5$ cpm/mg cell protein), i.e., by 90% with 24OH-C or by 87% with 27OH-C treatment (Figure 15 B). As expected, the cholesterol biosynthesis inhibitor simvastatin blocked cellular [^{14}C]-cholesterol synthesis by 98%. Cholesterol treatment resulted in a 25% decrease and also treatment with TO resulted in a marked (43%) decrease in radioactivity in the cholesterol fraction (Figure 15 B).

Regarding the amounts of cellular [^{14}C]-cholesterol esters counted in the corresponding TLC bands, levels comprised 4.5 ± 2.1% of intracellular unesterified cholesterol under control conditions (mean ± SEM, 15635 ± 5613 cpm/mg cell protein). In contrast to cholesterol biosynthesis, the formation of cellular cholesterol esters (Figure 15 C) was enhanced by 2-fold in the presence of 24OH-C and by 2.4-fold after 27OH-C treatment. The presence of cholesterol or TO did not significantly affect

cholesterol ester formation although there was a slight but non-significant trend towards increased incorporation of radioactivity in cholesterol esters.

To examine the possibility that pBCEC accumulate cholesterol esters and/or may form lipid droplets, Oil Red O staining (ORO) was performed in cholesterol-treated cells. Compared to ORO-positive cells (adipocytes), we have been unable to detect any neutral lipid staining in pBCEC treated with cholesterol (Figure 16).

As expected, [^{14}C]-cholesterol ester levels were decreased by 56% in cells treated with simvastatin (Figure 15 C). Taken together these results suggest that pBCEC are sensitive to modulation of cellular cholesterol levels and its distribution by sterols, LXR activation, and statin treatment.

Besides uptake and biosynthesis of cholesterol, efflux of cellular cholesterol to acceptor apo/lipoprotein particles is an important mechanism to maintain cellular cholesterol homeostasis. Previous *in vitro* studies in our group showed that in pBCEC the ABCA1/apoA-I pathway can be induced by LXR agonists (24OH-C or TO). In detail, ABCA1 is responsible for cholesterol efflux to apoA-I, synthesized and secreted by pBCEC and contributes to the formation of HDL-like particles at the basolateral side of the BBB [76]. To test regulation of the ABCA1/apoA-I pathway under the same conditions as applied here, apoA-I mediated efflux of cellular [^{3}H]-cholesterol was measured (Figure 15 D). During 24 h of incubation under control conditions 13 ± 2.4 % of total cellular [^{3}H]-activity was released to the medium containing apoA-I acceptors. TO was most potent in stimulating apoA-I dependent cholesterol efflux (4.3-fold), followed by cholesterol (2.9-fold), and 24OH-C (2.5-fold). There was a non-significant trend towards enhanced cholesterol efflux to apoA-I in pBCEC treated with 27OH-C, whereas cells incubated with simvastatin showed no altered cholesterol release.

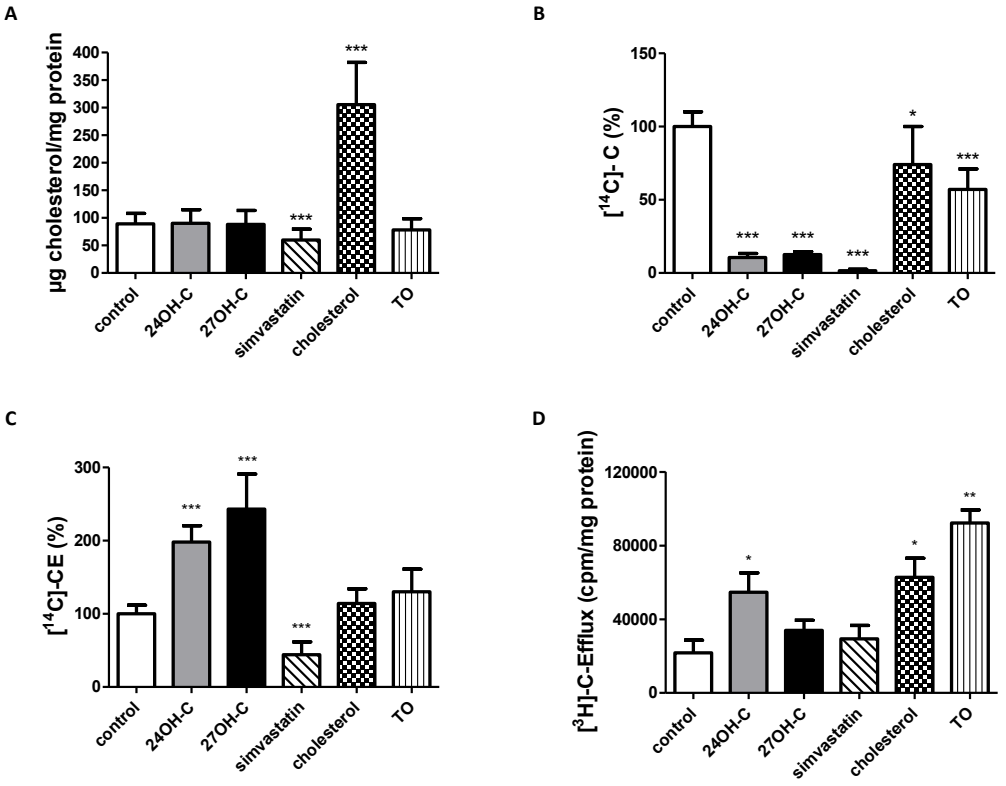

Figure 15: Altered cholesterol metabolism in pBCEC treated with LXR ligands, cholesterol and simvastatin. Cells were treated for 24 h with 10 µM 24OH-C, 10 µM 27OH-C, 5 µM simvastatin, 100 µM cholesterol, or 2 µM TO in serum-free medium. **(A)** Effects of cholesterol and simvastatin on cellular total cholesterol levels in pBCEC. After incubation, cells were washed and total cholesterol levels were determined by using an enzymatic kit (Greiner). Data represent mean ± SD of one experiment representative of 4 performed in quadruplicates. ***P < 0.001. **(B)** Biosynthesis of [^{14}C]-cholesterol ([^{14}C]-C) from [^{14}C]-acetate in pBCEC is decreased after treatment with oxysterols, cholesterol, simvastatin or TO. Primary pBCEC were exposed for 24 h to 10 µCi/mL [^{14}C]-acetate during the treatment with LXR agonists, cholesterol, or simvastatin. Cellular lipids were extracted and were analysed by TLC. Data represent mean ± SEM of three independent experiments performed in triplicates. *P < 0.05; ***P < 0.001. **(C)** Effects of oxysterols and simvastatin on cholesterol ester ([^{14}C]-CE) formation from [^{14}C]-acetate in pBCEC. BCEC were treated as indicated above and cellular lipids were extracted and analysed by TLC. Data represent mean ± SEM of three independent experiments performed in triplicates. ***P < 0.001. **(D)** LXR agonists and cholesterol promote apoA-I mediated cholesterol efflux from pBCEC. Cells were labeled with [^{3}H]-cholesterol in medium containing serum for 24 h followed by an equilibration time of 2 h in serum-free medium. After incubation with 10 µM 24OH-C, 10 µM 27OH-C, 5 µM simvastatin, 100 µM cholesterol, or 2 µM TO in serum-free medium in the presence or absence of apoA-I (20 µg/ml) for 24 h, cholesterol efflux was determined as the

radioactivity released to the supernatants. Data represent mean ± SD of cpm/mg cell protein of one experiment performed in triplicates. *P < 0.05, **P < 0.01, [169].

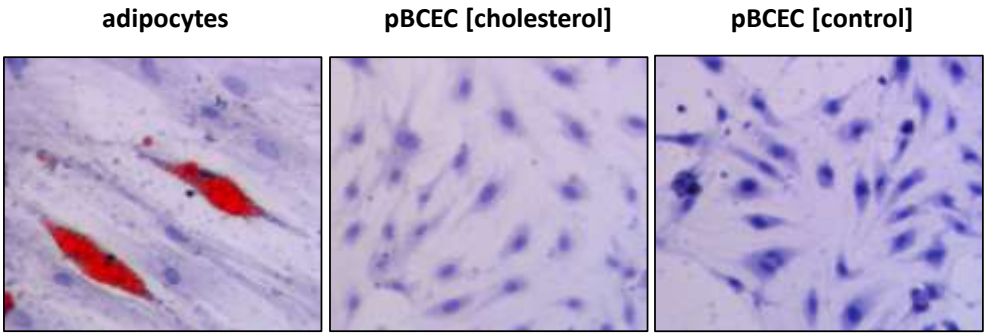

Figure 16: PBCEC do not form lipid droplets. PBCEC were treated for 24 h with 100 µM cholesterol in serum-free medium. ORO staining was performed as described in 'ORO staining of neutral lipids' in Materials and Methods. ORO staining (red) of control and cholesterol-treated pBCEC was negative compared to control pBCEC (ethanol treated) and ORO-positive adipocytes. Images were taken using a light microscope with 20-fold magnification and are representative for two independent experiments.

4.1.5. Alteration in expression levels of key genes of cholesterol metabolism

Since it was obvious that sterol treatment and/or LXR activation influenced cholesterol homeostasis in pBCEC, mRNA and protein expression levels of key enzymes and regulators in cholesterol metabolism were analysed by quantitative real-time PCR and immunoblotting (Figure 17, [169]).

In accordance with the reduced rate of cholesterol biosynthesis observed, HMGCR mRNA expression levels were down-regulated in pBCEC exposed to 24OH-C (by 81%), 27OH-C (by 59%), or cholesterol (by 42%). While the presence of simvastatin led to a drastic up-regulation (by 158%), TO did not significantly influence HMGCR gene expression levels in pBCEC (Figure 17 A). Consistent with the observed effects on mRNA expression levels, HMGCR protein levels (~97 kDa) were also reduced in pBCEC exposed to 24OH-C (by 39%), 27OH-C (by 40%), or cholesterol (by 40%). In contrast, the presence of simvastatin up-regulated HMGCR protein levels by 153%. One possible

explanation for elevated HMGCR mRNA and protein levels in pBCEC after simvastatin treatment is a compensatory mechanism which pBCEC use to stimulate their statin-mediated repressed cholesterol biosynthesis. Interestingly, we also observed an effect of TO treatment which down-regulated HMGCR protein levels by 70% (Figure 17 B).

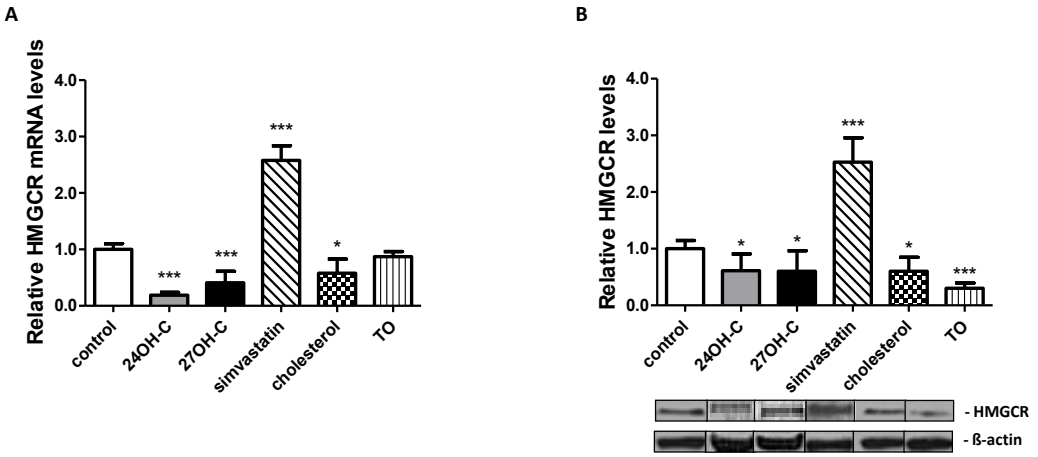

Figure 17: Modulation of HMGCR mRNA and protein levels in pBCEC treated with LXR ligands, cholesterol and simvastatin. Expression analysis of HMGCR gene and protein responsible for cholesterol biosynthesis. **(A)** Quantification of HMGCR mRNA levels analysed by real-time PCR. Cells were treated for 24 h with 10 µM 24OH-C, 10 µM 27OH-C, 5 µM simvastatin, 100 µM cholesterol or 2 µM TO in serum-free medium and quantitative real-time PCR was performed as described in Materials and Methods. HPRT1 mRNA was used for normalization. Data represent mean ± SEM of three independent experiments performed in triplicates. *P < 0.05; ***P < 0.001. **(B)** Quantification of HMGCR protein levels, normalized to the level of β-actin expression. pBCEC were treated as indicated for real-time experiments. Cells were lysed and intracellular APP expression was determined by immunoblotting. Shown is one representative immunoblot for HMGCR and β-actin. Data shown represent mean ± SEM of three independent experiments performed in triplicates. *P < 0.05, ***P < 0.001, [169].

Analysis of ACAT-1 and ACAT-2 expression in pBCEC by comparison of CT values obtained during RTQ PCR analyses, indicated that both genes are expressed at similar levels under basal conditions. None of the treatments altered the mRNA expression levels of ACAT-1 (Figure 18 A, [169]). However, despite the increase in CE formation in

pBCEC, the presence of either of the oxysterols significantly down-regulated gene expression of ACAT-2 after 24 h (by 90% with 24OH-C and by 79% with 27OH-C), whereas neither cholesterol nor TO altered cellular ACAT-2 levels. Elevation of ACAT-2 mRNA levels (by 2.6-fold) was observed in cells treated with simvastatin (Figure 18 B, [169]).

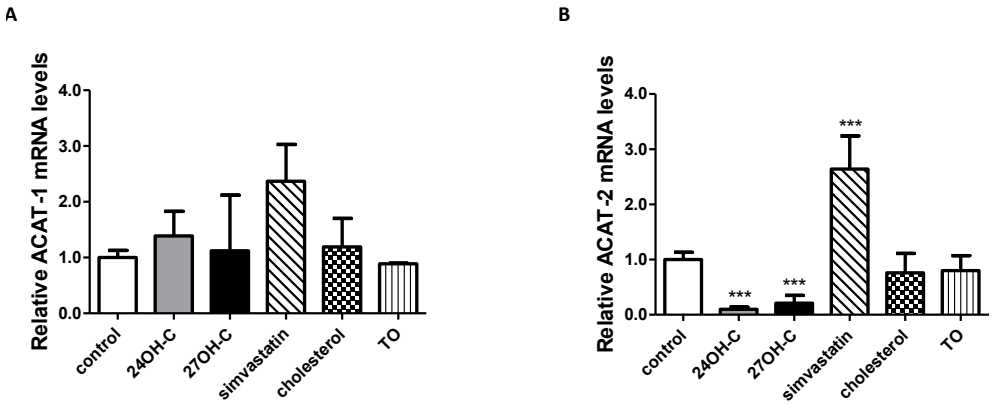

Figure 18: Alterations in ACAT mRNA expression in pBCEC treated with LXR ligands, cholesterol and simvastatin. Quantification of ACAT-1 **(A)** and ACAT-2 **(B)** mRNA levels analysed by real-time PCR. Cells were treated as indicated above and quantitative real-time PCR was performed in triplicates as described in Materials and Methods. HPRT1 mRNA was used for normalization. Data represent mean ± SEM of three independent experiments performed in triplicates. *P < 0.05; ***P < 0.001, [169].

Taken together, HMGCR and ACAT-2, two key genes responsible for cholesterol biosynthesis and esterification, are regulated by oxysterols and/or altered cholesterol levels in pBCEC.

To further examine the effects of LXR ligands, cholesterol, or simvastatin on expression of the direct LXR target gene ABCA1, we analysed ABCA1 mRNA and protein levels in pBCEC. Presence of 24OH-C led to a 1.6-fold induction of ABCA1 mRNA (Figure 19 A, [169]) and a 3.2-fold increase in ABCA1 protein levels (Figure 19 B, [169]). Similarly, the presence of 27OH-C in pBCEC resulted in a 1.4-fold increase of ABCA1 mRNA (Figure 19

A) and a 2.3-fold increase in ABCA1 protein (Figure 19 B). Compared to the oxysterols, the non-steroidal LXR ligand TO was even more potent to stimulate ABCA1 levels in pBCEC. The presence of TO in pBCEC enhanced ABCA1 mRNA expression 2.7-fold (Figure 19 A) and its protein expression 4.1-fold (Figure 19 B). Cholesterol however had no effect on ABCA1 mRNA expression in pBCEC (Figure 19 A), whereas it induced ABCA1 protein 2.2-fold (Figure 19 B). Simvastatin however, led to a significant down-regulation of ABCA1 mRNA levels (by 63%) but did not alter ABCA1 protein levels in pBCEC (Figure 19 B).

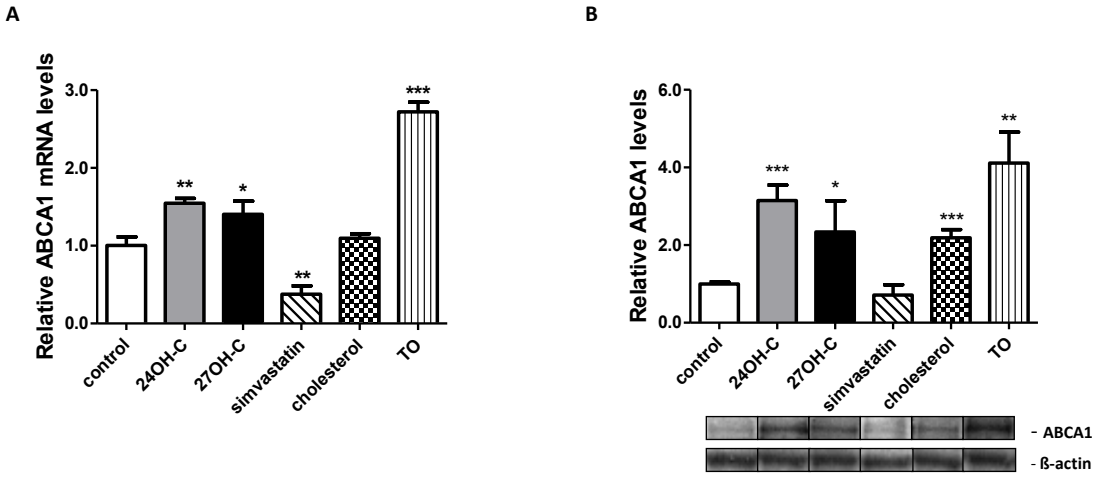

Figure 19: Modulation of ABCA1 mRNA and protein expression in pBCEC treated with LXR ligands, cholesterol and simvastatin. (A) Quantification of ABCA1 mRNA levels analysed by real-time PCR. Cells were treated as indicated above and quantitative real-time PCR was performed in triplicates as described in Materials and Methods. HPRT1 mRNA was used for normalization. Data represent mean ± SEM of two independent experiments performed in triplicates. *P < 0.05; ***P < 0.001. **(B)** Quantification of ABCA1 protein levels, normalized to the level of β-actin expression. pBCEC were treated as indicated for mRNA analysis. Cells were lysed and ABCA1 expression was determined by immunoblotting. Data shown represent mean ± SD of one experiment representative of 3 performed in triplicates. *P < 0.05, **P < 0.01, ***P < 0.001, [169].

HMGCR and ABCA1 are both target genes of SREBP-2, a key-regulator and transcription factor of cholesterol metabolism [170-172]. To further elucidate the molecular mechanisms of altered cholesterol synthesis in pBCEC we analysed SREBP-2 protein and mRNA expression levels. We observed decreased cellular SREBP-2 mRNA levels in cells treated with 24OH-C (by 65%), whereas 27OH-C, cholesterol, or TO did not significantly influence mRNA expression. Simvastatin however, significantly increased the expression of SREBP-2 mRNA expression by 84% (Figure 20 A, [169]).

Accordant to the data obtained from mRNA analyses, premature (p)SREBP–2 protein expression (~120 kDa, Figure 20 B, [169]) was reduced in pBCEC treated with 24OH-C (by 49%) and 27OH-C (by 64%), whereas the presence of simvastatin or cholesterol both led to an increase in pSREBP–2 protein levels, i.e., 1.7-fold with simvastatin and 5.7-fold with cholesterol. Cells exposed to TO exhibited no significant changes although there was a strong trend ($p = 0.065$) for decreased pSREBP–2 protein levels. Treatment with either of the two oxysterols significantly decreased protein expression levels of mature (m)SREBP–2 (~66 kDa, Figure 20 C, [169]) in pBCEC - by 58% for 24OH-C and by 72% for 27OH-C. Exposure to the non-steroidal LXR ligand TO similarly reduced mSREBP–2 protein levels (by 48%) in these cells. In contrast, exposure to simvastatin markedly increased mSREBP–2 protein levels (by 4.3-fold), whereas cholesterol showed no effect.

Taken together these data suggest that alterations of cholesterol biosynthesis in pBCEC treated with LXR agonists, cholesterol or simvastatin was (at least in part) due to modulations of SREBP-2 expression and that these modulations may affect APP expression and secretion.

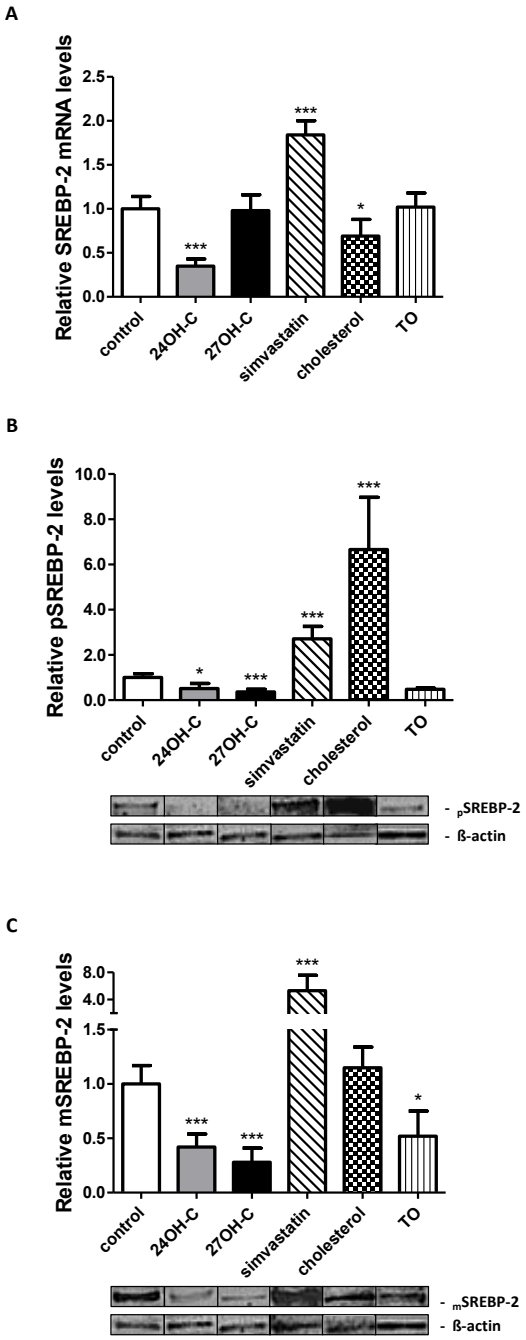

Figure 20: Analysis of SREBP-2 expression levels in pBCEC. Cells were treated for 24 h with 10 µM 24OH-C, 10 µM 27OH-C, 5 µM simvastatin, 100 µM cholesterol, or 2 µM TO in serum-free medium. **(A)** Quantification of SREBP-2 mRNA levels analysed by real-time PCR as described in Materials and Methods. HPRT1 mRNA expression levels were used for normalization. Data represent mean ± SEM of three independent experiments performed in triplicates. ***P < 0.001. **(B)** Quantification of premature (pSREBP-2; **B**) and mature (mSREBP-2; **C**) SREBP-2 protein levels (normalized to β-actin) was performed

by immunoblotting. Cells were lysed and intracellular pSREPB-2 **(B)** and mSREBP-2 **(C)** levels were determined. Shown is one representative immunoblot for pSREBP-2, mSREBP-2 and β-actin. Data shown represent mean ± SEM of three independent experiments performed in triplicates. *P < 0.05, ***P < 0.001, [169].

4.1.6. Both, depleted cellular cholesterol and isoprenoid intermediates are responsible for altered APP processing in pBCEC treated with simvastatin

Statins not only block cholesterol biosynthesis but also isoprenoid formation [173, 174]. To distinguish between cholesterol- versus isoprenoid-mediated effects on APP processing in simvastatin-treated pBCEC [124], we analyzed intracellular Aβ tetramer levels and secreted sAPPα in pBCEC incubated either under serum-free conditions or in medium supplemented with 10% ox serum, in the absence or presence of simvastatin and of mevalonate (Figure 22-Figure 23, [169]). In the presence of serum, cells are able to compensate their statin-blocked cholesterol biosynthesis via uptake of serum-derived cholesterol, but fail to circumvent their blocked isoprenoid formation. Thus, in the presence of serum, simvastatin treated pBCEC are confronted with a normal cholesterol but low isoprenoid environment (Figure 21 B, [169]). In contrast, pBCEC incubated with simvastatin under serum-free conditions not only fail to by-pass their low isoprenoid levels, but also to replenish their cholesterol pools, thus cells are situated in an environment with low cholesterol and low isoprenoid levels (Figure 21 A, [169]).

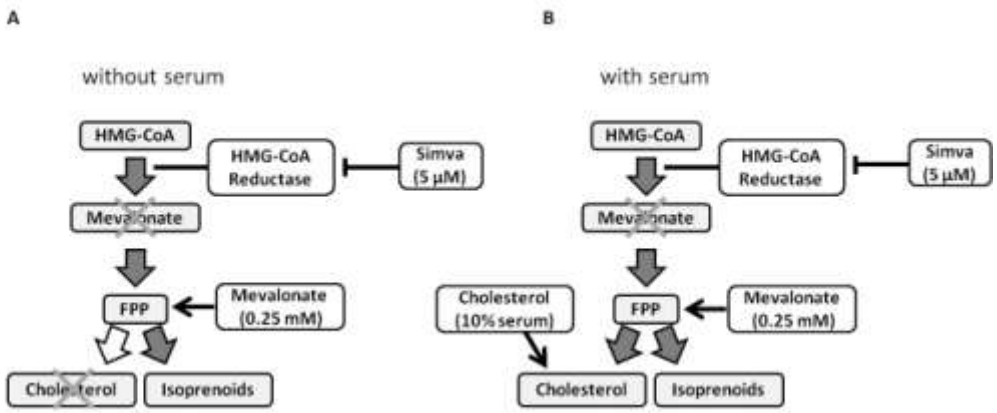

Figure 21: (A,B) Simplified schemes of cellular sterol biosynthesis pathways under the experimental

conditions employed. Farnesyl pyrophosphate (FPP). Cells were treated for 24 h with 5 µM simvastatin (simva) in the presence or absence of 0.25 mM mevalonate in either medium containing 10% Ox serum or serum-free medium, [169].

Exposure of pBCEC to simvastatin reduced cell-associated Aβ tetramer levels by 67% under serum-free conditions (Figure 22 A, [169]), but only by 6% in the presence of serum, respectively (Figure 22 B, [169]). This indicates that cholesterol is required for accumulation of intracellular Aβ oligomers. The addition of mevalonate (0.25 mM) only in part (by 26%) rescued the statin-induced inhibition of Aβ tetramer formation under serum-free conditions (Figure 22 A), but fully (100%) restored Aβ tetramer levels in pBCEC kept in the presence of serum (Figure 22 B). These results together suggest that both decreased cellular cholesterol-, and to apparently lesser extent decreased isoprenoids, are responsible for reducing Aβ oligomer accumulation in pBCEC by simvastatin treatment.

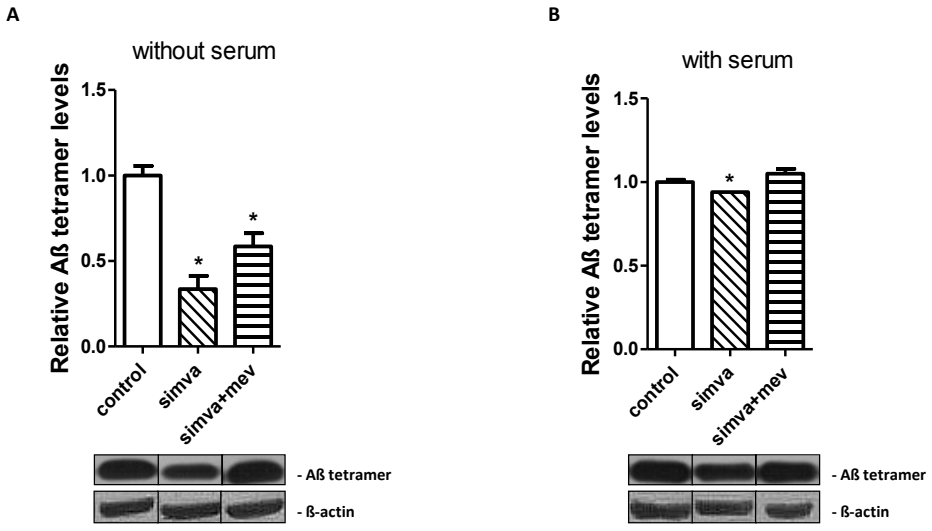

Figure 22: Low cellular cholesterol and low isoprenoid levels are responsible for simvastatin-mediated reduction of Aβ oligomers in pBCEC. Cells were treated for 24 h with 5 µM simvastatin in the presence or absence or 0.25 mM mevalonate in either serum-free medium **(A)** or medium containing 10% ox serum**(B)**. Effects of simvastatin (simva) or simvastatin plus mevalonate (simva+mev) on cellular Aβ tetramer levels in pBCEC in the absence **(A)** or in presence of serum (cholesterol) **(B)**. Cells were lysed and intracellular Aβ tetramer levels were determined by immunoblotting. Shown is one representative

immunoblot for Aβ tetramers and β-actin. Data represent mean ± SD of one experiment representative of 2 performed in triplicates. *P < 0.05, [169].

In parallel to decreased intracellular Aβ tetramer levels, the secretion of sAPPα was enhanced (13.6-fold) in pBCEC treated with simvastatin under serum-free conditions (Figure 23 A, [169]), but as well as in the presence of serum (14.2-fold, Figure 23 B, [169]). The addition of mevalonate completely reversed this effect in the absence (Figure 23 A, [169]) or in the presence of serum (Figure 23 B, [169]). This strongly indicates that inhibition of isoprenoid synthesis is responsible for the simvastatin-mediated modulation of the non-amyloidogenic, sAPPα APP processing pathway in pBCEC.

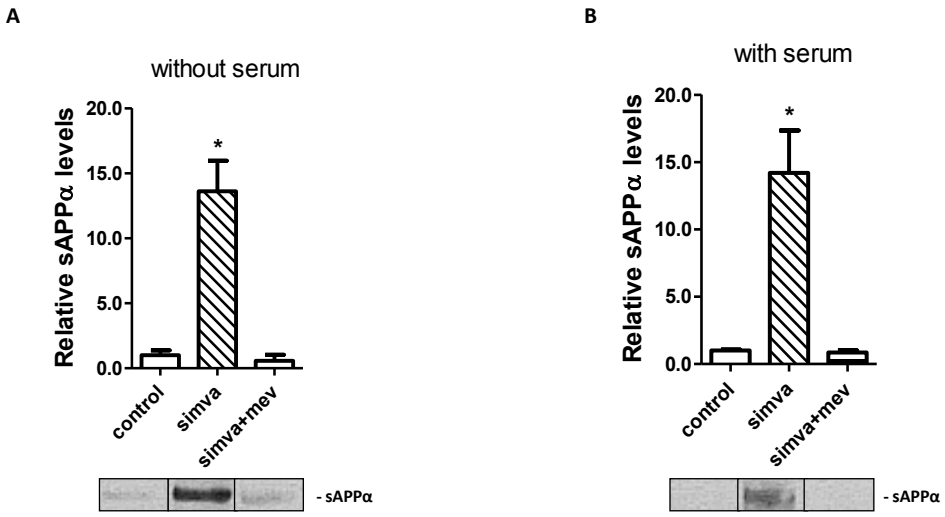

Figure 23: Isoprenoid-mediated effects on APP processing in pBCEC. Effects of simvastatin or simvastatin plus mevalonate on secreted sAPPα levels in pBCEC in the absence **(A)** or in presence **(B)** of serum (cholesterol). Secreted sAPPα was detected by immunoblotting of TCA-precipitated culture media as described in Materials and Methods. Shown are representative immunoblots for secreted sAPPα. Data represent mean ± SD of one experiment representative of 2 performed in triplicates. *P < 0.05, [169].

4.1.7. Polarized pBCEC secrete sAPPα preferentially to the basolateral/brain side of the *in vitro* BBB model

Highly specialized BCEC are the gate-keepers of the brain and represent a polarized interface between the CNS and the peripheral circulation. Therefore, we addressed the question whether or not pBCEC secrete sAPPα in a polarized manner and if treatment with LXR agonists, cholesterol or modulators of cholesterol (and isoprenoid) biosynthesis may affect sAPPα secretion. Cells were grown on Transwell filters and media of both basolateral (mimics the side facing the brain parenchymal tissue) and apical (mimics the side facing the peripheral circulation) compartments were analysed by immunoblotting (Figure 24, [169]). Notably, the amount of sAPPα secreted to the basolateral compartment was 5.9-fold higher as compared to sAPPα detected in the media of the apical compartment. (Figure 24 A). Furthermore, and in line with results obtained with pBCEC monolayers (Figure 13), sAPPα secretion was increased in response to 24OH-C (1.4-fold), 27OH-C (1.5-fold) and simvastatin (1.9-fold). In contrast, incubation of pBCEC with cholesterol led to decreased sAPPα levels (by 20%) in pBCEC. The presence of TO did not alter sAPPα levels secreted by pBCEC (Figure 24 B). These findings clearly show that pBCEC secrete the bulk of sAPPα into the abluminal direction and suggest that oxysterols and simvastatin stimulate non-amyloidogenic processing of APP in polarized pBCEC.

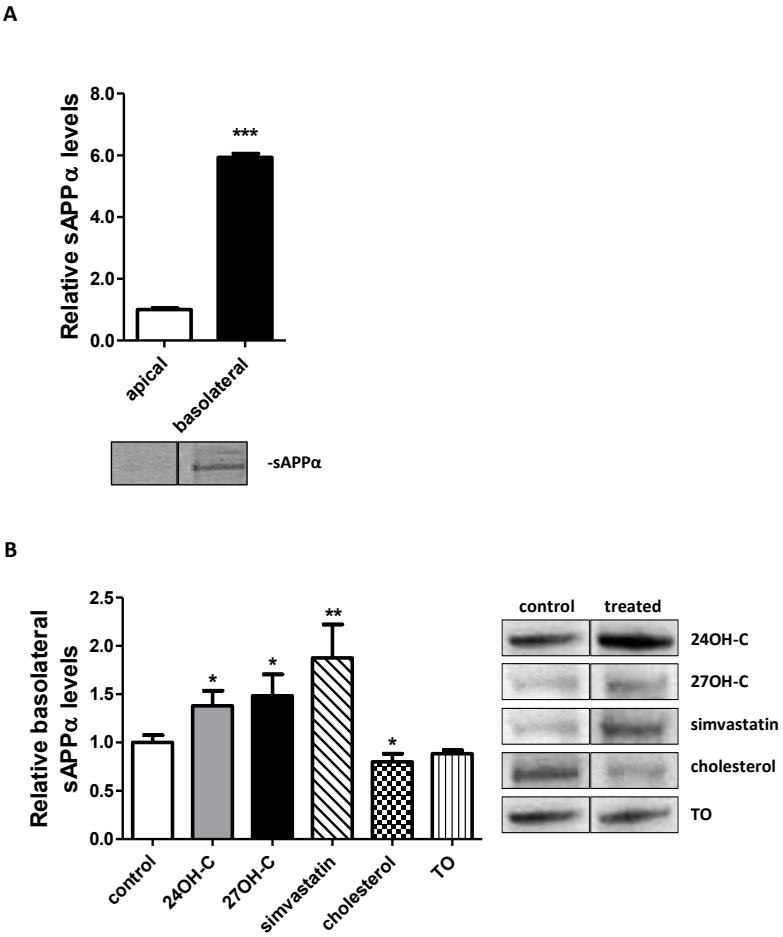

Figure 24: APP expression in an *in vitro* model of polarized pBCEC mimicking the BBB. Immunoblot analysis of sAPPα secreted to the apical or basolateral compartments of pBCEC monolayers grown on Transwell filters for 24 h in serum-free medium was performed as described in Materials and Methods. **(A)** Densitometric evaluation of apical versus basolateral sAPPα secretion. Data shown represent mean ± SD of one representative experiment of 3 performed in triplicates. ***P < 0.001. **(B)** Semiquantitative analysis of sAPPα release into the basolateral supernatants of pBCEC treated for 24 h with 10 µM 24OH-C, 10 µM 27OH-C, 5 µM simvastatin, 100 µM cholesterol, or 2 µM TO in serum-free medium. Secreted APPα was detected by immunoblotting of TCA-precipitated basolateral culture media as described in Materials and Methods. Data represent mean ± SD of one experiment representative of 3 performed in triplicates. *P < 0.05, **P < 0.01, [169].

4.1.8. LXR activation down-regulates expression of inflammatory genes in pBCEC

Since neuroinflammation is another major factor in the etiology of AD, we also examined the mRNA expression levels of inflammatory genes in pBCEC treated with natural and synthetic LXR agonists mRNA (Figure 25, [169]). Both, synthetic and natural LXR agonists significantly decreased transcription of COX2 between 25% (by 27OH-C or TO) and 37% (by 24OH-C) (Figure 25 A). Additionally, TNFα transcription was significantly decreased by TO treatment (by 70%) whereas a slight but non-significant trend towards reduced TNFα mRNA levels in pBCEC treated with 24OH-C and 27OH-C was observed (Figure 25 B). Our data corroborate the hypothesis that LXRs are potent targets for the treatment of AD since they modulate the expression of genes relevant to both cholesterol metabolism and inflammation [175].

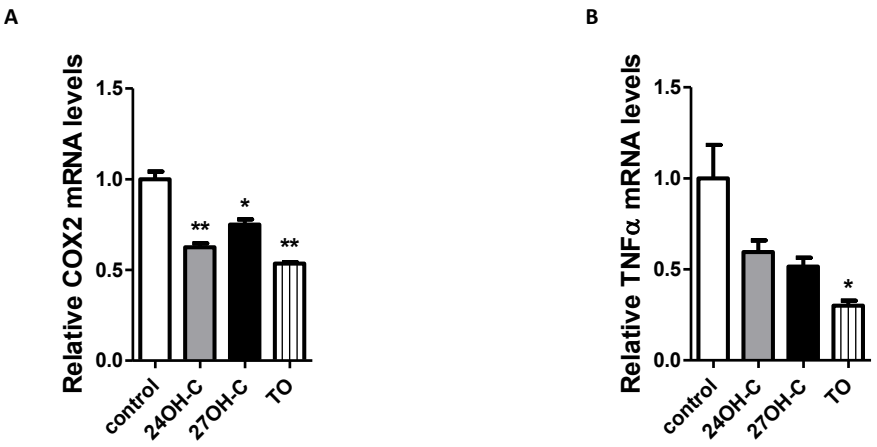

Figure 25: Downregulation of inflammatory genes expressed in pBCEC by LXR agonists. Quantification of COX2 **(A)** and TNFα **(B)** mRNA levels analysed by real-time PCR. Cells were treated for 24 h with 10 µM 24OH-C, 10 µM 27OH-C, or 2 µM TO in serum-free medium and quantitative real-time PCR was performed as described in Materials and Methods. HPRT1 mRNA expression levels were used for normalization. Data represent mean ± SD of one experiment representative of two performed in triplicates. *P < 0.05, **P < 0.01, [169].

4.1.9. Protein kinase C-mediated secretion of sAPPα in pBCEC can be modulated by oxysterols

Since oxysterols have been reported to lower protein kinase C (PKC)-mediated APP secretion in primary cortical neurons [176], we investigated possible effects of PKC activation on APPα secretion in the presence or absence of oxysterols in pBCEC (Figure 26). Activation of PKC by ionomycin drastically increased sAPPα secretion from pBCEC when compared to control cells (Figure 26, by 8.1-fold), whereas a co-incubation with 24OH-C reversed this effect (by 63%). Our data suggest that sAPPα secretion from pBCEC is (at least in part) regulated by PKC and can be modulated by the action of oxysterols.

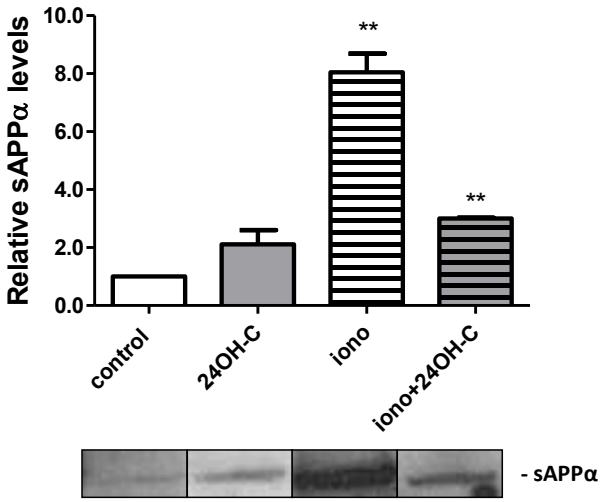

Figure 26: Protein kinase C-mediated sAPPα secretion from pBCEC. Cells were treated for 24 h with 10 µM 24OH-C and for 15 min with 1 µM ionomycin (iono) or DMSO (control) in serum-free medium. SDS-PAGE and immunoblotting for sAPPα was performed as described in Materials and Methods. Data represent mean ± SD of the densitometric evaluation of secreted sAPPα normalized to total cell protein of one experiment representative of two performed in triplicates. **P < 0.01.

4.2. Potential interactions between BBB-derived apo(lipo)proteins and Aβ turnover in BCEC

4.2.10. ApoA-I stimulates sAPPα secretion from pBCEC

The facts that pBCEC actively synthesize apoA-I and its deficiency has been reported to enhance cognitive decline and cerebral amyloid angiopathy (CAA) in an AD mouse model [177], prompted us to examine sAPPα secretion in the absence or presence of exogenous apoA-I (Figure 27). As compared to control cells, apoA-I-treatment (20 µg/ml) significantly increased sAPPα secretion from pBCEC (by 3.2-fold;Figure 27).

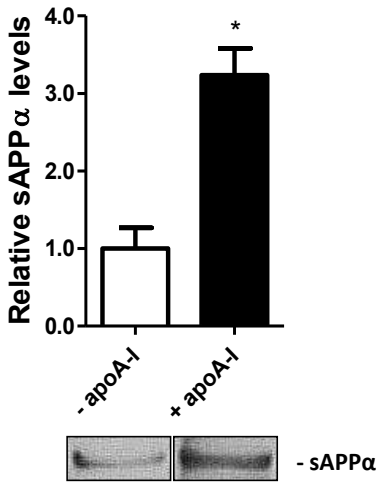

Figure 27: ApoA-I stimulates sAPPα secretion from pBCEC. Cells were treated for 24 h in the absence or presence with 20 µg/ml apoA-I in serum-free medium and immunoblotting for sAPPα was performed as described in Materials and Methods section '3.2.6 SDS-PAGE and immunoblotting' and sAPPα levels were normalized to total cell protein. Data represent mean ± SD of one experiment performed in triplicates. *P < 0.05.

4.2.11. Apolipoprotein profiles in pBCEC supernatants

Previous results of our group describe up-regulated apoA-I levels/secretion by LXR activation together with the up-regulation of ABCA1 in pBCEC and apoA-I/ABCA1-mediated cholesterol efflux, resulting in formation of HDL-like particles at the BBB [76]. To further characterize lipoprotein particles formed by pBCEC, cells were treated in the absence or presence of LXR ligands, simvastatin or cholesterol and density fractions of supernatants were isolated by density gradient ultracentrifugation after 24 h of incubation. Fractions were subjected to tryptic digest and analysis of peptide masses by LC-MS (performed by Dr. Ruth Birner-Gruenberger). Interestingly, we detected apoJ (clusterin) as a major secreted protein in addition to apoA-I, which we (and others [91]) have previously described [76].

To be able to quantify the apolipoproteins, more experiments have to be performed. As can be seen from immunoblotting experiments carried out on density fractions isolated from pBCEC supernatants (Figure 28), the majority of apoJ (Fig. 27 A) was detected in fraction 1 (mean density Ω= 1.0 g/ml), corresponding to plasma VLDL and LDL, a minor amount was also present in fraction 3 which corresponds to the density of plasma HDL particles (Ω= 1.10 g/ml). Interestingly, exclusively in the presence of cholesterol (100 µM), apoJ was detected in fraction 2 corresponding to the LDL density range (Ω= 1.05 g/ml).

In accordance with previous findings [76], apoA-I was detected in density fraction 3 - which corresponds to the density of plasma HDL particles, and 4 - lipid-free apoA-I (Figure 28, C). Results from this single set of experiments did not show obvious effects of LXR ligands (24OH-C, Fig. 27C) on apoA-I expression, however, we know from previous studies that LXR activation induces secretion of apoA-I by pBCEC (detected by immunoblotting; [76]).

Complementary immunoblot analysis of APP (Fig. 28, B) in pBCEC-derived density fractions revealed that sAPPα is present mainly in density fraction 3, a minor amount was also immunodetected in density fraction 1 (control conditions). The presence of cholesterol and 24OH-C changed the APP expression pattern. APP arose in fractions 1,

2 and 4 in pBCEC treated with 24OH-C (no signal in controls). This is in line with results obtained for APP protein expression levels and secretion in pBCEC monolayers (6-wells) treated with 24-OH-C (Figure 11 and Figure 13) and indicates that the oxysterol stimulates APP protein expression/secretion. Incubation of pBCEC with cholesterol also stimulated APP secretion in fractions 1 and 2 but failed to induce secretion of APP to fraction 4. This partly reflects our results obtained in pBCEC grown as monolayers (multiwell plates) where we found increased APP expression, but no significant alterations in APP secretion (Figure 11 and Figure 13). Interestingly, the expression pattern of apoJ and APP over-lapped: under control conditions and in the presence of 24OH-C fraction 1 and 3 contained both, apoJ and APP, and in the presence of cholesterol apoJ and APP shifted to lower density fractions 1, 2, and 3 (Figure 28, A and B).

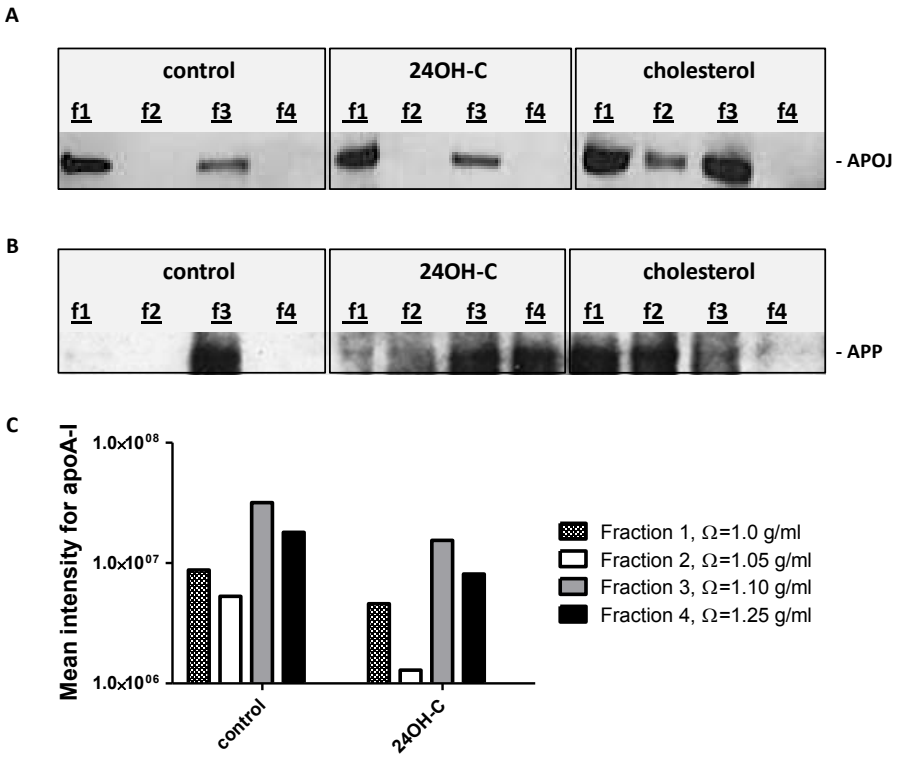

Figure 28: ApoJ, APP and apoA-I expression in lipoprotein density fractions secreted from pBCEC. Cells were grown on 10 cm petri dishes and incubated for 24 h with 10 µM 24OH-C or 100 µM cholesterol in serum-free medium. Lipoprotein fractions were isolated, proteins TCA precipitated, separated by SDS-PAGE and immunoblotted for apoJ (A) and APP (B) as described in Materials and Methods section '3.2.6

SDS-PAGE and immunoblotting'. Graph represents one experiment performed in duplicates. (C) Cells were treated as described for A. Lipoproteins were isolated from cellular supernatants by density gradient ultracentrifugation, proteins subjected to tryptic digest, and peptide masses analyzed by LC-MS analysis by our collaborator Dr. Ruth Birner-Gruenberger. Data shown represent mean peptide spectra intensities of apoA-I of one experiment performed in duplicates.

Since we found that apoJ and APP protein expression in lipoprotein density fractions over-lapped (Figure 28, A and B), and apoJ was reported to localize around senile plaques [153] and to transport Aβ [96, 157], to examine possible interaction/binding of the two proteins we immunoprecipitated apoJ and APP of pBCEC culture supernatants (Figure 29). Therefore, pBCEC were incubated for 24 h in serum-free medium, supernatants were incubated with magnetic beads carrying cross-linked antibodies specific for apoJ or APP. After several washing steps, bound antigens were gently removed from their capturing antibodies and samples were further analyzed via SDS-PAGE and immunoblotting (for further details please refer to Materials and Methods section '3.2.5 Immunoprecipitation'). For detection via immunoblot we used a primary antibody specific for apoJ and expected signals in both samples: samples precipitated with the apoJ-specific and APP-specific antibody. In parallel, to our immunoprecipitated samples, as apoJ-positive control, we analyzed human serum (5 µl of a 1:200 dilution). Figure 29, B shows that the apoJ immunoprecipitate displays the exact same pattern as the positive control, Figure 29, A. Interestingly, we detected an additional band > 80 kDa (Figure 29, B *) in the apoJ immunoprecipitate. The analyses of the APP immunoprecipitate revealed the presence of a band of same size > 80 kDa (Figure 29, C *) and additionally the most prominent band of apoJ (~55 kDa). Our data, so far, suggest that apoJ and APP interact since they co-localize in the same lipoprotein density fractions and they appeared to physically interact (co-immunoprecipitation).

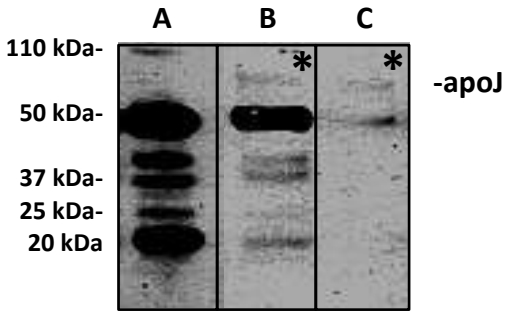

Figure 29: ApoJ binds APP/Aβ in pBCEC. Cells were grown on petri dishes and incubated for 24 h in serum-free medium. Immunoprecipitation was performed as described in Materials and Methods section '3.2.5 Immunoprecipitation' using antibodies specific for apoJ and APP. Immunoprecipitates were further analyzed by immunoblotting as described in Materials and Methods section '3.2.6 SDS-PAGE and immunoblotting'. (A-C) Immunoblot of apoJ protein. (A) Human serum, positive control for apoJ. (B) ApoJ immunoprecipitate – beside the 'typical' pattern of apoJ (compared to serum sample) an additional band at > 80 kDa appeared. (C) APP immunoprecipitate – a band at > 80 kDa represents APP, the lower band at ~55 kDa shows apoJ. *Band > 80 kDa represents APP.

To further characterize regulation of ApoJ protein and mRNA expression by LXR ligands, cholesterol and simvastatin, immunoblotting and quantitative real-time PCR were performed. We detected a 2.3-fold up-regulation of intracellular apoJ protein levels in pBCEC (Figure 30, A), whereas supernatant levels of both apoJ subunits (α- and β-chain) were markedly decreased: by 84% in cells treated with 24OH-C, by 99% in TO-treated cells, and by 65% in cells incubated with simvastatin. In contrast, cholesterol did not show any effects on the secreted amounts of ApoJ. (Figure 30, B).

ApoJ mRNA levels in pBCEC treated with LXR ligands or cholesterol were significantly decreased (Figure 31) with TO being the most potent agent to decrease ApoJ mRNA levels (67% reduction), followed by the natural LXR ligand 24OH-C (54% reduction) and cholesterol (53% reduction).

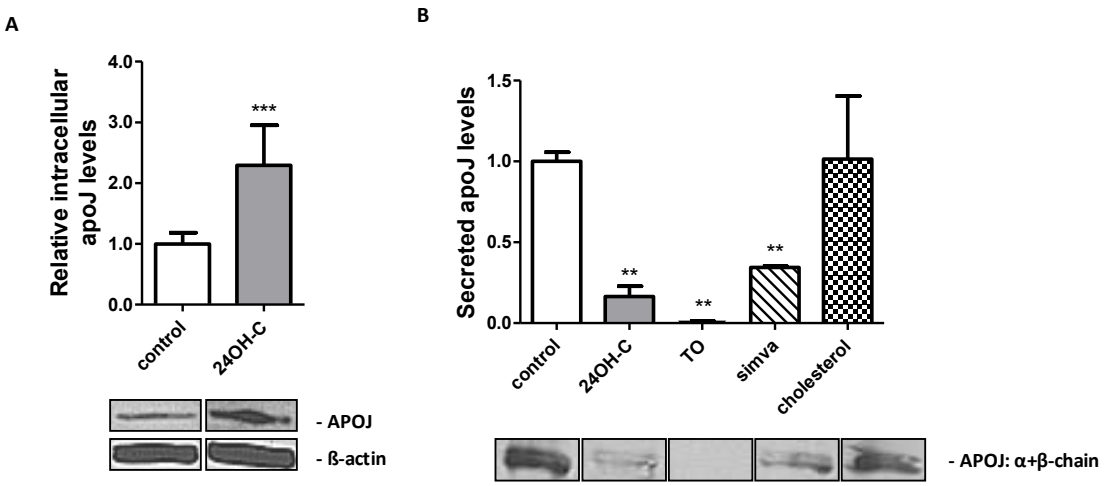

Figure 30: ApoJ protein expression levels are modulated upon LXR-activation and y simvastatin treatment in pBCEC. Cells were treated for 24 h with 10 µM 24OH-C, 2 µM TO, 5 µM simvastatin or 100 µM cholesterol in serum-free medium and immunoblotting for intracellular (A) and secreted apoJ (B) was performed as described in Materials and Methods section '3.2.6 SDS-PAGE and immunoblotting'. (A) Intracellular apoJ levels in pBCEC rise after stimulation with 24OH-C. Data represent mean ± SD of one experiment representative of two performed in triplicates. *** $P < 0.001$. (B) Decreased secreted ApoJ levels in pBCEC after LXR-activation or incubation with simvastatin. Data represent mean ± SD of one representative experiment performed in duplicates. ** $P < 0.01$.

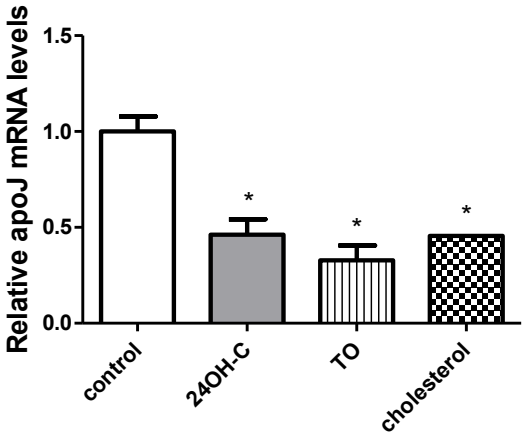

Figure 31: ApoJ mRNA expression is down-regulated by LXR-ligands or cholesterol treatment. Cells were treated for 24 h with 10 µM 24OH-C, 2 µM TO or 100 µM cholesterol in serum-free medium and real-time analysis for ApoJ mRNA expression was performed as described in Material and Methods section '3.2.6 SDS-PAGE and immunoblotting'. HPRT1 mRNA expression levels were used for

normalization. Data represent mean ± SD of one experiment representative of two performed in triplicates. *P < 0.05.

Our data confirm and indicate that pBCEC express and secrete apoA-I and apoJ, respectively, and that expression and secretion of apoA-I/apoJ can be modulated by LXR activation and/or altered cholesterol homeostasis.

4.2.12. Transport of radiolabeled Aβ peptide across the BBB *in vitro*

To investigate if pBCEC are capable of transporting 'exogenous' Aβ and to simulate the BBB *in vitro*, a Transwell system (Vitaris AG) was used. To obtain a polarized, tight monolayer, pBCEC were cultured on porous membrane filters that allow separate access to the apical (representing the 'blood' side) and the basolateral (representing the 'brain parenchymal' side) compartment. Tight junction formation upon the addition of hydrocortisone-containing medium increases the electrical resistance which is monitored using an Ohmmeter (Materials and Methods section '3.2.3 Transwell experiments' and [76]). Radiolabeled $A\beta_{1\text{-}40}$ peptide (^{125}I- Aβ) was added either to the basolateral or apical compartment. Time-dependent transport of Aβ was determined by counting aliquots of the culture media.

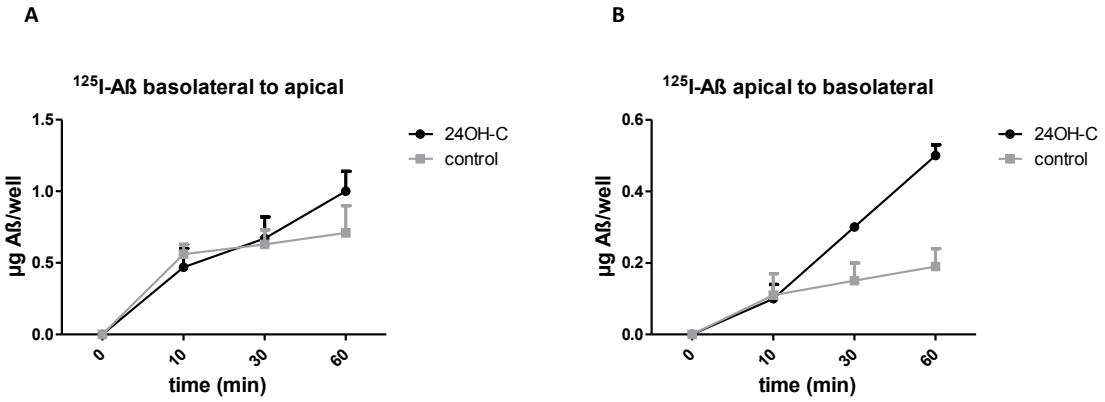

Figure 32: Transport of ^{125}I- Aβ in pBCEC. pBCEC were cultured on Transwell in the absence or presence of 10 µM 24*(S)*OH-cholesterol for 16 h. Subsequently, ^{125}I- Aβ (0.5 µg/ml) was added to the basolateral (A), or apical (B) compartment. At the indicated time points aliquots of the media were counted on a gamma counter. Results represent means ± SD from one representative experiment performed in triplicates.

Our initial experiments showed that Aβ transport across pBCEC takes place in both directions, from apical to basolateral and vice versa (Figure 32, A&B) and indicate that LXR activation by 24*(S)*OH-cholesterol may enhance the transport of Aβ. These results have to be confirmed during future experiments.

4.2.13. Transport of radiolabeled ApoA-I across the BBB *in vitro*

From previous and the present studies we know that pBCEC express and secrete apoA-I [76]; Figure 28, C). To examine the transport of exogenous apoA-I across polarized pBCEC, cells were cultured on Transwell filters and increasing concentrations of ^{125}I-apoA-I were added to the apical media. At indicated time points aliquots from the basolateral compartment were counted to determine apoA-I transcytosis (Figure 33, A). Up to approx. 100 ng of apoA-I were transported across the monolayer at 3 h of incubation and the highest concentration of apoA-I used, which corresponds to approx. 1% of apically added apoA-I. In contrast, cell-associated activity at the end of incubation accounted for only up to 0.1% of total radioactivity (Figure 33, B).

During tracer assays we could observe ^{125}I- Aβ transport across polarized pBCEC in both directions (Figure 32). Additionally we were able to show that ^{125}I-apoA-I undergoes dose- and time-dependent transcytosis across pBCEC from the apical to the basolateral compartment and vice versa (Figure 33 and Figure 34). Preliminary findings indicate that the presence of HDL_3 might support the transport of apoA-I across the monolayer. In future experiments we will investigate potential interactions of apoA-I and HDL with Aβ-transport in this *in vitro* BBB model and we will further analyse effects of LXR activation and/or cholesterol treatment in these processes.

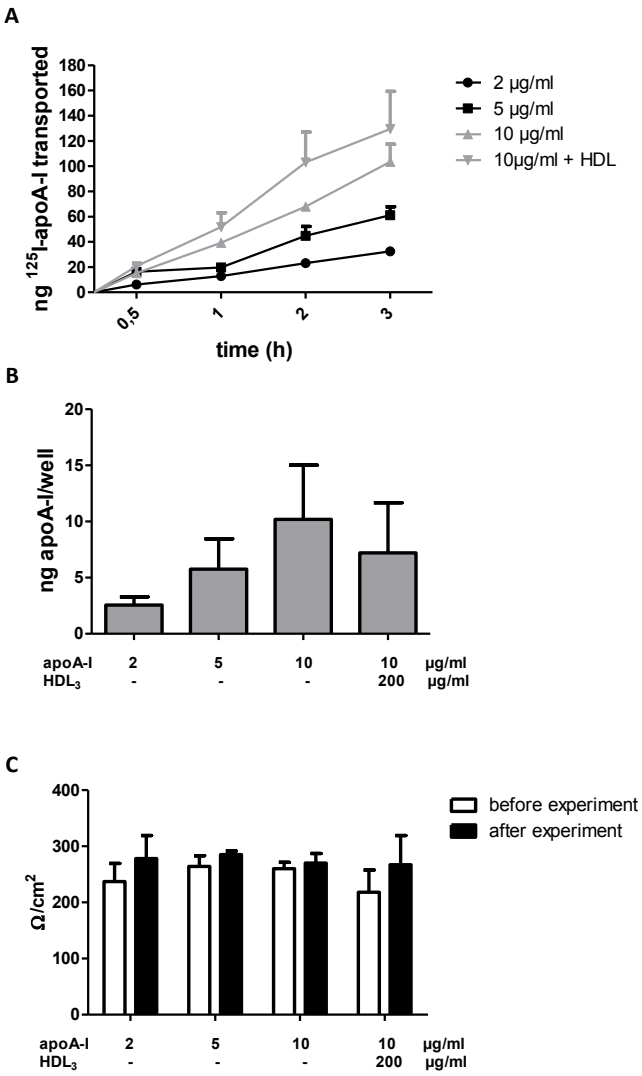

Figure 33 Time- and dose dependent transport of apoA-I across pBCEC (apical to basolateral). (A) pBCECs were cultivated in 12-well Transwells and were incubated apical with ^{125}I-apoA-I (1 - 5 µg/well = 2 - 10 µg/ml) +/- HDL_3 (100 µg/well (= 200 µg/ml)). ApoA-I has been iodinated on the same day. At indicated time points 400 µl aliquots from the basolateral compartment were counted on a gamma counter and were replaced with fresh medium. **(B)** After 3 h cells were washed with PBS and lysed in 0.3 N NaOH o/n to determine ng apoA-I/mg cell protein. **(C)** TEER values were determined at the beginning and the end of the experiment as described under Materials and Methods section '3.2.3 Transwell experiments'.

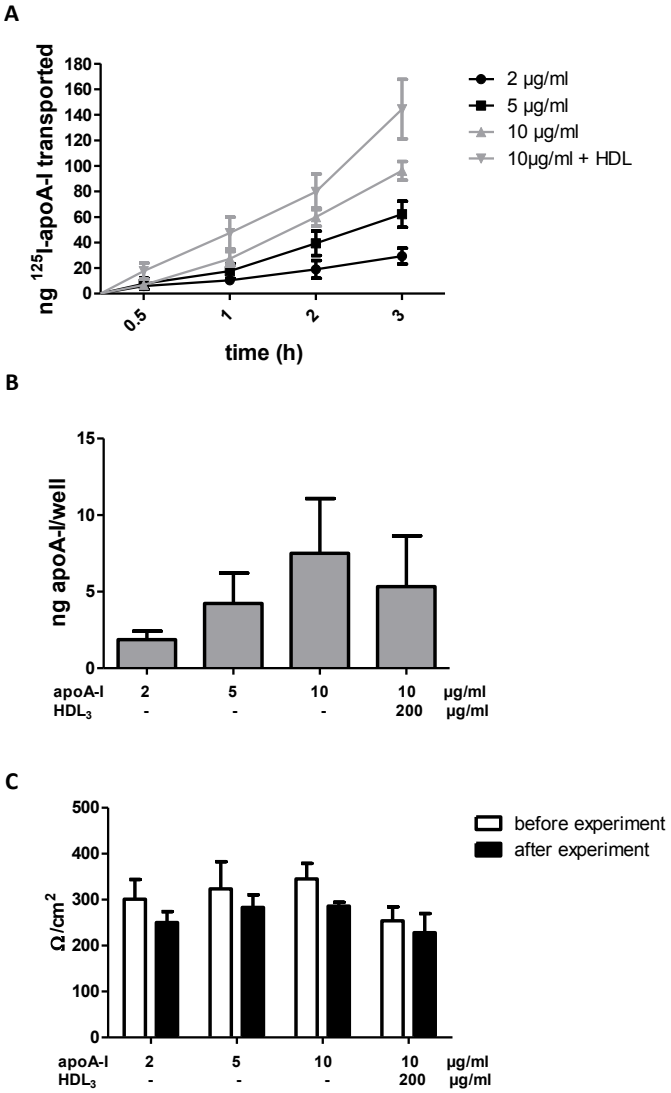

Figure 34: Time- and dose dependent transport of apoA-I across pBCEC (basolateral to apical). (A) pBCECs were cultivated in 12-well Transwells and were incubated basolateral with ^{125}I-apoA-I (1 - 5 µg/well = 2 - 10 µg/ml) +/- HDL_3 (100 µg/well (= 200 µg/ml)). ApoA-I has been iodinated on the same day. At indicated time points 400 µl aliquots from the apical compartment were counted on a gamma counter and were replaced with fresh medium. **(B)** After 3 h cells were washed with PBS and lysed in 0.3 N NaOH o/n to determine ng apoA-I/mg cell protein. **(C)** TEER values were determined at the beginning and the end of the experiment as described under Materials and Methods section '3.2.3 Transwell experiments'.

4.2.14. Binding and uptake of Alexa-Aβ at the BBB *in vitro*

During experiments described above we observed a time-dependent transport of [^{125}I]-Aβ across pBCEC grown on Transwell filter inserts (Figure 32). Additional experiments should clarify which receptors might be involved in this transport process. Preliminary data obtained during FACS experiments (performed in co-operation with Gunther Marsche and Michael Holzer, Institute of Experimental and Clinical Pharmacology, Medical University of Graz) on BW transductants (B – lymphocytes which over-express certain types of scavenger receptors) have provided evidence for two scavenger receptors to be able to bind Alexa-Aβ (Figure 35), namely scavenger receptor expressed on endothelial cells (SREC-I) and scavenger receptor A1 (SR-AI).

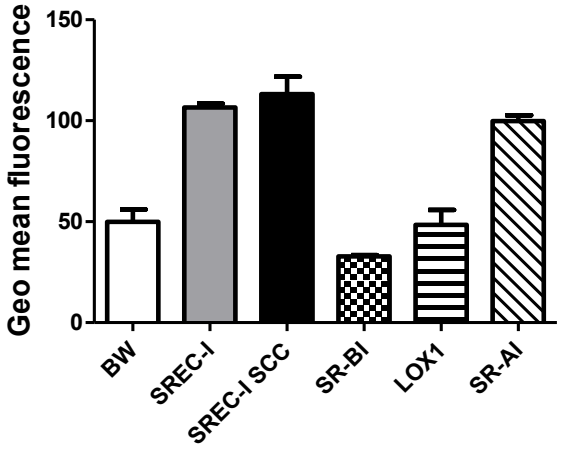

Figure 35: SREC-I and SR-AI are able to bind Aβ in BW transductants. BW cells were grown on 96 well plates, incubated with fluorescently-labeled Aβ and analyzed using a flow cytometer. Graph bars show the geo mean of fluorescence ± SD of one single measurement performed in duplicates (performed by Michael Holzer).

Analysis of SREC-I, SR-AI, RAGE and LPR1 mRNA levels, candidate or known receptors for Aβ (Figure 36) was performed via quantitative real-time PCR as indicated in Materials and Methods. We found that pBCEC do express SREC-I, RAGE and LRP1 but they do not express SR-AI.

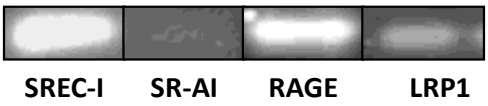

Figure 36: pBCEC express SREC-I, RAGE and LRP1 but not SR-AI. Cells were grown on 6 well plates in serum-free medium for 24 h. Cells were harvested and real-time for SREC-I, LPR1 and RAGE was performed as described in Materials and Methods. Shown is one representative separation of PCR products on a 1% agarose gel.

Since pBCEC only express SREC-I, but not SR-AI (Figure 37), we next investigated binding and uptake of fluorescently labeled Aβ (25µg/ml) in BW- SREC-I cells in the absence or presence of fucoidan (50µg/ml), a known inhibitor of class A macrophage scavenger receptors (Figure 37). We found a reduction in Aβ binding (4°C) by BW cells (by 75%) and by SREC-I overexpressing BW cells (by 85%) and in Aβ uptake (37°C) by BW cells (by 81%) and by SREC-I overexpressing BW cells (by 67%).

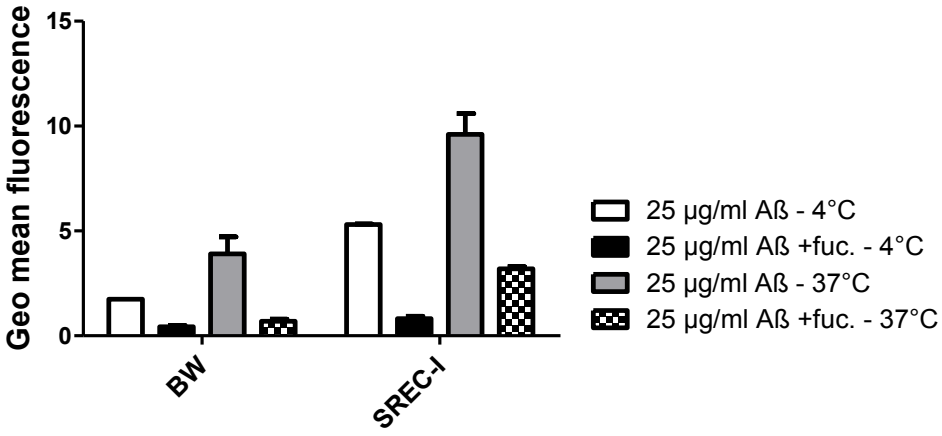

Figure 37: Binding and uptake of Aβ by BW transductants is inhibited by fucoidan. BW cells were grown on 96 well plates, incubated with Alexa-Aβ (25 µg/ml) in the absence or presence of fucoidan (50 µg/ml) and analyzed using a flow cytometer. Graph bars show the geo mean fluorescence ± SD of one single measurement performed in duplicates (performed by Michael Holzer).

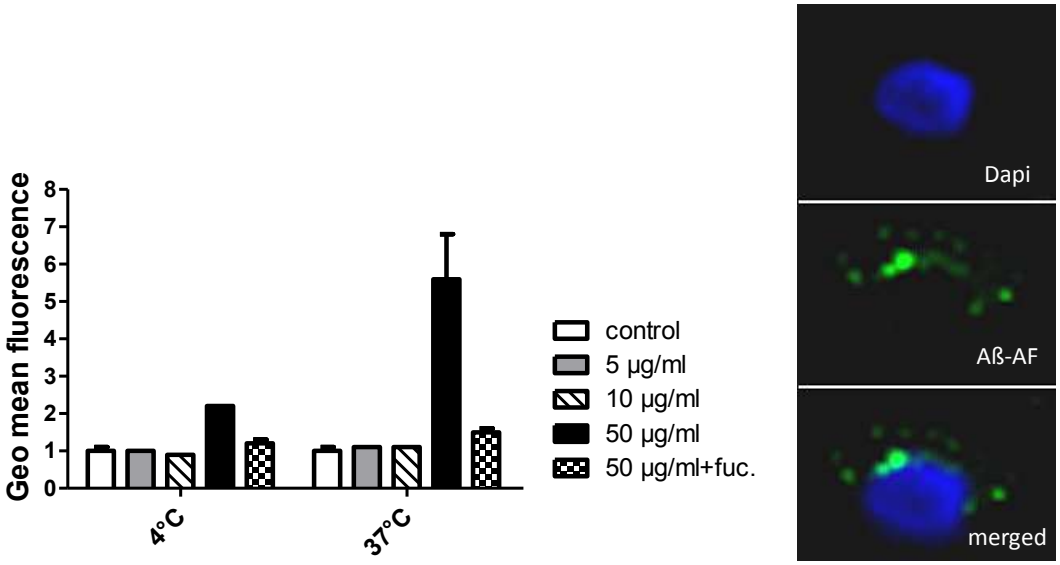

Figure 38: Binding and uptake of Alexa-Aβ peptide to pBCEC is blocked by fucoidan. (Left panel) Cells grown on 48 well plates were incubated with 0-50 µg/ml fluorescently-labeled $A\beta_{1-40}$ peptide for 2 h at either 4°C (binding) or 37°C (uptake). Cells were then harvested, washed, fixed an analysed using a flow cytometer. Data shown represent geo mean fluorescence ± SD of one single experiment performed in duplicates. **(right panel)** Cells were grown on collagen-coated FlexiPerm slides and incubated for 2 h at 37°C with Alexa 488-labeled $A\beta_{1-40}$ peptides (50 µg/ml). Then cells were washed, fixed with acetone and mounted with Vectashield containing Dapi. Visualization was carried out using a Leica fluorescence microscope (40x magnification). Dapi, Dapi-staining of cell nucleus; Aβ-AF, fluorescent signal of bound/internalized Aβ; merged, overlay of Dapi and fluorescent picture.

To further approve involvement of SREC-I, Aβ binding in BW cells and in BW cells overexpressing SREC-I was examined in the absence or presence of SREC-I antibody. Interestingly we found a drastically decreased Aβ binding (by 84%) in BW cells overexpressing SREC-I in the presence of inhibiting SREC-I antibody Figure 39).

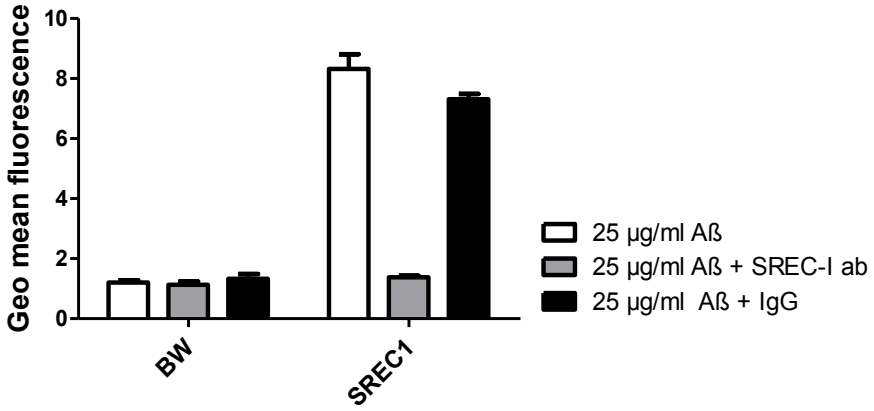

Figure 39: Binding of Aβ peptide is blocked by SREC-I antibody-inhibition. BW cells grown on 48 well plates were incubated with 25 µg/ml fluorescently-labeled $A\beta_{1-40}$ peptide for 1 h at 4° in the presence or absence of SREC-I antibody (10 µg/ml). Cells were then harvested, washed, fixed an analysed using a flow cytometer. Data shown represent geo mean fluorescence ± SD of one single experiment performed in duplicates (performed by Michael Holzer).

Within further experiments we reduced the amount of fluorescently-labeled Aβ to 15 µg/ml and increased the sample size (Figure 40). We observed similar results as for the experiments performed with 50 µg/ml Aβ: pBCEC bind (4°C) and actively internalize Aβ peptides (37°C). Interestingly, the addition of fucoidan only significantly inhibited Aβ internalization (by 36%) but did not influence the binding of Aβ by pBCEC.

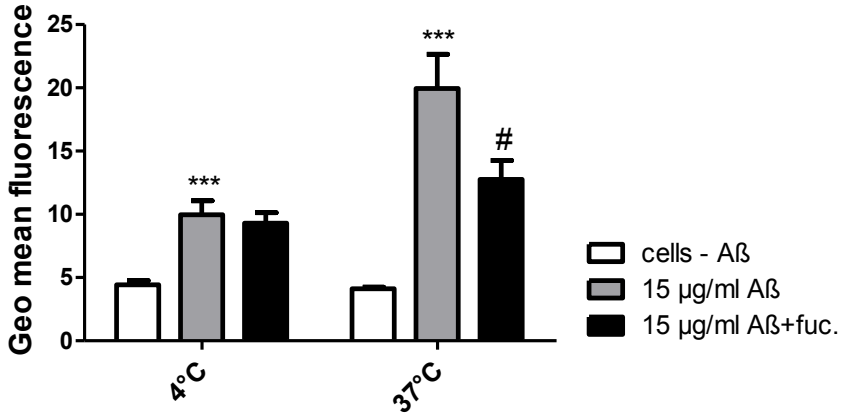

Figure 40: Binding and uptake of Aβ peptide to pBCEC is blocked by fucoidan. Cells grown on 48 well plates were incubated with 15 µg/ml fluorescently-labeled $A\beta_{1-40}$ peptide for 2 h at either 4°C (binding) or 37°C (uptake). Cells were then harvested, washed, fixed an analysed using a flow cytometer. Data

shown represent geo mean fluorescence ± SEM of 2 independent experiments performed in triplicates *** P < 0.001 (compared to cells – Aβ), # P < 0.01 (compared to 15 µg/ml Aβ).

However, in contrast to drastically decreased Aβ binding in BW cells overexpressing SREC-I in the presence of SREC-I antibody (Figure 39), Aβ binding in pBCEC did not change in the presence of SREC-I antibody (Figure 41). This may indicate that other Aβ peptide receptors do prevail.

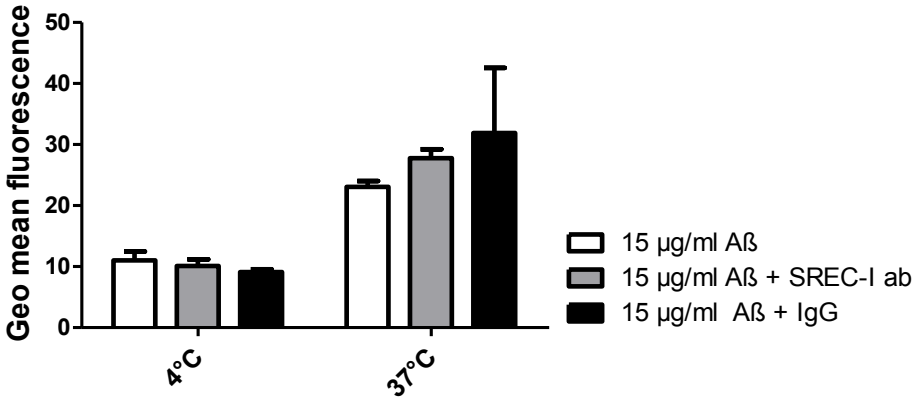

Figure 41: Binding of Aβ peptide in the presence of SREC-I antibody in pBCEC. Cells grown on 48 well plates were incubated with 15 µg/ml fluorescently-labeled $A\beta_{1\text{-}40}$ peptide for 2 h at either 4° or 37°C in the presence or absence of SREC-I antibody (10 µg/ml). Cells were then harvested, washed, fixed an analysed using a flow cytometer. Data shown represent geo mean fluorescence ± SD of one single experiment performed in triplicates.

Our results show that addition of the inhibitor fucoidan significantly lowers the uptake and binding of Aβ in BW cells overexpressing SREC-I and pBCEC, suggesting that SREC-I may represent a novel candidate-receptor for Aβ at the BBB. To further confirm which receptors are responsible for the transport of Aβ at the BBB, RNAi and further antibody inhibition experiments in pBCEC are crucial.

5. Discussion

5.1. Characterization of APP and cholesterol metabolism in BCEC

There is striking evidence that cerebral Aβ production and cholesterol homeostasis are closely linked. Not surprisingly various studies have concentrated on the relationship between APP processing and the effects of cholesterol and/or LXR activation in cellular models overexpressing APP, in neurons, and astrocytes, as well as in various mouse models of AD [178-180]. The involvement of the BBB in these processes is just one open question in the etiology of neurodegenerative diseases such as AD. BBB dysfunction has been discussed as one possible explanation for hypercholesterolemia-induced Aβ production in rabbits and mouse models of AD [97-101]. In addition, enhanced clearance of Aβ to peripheral circulation has been suggested as one pathway mediating the protective effects of statins in AD [181].

The first goal of the present *in vitro* study was to determine the contribution of BCEC to APP synthesis and processing and to clarify the impact of pharmacological antagonists of cholesterol biosynthesis on APP processing. We focused on APP biosynthesis and processing in response to exogenously supplied synthetic (TO) and natural (24 and 27OH-C) LXR agonists, simvastatin, and cholesterol. Our study strengthens the concept of an active contribution of the cerebrovasculature [182] in AD for the following reasons: i) BCEC express all key mRNAs that are involved in APP processing, i.e. α-, β-, and γ- secretases; ii) we show that pBCEC synthesize APP, sAPPα, and Aβ, and iii) our data illustrate that inhibition of *de novo* cholesterol biosynthesis by LXR ligands, the HMGCR inhibitor simvastatin, and exogenously supplied cholesterol are effectors of APP processing in BCEC. In light of the huge surface area of the cerebrovasculature (approx. 20 m^2) this might be of therapeutic importance: The apical side of pBCEC is in constant contact with the peripheral circulation and could thereby represent a compartment that is better accessible to targeted interventions than the isolated deeper regions of the brain.

In line with previous reports [35, 123, 183, 184] we demonstrate the expression of α, β and γ-secretase in pBCEC. In agreement with results obtained in APP-overexpressing HEK cells [118], the non-amyloidogenic α-secretase pathway is most prevalent in pBCEC. The majority of secreted sAPPα was detected in the basolateral compartment, indicating that pBCEC-derived sAPPα could exert neurotrophic and neuroprotective effects [178, 180] in deeper regions of the brain. In contrast to sAPPα, sAPPβ and Aβ was much less abundant. Of note, a remarkable portion of Aβ oligomers was detected intracellularly as described until now only for neuronal and glial cells [10].

Moreover, our data illustrate for the first time that oxysterols (24OH-C and 27OH-C), the non-steroidal LXR ligand TO901317 (TO), cholesterol and the HMG-CoA reductase inhibitor simvastatin can influence APP processing in the cerebral microvasculature. This is of potential physiological importance since BCEC *in vivo* are exposed to plasma cholesterol, pharmacological agonists, statins and oxysterols that 'diffuse' across the BBB from brain to blood (i.e. 24OH-C) or vice versa (i.e. 27OH-C). In detail, we found that 24OH-C and 27OH-C as well as TO, cholesterol and simvastatin led to an increase in total brain endothelial APP protein levels without significantly altering APP mRNA expression, emphasizing that the changes observed were only related to changes on the post-translational level. Concordant with our findings, it has been reported in human neuroblastoma SH-SY5Y and in CHO cells stably expressing human APP that oxysterols can increase intracellular APP protein levels [185, 186]. Our findings that simvastatin treatment enhanced intracellular APP levels in pBCEC are in line with those reporting an accumulation of APP in mouse Na2 neuroblastoma cells and APPsw-293 cells, both postulating inhibition of protein isoprenylation as the responsible mechanism [124, 126]. In agreement with results reported by Bodovitz and Klein, in APP stably transfected HEK 293 cells [118], we also detected elevated mature and immature APP protein levels in pBCEC treated with cholesterol. Our finding that in addition to oxysterol agonists, also the non-steroidal LXR agonist TO901317 elevated intracellular APP protein levels in pBCEC, suggests that LXR activation is involved.

Concomitant with the enhanced full-length APP protein levels we observed decreased Aβ oligomer levels in pBCEC exposed to synthetic and endogenous LXR ligands, simvastatin or cholesterol. Accordant with reduced Aβ oligomer levels, mRNA levels of the β-secretase BACE1 were also decreased in the presence of oxysterols, TO, or simvastatin, suggesting that pBCEC in the presence of LXR agonists or HMG-CoA reductase inhibitors favour non-amyloidogenic cleavage events. Further analyses of the mechanism(s) underlying reduced Aβ oligomer levels revealed that both low cholesterol and isoprenoid levels down-regulated Aβ oligomer formation in simvastatin-treated pBCEC.

Accordant with reduced β-secretase cleavage products, the amount of sAPPα secreted by pBCEC incubated with simvastatin was enhanced. Interestingly, this phenomenon seemed to be caused by decreased levels of cellular isoprenoid intermediates in the cholesterol biosynthesis pathway and independent of cholesterol depletion itself. In parallel, and only by simvastatin treatment, ADAM10 transcription was enhanced in pBCEC, indicating a direct regulatory effect of HMG-CoA reductase inhibitors on the α-secretase pathway to occur, in line with previous reports [125]. Our findings of significantly increased amounts of secreted APPα upon incubation with 24OH-C or 27OH-C, suggest that regulatory effects of oxysterols are beneficial against Aβ peptide generation, as well. Similar reports refer to enhanced sAPPα secretion in human neuroblastoma cells treated with 24OH-C, but not with 27OH-C [186, 187]. The fact that the presence of the non-steroidal LXR ligand TO901317 also decreased Aβ oligomer levels in pBCEC, indicates the involvement of LXR activation in APP processing. Several *in vivo* and *in vitro* studies support this suggestion, since APP overexpressing CHO-, and mouse neuroblastoma cells treated with TO showed similar Aβ-reducing effects [130, 132]. AD mice treated with TO establish reduced total cerebral Aβ levels and improved cognitive performance [132, 188]. Further strong support for a beneficial role of LXR activation during AD development/pathogenesis comes from reports demonstrating enhanced senile plaque formation in AD mice lacking LXRs [175].

Our observation that the presence of cholesterol decreased sAPPα levels in (polarized) pBCEC agrees with those of Bodovitz and Klein reported in APP stably transfected HEK 293 cells [118]. The authors hypothesized that α-secretase activity may be inhibited by increased cellular cholesterol levels and thus be responsible for the observed effect.

5.1.1. Cholesterol biosynthesis

In this study we were able to identify and link the impact of LXR ligands, cholesterol, and simvastatin on APP processing and cholesterol homeostasis in pBCEC. Pharmacological modulation of intracellular cholesterol homeostasis resulted in pronounced alterations of APP synthesis and processing by pBCEC. In parallel, total cellular cholesterol mass was down-regulated by simvastatin and up-regulated by exogenously added cholesterol. LXR ligands did not affect total cellular cholesterol content. However, all agonists significantly attenuated cellular *de novo* cholesterol biosynthesis. As a uniform response to inhibited cholesterol biosynthesis we have observed increased APP synthesis, decreased BACE mRNA levels, and lower intracellular Aβ oligomer deposition. Data from the present study suggest that decreased *de novo* cholesterol synthesis induces a non-amyloidogenic pBCEC phenotype, probably as a response to redistribution of different cellular cholesterol pools.

In addition, under conditions where *de novo* cholesterol biosynthesis was most effectively inhibited (oxysterols and simvastatin), the levels of secreted, anti-amyloidogenic sAPPα were significantly elevated. On the transcriptional level, only simvastatin treatment induced a significant increase of ADAM10 mRNA. These findings, in line with a previous report [125], indicate a direct regulatory effect of HMGCR inhibitors on the α-secretase pathway. Statins inhibit isoprenylation of GTPases thereby leading to reduced Aβ production [126]. Accordingly, in the present study sAPPα secretion was increased under mevalonate limiting conditions, while Aβ deposition was decreased. Reversing the mevalonate block resulted in either complete (sAPPα) or partial (Aβ) reversal of this phenotype.

Oxysterol-mediated inhibition of SREBP processing or activation of LXR [189] might account for altered transcription of HMGCR and multiple other genes involved in cholesterol homeostasis. SREBP-2 contains a sterol regulatory element (SRE) in its own promoter region and is capable of regulating its own transcription [190]. In oxysterol treated pBCEC a decrease in mature SREBP-2 protein may result in reduced SRE-mSREBP-2 binding and thus decreased SREBP-2 mRNA levels in oxysterol treated BCEC. Cholesterol treatment elevated premature SREBP-2 protein levels, whereas the presence of TO slightly decreased mature SREBP-2 protein levels, but neither compound altered SREBP-2 mRNA levels in pBCEC. This is in accordance with previous reports in human neuroblastoma cells SY5Y, HEK 293 cells and a mouse microglial cell line [191]. We encountered enhanced SREBP-2 mRNA levels and elevated premature and mature SREBP-2 protein levels in the presence of simvastatin in pBCEC which is concordant with results obtained in SY5Y cells [192] and is a result of both enhanced SREBP-2 activity and transcription in a low cholesterol environment.

Up-regulation of HMGCR in pBCEC by simvastatin on mRNA and protein level was unexpected. However, such an effect was also observed in neuroblastoma cells [192] and ascribed to increased transcription, translation and protein stability of HMGCR in the presence of statins [193]. Another possible explanation is a compensatory mechanism, pBCEC use to deplete decreased cholesterol levels and biosynthesis upon simvastatin treatment.

5.1.2. Cholesterol storage

Also ACAT, catalyzing intracellular cholesterol esterification, has been linked to amyloidogenesis in several studies. Increasing CE levels enhances Aβ release from cells, whereas pharmacological inhibition of ACAT-1 was shown to reduce intracellular CE levels and Aβ release [129, 194]. ACAT-1 inhibition decreased plaque burden in APP mice by reducing secretion and increasing clearance of Aβ [195]. During the present study, ACAT-1 mRNA levels were unaffected by the agonists used. In contrast, ACAT-2 mRNA levels were up- (simvastatin), down- (oxysterols) or un-regulated (TO, cholesterol) and did not clearly correlate with the induction of either a pro- or anti-

amyloidogenic pBCEC phenotype. Therefore, we are currently unable to draw firm conclusions about the role of ACAT in APP processing in pBCEC.

5.1.3. Cholesterol efflux

Increased LXR/ABCA1/apoA-I dependent cholesterol efflux (Fig. 3D) from pBCEC is most probably a protective pathway preventing accumulation of toxic concentrations of cholesterol [76]. The LXR/ABCA1/apoE axis in brain is now considered as a promising therapeutic target in AD [196]. In line, a crucial role of ABCA1 has been suggested in plaque formation, since lack of ABCA1 protein leads to enhanced Aβ deposition in APP23/ABCA1$^{-/-}$ mice [197]. In agreement, our data demonstrate a reduction in intracellular Aβ deposits under conditions of LXR-mediated ABCA1 up-regulation. In contrast and despite of down-regulated ABCA1 expression (an event mediated by SREBP-2; [172]) intracellular Aβ oligomer formation was still reduced in response to BCEC treatment with simvastatin.

5.1.4. PKC action on APP secretion

Already in the 1990's Buxbaum et al. reported that APP processing is sensitive to regulators of protein-phosphorylation, e.g. PKC activators decreased APP processing via the amyloidogenic pathway [198]. More recent data point towards a role of PKC in the cellular trafficking of APP [199] and highlight modulating effects of oxysterol-action on protein kinase activity and APP processing [176].

To clarify if PKC also takes part in APP processing at the BBB we examined effects of PKC activation on APPα secretion in pBCEC. Indeed we observed a drastically increased sAPPα secretion from BCEC incubated with ionomycin (a PKC activator) compared to control cells. Enhanced sAPPα secretion from pBCEC might be explained by the findings of Pangrsic et. al, that ionomycin stimulates exocytic cargo release (e.g. ATP release from cultured astrocytes) [200]. Furthermore we found that addition of 24OH-C reversed this effect. Our data are in line with those found in primary cortical neurons [176] and emphasize that APP processing in BCEC is (at least in part) regulated by PKC and can be modulated by the action of oxysterols.

5.2. Investigation of BBB-derived (apo) lipoproteins and Aβ turnover at the BBB

5.2.1. ApoA-I stimulates sAPPα secretion from pBCEC

Previous studies of our group highlight that pBCEC actively synthesize HDL-like particles containing apoA-I [76]. In addition, within this study we found that apoA-I treatment of pBCEC significantly increased sAPPα secretion as compared to control cells. The underlying mechanism for enhanced sAPPα secretion is not known at present, however, one could speculate that interaction of apoA-I with APP may induce its increased formation/release, since apoA-I has been reported to interact with at least one extracellular domain of APP [201]. Alternatively (or in addition), the presence of apoA-I may activate PKC signaling [202, 203]in pBCEC and thereby induce the release of neuroprotective sAPPα at the BBB (see above). It is perhaps plausible that enhanced release of sAPPα upon apoA-I stimulation in BCEC could contribute to the extenuating effects of apoA-I overexpression on neurodegenerative symptoms in AD mouse models [177, 204].

5.2.2. Apolipoprotein profiles in pBCEC

Another aim of the present *in vitro* study was to characterize the (apo)lipoprotein profile in pBCEC supernatants. We found that pBCEC express and secrete significant amounts of apoA-I and apoJ. Previous results of our group showed that HDL-like particles (that contain apoA-I) are formed at the basolateral side of the *in vitro* BBB model [76]. Our new findings suggest that pBCEC can also form lipoprotein particles that contain apoJ or possibly both apoJ and apoA-I as it has been described for a small fraction of plasma-derived small and lipid-poor apoJ-containing HDL particles [205] and lipoprotein particles containing apoJ have been also found in hepatocytes and astrocytes [93, 206]. However, the majority of pBCEC-derived apoJ was detected in density fraction 1 and 3 under all conditions explored. These findings are partly in line

with those of De Silva et al. and suggest that apoJ may associate with VLDL, LDL and HDL_3 [207].

ApoJ or clusterin is involved in many processes, e.g. cholesterol efflux [95], inhibition of complement activation [208], and was shown to bind Aβ *in vivo* and *in vitro* [209, 210]. Soluble plasma Aβ (sAβ) is mainly complexed with apoJ [209] and is found in HDL [206], HDL_3 and VHDL [211]. ApoJ–$sA\beta_{1\text{-}40}$–complexes can bind to microvessels and can be transported from blood-to brain *in vivo* [51]. Since Aβ binding to apoE depends on the lipidation status of the apolipoprotein [212], and BCEC secrete lipid-rich apoJ, similar mechanisms could occur in microvascular endothelial cells forming the BBB. Future studies should further investigate this interesting question.

During this study we observed increased intracellular apoJ protein levels in pBCEC treated with 24OH-C in parallel to decreased apoJ secretion and gene expression. Since apoJ is no reported LXR target gene the effects of 24OH-C on apoJ expression might also be independent of LXR activation. The decreased secretion and gene expression of apoJ may represent a feed-back regulatory mechanism due to increased intracellular apoJ protein levels. TO also decreased apo J secretion and gene expression in pBCEC. However, there is no data on intracellular apoJ levels in this cell type treated with TO or 27OH-C until so far. Similar results (for both synthetic and non-synthetic LXR ligands) would suggest LXR-dependent regulation of apoJ expression in pBCEC Future experiments should address this issue. The finding that both cholesterol and simvastatin altered apoJ secretion and gene expression in BCEC indicates that altered cholesterol homeostasis might also influence apoJ expression at the BBB.

During this study we could show that the pattern of distribution of apoJ and APP in (lipoprotein) density fractions over-lapped and that apoJ and APP/Aβ physically interact. We speculate that intracellular apoJ and extracellular apoJ and/or HDL-like particles formed by pBCEC could be transport shuttles for brain-derived and endogenously (in BCEC) synthesized Aβ and be involved in the clearance of excess Aβ across the BBB. Future studies will address these questions.

5.2.3. Transport of Aβ peptide across the BBB in vitro

The maintenance of cerebral Aβ homeostasis involves Aβ clearance and uptake across the BBB, processes in which several cellular receptors and transporters are reported to be involved [213] in addition to the presently best described candidates, LRP1 and RAGE [214]. During this study we addressed the questions if time-dependent transport of Aβ peptide can be measured using the *in vitro* Transwell model of the BBB and if known and/or novel Aβ-binding candidates are expressed in pBCEC.

In our initial experiments, radiolabeled $A\beta_{1\text{-}40}$ was added to either the apical (mimicking the blood side) or the basolateral side (simulating the brain side) of pBCEC grown on Transwell filters (BBB *in vitro* model) on and Aβ transport to the other compartment was monitored over-time. A time-dependent transport of $A\beta_{1\text{-}40}$ from both apical to basolateral and vice versa was observed, that seemed to be enhanced after LXR activation by using its endogenous ligand 24OH-C.

During this study we found that APP and apoA-I/apoJ expression in lipoprotein density fractions over-lapped and that addition of apoA-I to the culture medium of pBCEC enhances non-amyloidogenic processing of APP. We therefore speculate that HDL-like particles (containing apoA-I and/or apoJ) could be Aβ-transport vehicles and thus investigated transport of radiolabeled apoA-I in our Transwell system. Interestingly also apoA-I was transported into both directions across the cellular model of the BBB.

To characterize novel receptors involved in the Aβ transport observed, we performed FACS analyses to monitor fluorescently labeled Aβ uptake by BW transductants (B–lymphocytes which over-express certain types of scavenger receptors). This allowed us to detect two promising candidates, namely scavenger receptor expressed on endothelial cells (SREC-I) and scavenger receptor A1 (SR-AI). Reduced Aβ binding and uptake in SREC-I overexpressing BW cells in the presence of fucoidan and inhibiting SREC-I antibody further approved the involvement of SREC-I in Aβ binding in BW cells. In pBCEC only SREC-I was expressed and fucoidan significantly inhibited Aβ uptake by pBCEC. In contrast to BW cells, Aβ binding in pBCEC in the presence of SREC-I antibody did not change.

Our results suggest SREC-I as a new candidate-receptor for Aβ at the BBB. Although RNAi and further antibody inhibition experiments in pBCEC are crucial to further strengthen this hypothesis.

Data of the present study revealed that cerebrovascular endothelial cells actively contribute to cerebral APP/Aβ synthesis. Dysfunctional cerebrovascular cholesterol and/or APP homeostasis might therefore contribute to the pathogenesis of AD. Pharmacological modulation of cellular lipoprotein, cholesterol and isoprenoid metabolism could contribute to redirect APP synthesis and processing by cerebromicrovascular endothelial cells towards the beneficial, non-amyloidogenic pathway. In particular cerebrovascular LXRs may represent promising targets for such intervention strategies, due to their ability to modulate cholesterol and lipoprotein metabolism, APP processing, and inflammatory gene expression at the BBB.

6. Bibliography

[1] Burns A, Byrne EJ, Maurer K (2002) Alzheimer's disease. *Lancet* **360**, 163-165.

[2] Yves D, Vincent B, Regis L, Audrey G, Valerie Cde C, Sophie B, Philippe P (2011) Increased perfusion in supplementary motor area during a REM sleep behaviour episode. *Sleep Med* **12**, 531-532.

[3] Goate A, Chartier-Harlin MC, Mullan M, Brown J, Crawford F, Fidani L, Giuffra L, Haynes A, Irving N, James L, et al. (1991) Segregation of a missense mutation in the amyloid precursor protein gene with familial Alzheimer's disease. *Nature* **349**, 704-706.

[4] Levy-Lahad E, Wasco W, Poorkaj P, Romano DM, Oshima J, Pettingell WH, Yu CE, Jondro PD, Schmidt SD, Wang K, et al. (1995) Candidate gene for the chromosome 1 familial Alzheimer's disease locus. *Science* **269**, 973-977.

[5] Sherrington R, Rogaev EI, Liang Y, Rogaeva EA, Levesque G, Ikeda M, Chi H, Lin C, Li G, Holman K, Tsuda T, Mar L, Foncin JF, Bruni AC, Montesi MP, Sorbi S, Rainero I, Pinessi L, Nee L, Chumakov I, Pollen D, Brookes A, Sanseau P, Polinsky RJ, Wasco W, Da Silva HA, Haines JL, Perkicak-Vance MA, Tanzi RE, Roses AD, Fraser PE, Rommens JM, St George-Hyslop PH (1995) Cloning of a gene bearing missense mutations in early-onset familial Alzheimer's disease. *Nature* **375**, 754-760.

[6] Corder EH, Saunders AM, Strittmatter WJ, Schmechel DE, Gaskell PC, Small GW, Roses AD, Haines JL, Pericak-Vance MA (1993) Gene dose of apolipoprotein E type 4 allele and the risk of Alzheimer's disease in late onset families. *Science* **261**, 921-923.

[7] Saunders AM, Strittmatter WJ, Schmechel D, George-Hyslop PH, Pericak-Vance MA, Joo SH, Rosi BL, Gusella JF, Crapper-MacLachlan DR, Alberts MJ, et al. (1993) Association of apolipoprotein E allele epsilon 4 with late-onset familial and sporadic Alzheimer's disease. *Neurology* **43**, 1467-1472.

[8] Strittmatter WJ, Roses AD (1995) Apolipoprotein E and Alzheimer disease. *Proc Natl Acad Sci U S A* **92**, 4725-4727.

[9] Corder EH, Saunders AM, Risch NJ, Strittmatter WJ, Schmechel DE, Gaskell PC, Jr., Rimmler JB, Locke PA, Conneally PM, Schmader KE, et al. (1994) Protective effect of apolipoprotein E type 2 allele for late onset Alzheimer disease. *Nat Genet* **7**, 180-184.

[10] LaFerla FM, Green KN, Oddo S (2007) Intracellular amyloid-beta in Alzheimer's disease. *Nat Rev Neurosci* **8**, 499-509.

[11] McKhann G, Drachman D, Folstein M, Katzman R, Price D, Stadlan EM (1984) Clinical diagnosis of Alzheimer's disease: report of the NINCDS-ADRDA Work Group under the auspices of Department of Health and Human Services Task Force on Alzheimer's Disease. *Neurology* **34**, 939-944.

[12] Alzheimer A, Stelzmann RA, Schnitzlein HN, Murtagh FR (1995) An English translation of Alzheimer's 1907 paper, "Uber eine eigenartige Erkankung der Hirnrinde". *Clin Anat* **8**, 429-431.

[13] Glenner GG, Wong CW (1984) Alzheimer's disease: initial report of the purification and characterization of a novel cerebrovascular amyloid protein. *Biochem Biophys Res Commun* **120**, 885-890.

[14] Masters CL, Simms G, Weinman NA, Multhaup G, McDonald BL, Beyreuther K (1985) Amyloid plaque core protein in Alzheimer disease and Down syndrome. *Proc Natl Acad Sci U S A* **82**, 4245-4249.

[15] Goedert M, Wischik CM, Crowther RA, Walker JE, Klug A (1988) Cloning and sequencing of the cDNA encoding a core protein of the paired helical filament of Alzheimer disease: identification as the microtubule-associated protein tau. *Proc Natl Acad Sci U S A* **85**, 4051-4055.

[16] Grundke-Iqbal I, Iqbal K, Tung YC, Quinlan M, Wisniewski HM, Binder LI (1986) Abnormal phosphorylation of the microtubule-associated protein tau (tau) in Alzheimer cytoskeletal pathology. *Proc Natl Acad Sci U S A* **83**, 4913-4917.

[17] Ihara Y, Nukina N, Miura R, Ogawara M (1986) Phosphorylated tau protein is integrated into paired helical filaments in Alzheimer's disease. *J Biochem* **99**, 1807-1810.

[18] Kosik KS, Joachim CL, Selkoe DJ (1986) Microtubule-associated protein tau (tau) is a major antigenic component of paired helical filaments in Alzheimer disease. *Proc Natl Acad Sci U S A* **83**, 4044-4048.

[19] Mohandas E, Rajmohan V, Raghunath B (2009) Neurobiology of Alzheimer's disease. *Indian J Psychiatry* **51**, 55-61.

[20] Ehrlich P (1904) Ueber die Beziehungen von chemischer Konstitution, Verteilung und pharmakologischer Wirkung *Gesammelte Arbeiten zur Immunitaetsforschung*, 574.

[21] Goldmann E (1913) Vitalfaerbung am Zentralnervensystem. *Abhandl Konigl preuss Akad Wiss* **1**, 1-60.

[22] Carvey PM, Hendey B, Monahan AJ (2009) The blood-brain barrier in neurodegenerative disease: a rhetorical perspective. *J Neurochem* **111**, 291-314.

[23] Kniesel U, Wolburg H (2000) Tight junctions of the blood-brain barrier. *Cell Mol Neurobiol* **20**, 57-76.

[24] Diaz-Flores L, Gutierrez R, Varela H, Rancel N, Valladares F (1991) Microvascular pericytes: a review of their morphological and functional characteristics. *Histol Histopathol* **6**, 269-286.

[25] Ho KL (1985) Ultrastructure of cerebellar capillary hemangioblastoma. IV. Pericytes and their relationship to endothelial cells. *Acta Neuropathol* **67**, 254-264.

[26] Balabanov R, Dore-Duffy P (1998) Role of the CNS microvascular pericyte in the blood-brain barrier. *J Neurosci Res* **53**, 637-644.

[27] Hawkins BT, Davis TP (2005) The blood-brain barrier/neurovascular unit in health and disease. *Pharmacol Rev* **57**, 173-185.

[28] Fenstermacher J, Kaye T (1988) Drug "diffusion" within the brain. *Ann N Y Acad Sci* **531**, 29-39.
[29] Oldendorf WH, Cornford ME, Brown WJ (1977) The large apparent work capability of the blood-brain barrier: a study of the mitochondrial content of capillary endothelial cells in brain and other tissues of the rat. *Ann Neurol* **1**, 409-417.
[30] Sedlakova R, Shivers RR, Del Maestro RF (1999) Ultrastructure of the blood-brain barrier in the rabbit. *J Submicrosc Cytol Pathol* **31**, 149-161.
[31] Stevenson BR, Keon BH (1998) The tight junction: morphology to molecules. *Annu Rev Cell Dev Biol* **14**, 89-109.
[32] Begley DJ, Brightman MW (2003) Structural and functional aspects of the blood-brain barrier. *Prog Drug Res* **61**, 39-78.
[33] Shibata M, Yamada S, Kumar SR, Calero M, Bading J, Frangione B, Holtzman DM, Miller CA, Strickland DK, Ghiso J, Zlokovic BV (2000) Clearance of Alzheimer's amyloid-ss(1-40) peptide from brain by LDL receptor-related protein-1 at the blood-brain barrier. *J Clin Invest* **106**, 1489-1499.
[34] Zlokovic BV (2004) Clearing amyloid through the blood-brain barrier. *J Neurochem* **89**, 807-811.
[35] Deane R, Du Yan S, Submamaryan RK, LaRue B, Jovanovic S, Hogg E, Welch D, Manness L, Lin C, Yu J, Zhu H, Ghiso J, Frangione B, Stern A, Schmidt AM, Armstrong DL, Arnold B, Liliensiek B, Nawroth P, Hofman F, Kindy M, Stern D, Zlokovic B (2003) RAGE mediates amyloid-beta peptide transport across the blood-brain barrier and accumulation in brain. *Nat Med* **9**, 907-913.
[36] Zhao C, Ling Z, Newman MB, Bhatia A, Carvey PM (2007) TNF-alpha knockout and minocycline treatment attenuates blood-brain barrier leakage in MPTP-treated mice. *Neurobiol Dis* **26**, 36-46.
[37] Bell RD, Zlokovic BV (2009) Neurovascular mechanisms and blood-brain barrier disorder in Alzheimer's disease. *Acta Neuropathol* **118**, 103-113.
[38] Patel NV, Forman BM (2004) Linking lipids, Alzheimer's and LXRs? *Nucl Recept Signal* **2**, e001.
[39] Grosgen S, Grimm MO, Friess P, Hartmann T (2010) Role of amyloid beta in lipid homeostasis. *Biochim Biophys Acta* **1801**, 966-974.
[40] Zheng H, Koo EH (2006) The amyloid precursor protein: beyond amyloid. *Mol Neurodegener* **1**, 5.
[41] Kang J, Muller-Hill B (1990) Differential splicing of Alzheimer's disease amyloid A4 precursor RNA in rat tissues: PreA4(695) mRNA is predominantly produced in rat and human brain. *Biochem Biophys Res Commun* **166**, 1192-1200.
[42] Rohan de Silva HA, Jen A, Wickenden C, Jen LS, Wilkinson SL, Patel AJ (1997) Cell-specific expression of beta-amyloid precursor protein isoform mRNAs and proteins in neurons and astrocytes. *Brain Res Mol Brain Res* **47**, 147-156.
[43] Menendez-Gonzalez M, Perez-Pinera P, Martinez-Rivera M, Calatayud MT, Blazquez Menes B (2005) APP processing and the APP-KPI domain involvement in the amyloid cascade. *Neurodegener Dis* **2**, 277-283.
[44] Zhang YW, Thompson R, Zhang H, Xu H (2011) APP processing in Alzheimer's disease. *Mol Brain* **4**, 3.

[45] Chow VW, Mattson MP, Wong PC, Gleichmann M (2010) An overview of APP processing enzymes and products. *Neuromolecular Med* **12**, 1-12.
[46] Martins IJ, Berger T, Sharman MJ, Verdile G, Fuller SJ, Martins RN (2009) Cholesterol metabolism and transport in the pathogenesis of Alzheimer's disease. *J Neurochem* **111**, 1275-1308.
[47] Kojro E, Fahrenholz F (2005) The non-amyloidogenic pathway: structure and function of alpha-secretases. *Subcell Biochem* **38**, 105-127.
[48] Haass C, Hung AY, Schlossmacher MG, Teplow DB, Selkoe DJ (1993) beta-Amyloid peptide and a 3-kDa fragment are derived by distinct cellular mechanisms. *J Biol Chem* **268**, 3021-3024.
[49] Jarrett JT, Berger EP, Lansbury PT, Jr. (1993) The carboxy terminus of the beta amyloid protein is critical for the seeding of amyloid formation: implications for the pathogenesis of Alzheimer's disease. *Biochemistry* **32**, 4693-4697.
[50] Younkin SG (1998) The role of A beta 42 in Alzheimer's disease. *J Physiol Paris* **92**, 289-292.
[51] Zlokovic BV (1996) Cerebrovascular transport of Alzheimer's amyloid beta and apolipoproteins J and E: possible anti-amyloidogenic role of the blood-brain barrier. *Life Sci* **59**, 1483-1497.
[52] Allinson TM, Parkin ET, Turner AJ, Hooper NM (2003) ADAMs family members as amyloid precursor protein alpha-secretases. *J Neurosci Res* **74**, 342-352.
[53] Hussain I, Powell D, Howlett DR, Tew DG, Meek TD, Chapman C, Gloger IS, Murphy KE, Southan CD, Ryan DM, Smith TS, Simmons DL, Walsh FS, Dingwall C, Christie G (1999) Identification of a novel aspartic protease (Asp 2) as beta-secretase. *Mol Cell Neurosci* **14**, 419-427.
[54] Sinha S, Anderson JP, Barbour R, Basi GS, Caccavello R, Davis D, Doan M, Dovey HF, Frigon N, Hong J, Jacobson-Croak K, Jewett N, Keim P, Knops J, Lieberburg I, Power M, Tan H, Tatsuno G, Tung J, Schenk D, Seubert P, Suomensaari SM, Wang S, Walker D, Zhao J, McConlogue L, John V (1999) Purification and cloning of amyloid precursor protein beta-secretase from human brain. *Nature* **402**, 537-540.
[55] Vassar R, Bennett BD, Babu-Khan S, Kahn S, Mendiaz EA, Denis P, Teplow DB, Ross S, Amarante P, Loeloff R, Luo Y, Fisher S, Fuller J, Edenson S, Lile J, Jarosinski MA, Biere AL, Curran E, Burgess T, Louis JC, Collins F, Treanor J, Rogers G, Citron M (1999) Beta-secretase cleavage of Alzheimer's amyloid precursor protein by the transmembrane aspartic protease BACE. *Science* **286**, 735-741.
[56] Francis R, McGrath G, Zhang J, Ruddy DA, Sym M, Apfeld J, Nicoll M, Maxwell M, Hai B, Ellis MC, Parks AL, Xu W, Li J, Gurney M, Myers RL, Himes CS, Hiebsch R, Ruble C, Nye JS, Curtis D (2002) aph-1 and pen-2 are required for Notch pathway signaling, gamma-secretase cleavage of betaAPP, and presenilin protein accumulation. *Dev Cell* **3**, 85-97.
[57] Levitan D, Lee J, Song L, Manning R, Wong G, Parker E, Zhang L (2001) PS1 N- and C-terminal fragments form a complex that functions in APP processing and Notch signaling. *Proc Natl Acad Sci U S A* **98**, 12186-12190.

[58] Steiner H, Winkler E, Edbauer D, Prokop S, Basset G, Yamasaki A, Kostka M, Haass C (2002) PEN-2 is an integral component of the gamma-secretase complex required for coordinated expression of presenilin and nicastrin. *J Biol Chem* **277**, 39062-39065.

[59] Wolfe MS, Xia W, Ostaszewski BL, Diehl TS, Kimberly WT, Selkoe DJ (1999) Two transmembrane aspartates in presenilin-1 required for presenilin endoproteolysis and gamma-secretase activity. *Nature* **398**, 513-517.

[60] Yu G, Nishimura M, Arawaka S, Levitan D, Zhang L, Tandon A, Song YQ, Rogaeva E, Chen F, Kawarai T, Supala A, Levesque L, Yu H, Yang DS, Holmes E, Milman P, Liang Y, Zhang DM, Xu DH, Sato C, Rogaev E, Smith M, Janus C, Zhang Y, Aebersold R, Farrer LS, Sorbi S, Bruni A, Fraser P, St George-Hyslop P (2000) Nicastrin modulates presenilin-mediated notch/glp-1 signal transduction and betaAPP processing. *Nature* **407**, 48-54.

[61] Snipes GJ, Suter U (1997) Cholesterol and myelin. *Subcell Biochem* **28**, 173-204.

[62] Dietschy JM, Turley SD (2001) Cholesterol metabolism in the brain. *Curr Opin Lipidol* **12**, 105-112.

[63] Muse ED, Jurevics H, Toews AD, Matsushima GK, Morell P (2001) Parameters related to lipid metabolism as markers of myelination in mouse brain. *J Neurochem* **76**, 77-86.

[64] Bjorkhem I, Diczfalusy U, Lutjohann D (1999) Removal of cholesterol from extrahepatic sources by oxidative mechanisms. *Curr Opin Lipidol* **10**, 161-165.

[65] Bjorkhem I, Meaney S (2004) Brain cholesterol: long secret life behind a barrier. *Arterioscler Thromb Vasc Biol* **24**, 806-815.

[66] Dietschy JM, Turley SD (2004) Thematic review series: brain Lipids. Cholesterol metabolism in the central nervous system during early development and in the mature animal. *J Lipid Res* **45**, 1375-1397.

[67] Vance JE, Hayashi H, Karten B (2005) Cholesterol homeostasis in neurons and glial cells. *Semin Cell Dev Biol* **16**, 193-212.

[68] Funfschilling U, Saher G, Xiao L, Mobius W, Nave KA (2007) Survival of adult neurons lacking cholesterol synthesis in vivo. *BMC Neurosci* **8**, 1.

[69] Saher G, Brugger B, Lappe-Siefke C, Mobius W, Tozawa R, Wehr MC, Wieland F, Ishibashi S, Nave KA (2005) High cholesterol level is essential for myelin membrane growth. *Nat Neurosci* **8**, 468-475.

[70] Bjorkhem I, Lutjohann D, Diczfalusy U, Stahle L, Ahlborg G, Wahren J (1998) Cholesterol homeostasis in human brain: turnover of 24S-hydroxycholesterol and evidence for a cerebral origin of most of this oxysterol in the circulation. *J Lipid Res* **39**, 1594-1600.

[71] Lund EG, Guileyardo JM, Russell DW (1999) cDNA cloning of cholesterol 24-hydroxylase, a mediator of cholesterol homeostasis in the brain. *Proc Natl Acad Sci U S A* **96**, 7238-7243.

[72] Janowski BA, Willy PJ, Devi TR, Falck JR, Mangelsdorf DJ (1996) An oxysterol signalling pathway mediated by the nuclear receptor LXR alpha. *Nature* **383**, 728-731.

[73] Wang L, Schuster GU, Hultenby K, Zhang Q, Andersson S, Gustafsson JA (2002) Liver X receptors in the central nervous system: from lipid homeostasis to neuronal degeneration. *Proc Natl Acad Sci U S A* **99**, 13878-13883.

[74] Baranowski M (2008) Biological role of liver X receptors. *J Physiol Pharmacol* **59 Suppl 7**, 31-55.

[75] Abildayeva K, Jansen PJ, Hirsch-Reinshagen V, Bloks VW, Bakker AH, Ramaekers FC, de Vente J, Groen AK, Wellington CL, Kuipers F, Mulder M (2006) 24(S)-hydroxycholesterol participates in a liver X receptor-controlled pathway in astrocytes that regulates apolipoprotein E-mediated cholesterol efflux. *J Biol Chem* **281**, 12799-12808.

[76] Panzenboeck U, Balazs Z, Sovic A, Hrzenjak A, Levak-Frank S, Wintersperger A, Malle E, Sattler W (2002) ABCA1 and scavenger receptor class B, type I, are modulators of reverse sterol transport at an in vitro blood-brain barrier constituted of porcine brain capillary endothelial cells. *J Biol Chem* **277**, 42781-42789.

[77] Panzenboeck U, Kratzer I, Sovic A, Wintersperger A, Bernhart E, Hammer A, Malle E, Sattler W (2006) Regulatory effects of synthetic liver X receptor- and peroxisome-proliferator activated receptor agonists on sterol transport pathways in polarized cerebrovascular endothelial cells. *Int J Biochem Cell Biol* **38**, 1314-1329.

[78] Sinensky M (1977) Isolation of a mammalian cell mutant resistant to 25-hydroxy cholesterol. *Biochem Biophys Res Commun* **78**, 863-867.

[79] Heverin M, Meaney S, Lutjohann D, Diczfalusy U, Wahren J, Bjorkhem I (2005) Crossing the barrier: net flux of 27-hydroxycholesterol into the human brain. *J Lipid Res* **46**, 1047-1052.

[80] Zelcer N, Tontonoz P (2006) Liver X receptors as integrators of metabolic and inflammatory signaling. *J Clin Invest* **116**, 607-614.

[81] Collet X, Francone O, Besnard F, Fielding CJ (1999) Secretion of lecithin:cholesterol acyltransferase by brain neuroglial cell lines. *Biochem Biophys Res Commun* **258**, 73-76.

[82] Bassett CN, Montine KS, Neely MD, Swift LL, Montine TJ (2000) Cerebrospinal fluid lipoproteins in Alzheimer's disease. *Microsc Res Tech* **50**, 282-286.

[83] Ladu MJ, Reardon C, Van Eldik L, Fagan AM, Bu G, Holtzman D, Getz GS (2000) Lipoproteins in the central nervous system. *Ann N Y Acad Sci* **903**, 167-175.

[84] Martel CL, Mackic JB, Matsubara E, Governale S, Miguel C, Miao W, McComb JG, Frangione B, Ghiso J, Zlokovic BV (1997) Isoform-specific effects of apolipoproteins E2, E3, and E4 on cerebral capillary sequestration and blood-brain barrier transport of circulating Alzheimer's amyloid beta. *J Neurochem* **69**, 1995-2004.

[85] Rebeck GW (2004) Cholesterol efflux as a critical component of Alzheimer's disease pathogenesis. *J Mol Neurosci* **23**, 219-224.

[86] Hirsch-Reinshagen V, Burgess BL, Wellington CL (2009) Why lipids are important for Alzheimer disease? *Mol Cell Biochem* **326**, 121-129.

[87] Yu C, Youmans KL, LaDu MJ (2010) Proposed mechanism for lipoprotein remodelling in the brain. *Biochim Biophys Acta* **1801**, 819-823.

[88] Tarr PT, Edwards PA (2008) ABCG1 and ABCG4 are coexpressed in neurons and astrocytes of the CNS and regulate cholesterol homeostasis through SREBP-2. *J Lipid Res* **49**, 169-182.

[89] Wang N, Yvan-Charvet L, Lutjohann D, Mulder M, Vanmierlo T, Kim TW, Tall AR (2008) ATP-binding cassette transporters G1 and G4 mediate cholesterol and desmosterol efflux to HDL and regulate sterol accumulation in the brain. *FASEB J* **22**, 1073-1082.

[90] Herz J, Bock HH (2002) Lipoprotein receptors in the nervous system. *Annu Rev Biochem* **71**, 405-434.

[91] Mockel B, Zinke H, Flach R, Weiss B, Weiler-Guttler H, Gassen HG (1994) Expression of apolipoprotein A-I in porcine brain endothelium in vitro. *J Neurochem* **62**, 788-798.

[92] DeMattos RB, Brendza RP, Heuser JE, Kierson M, Cirrito JR, Fryer J, Sullivan PM, Fagan AM, Han X, Holtzman DM (2001) Purification and characterization of astrocyte-secreted apolipoprotein E and J-containing lipoproteins from wild-type and human apoE transgenic mice. *Neurochem Int* **39**, 415-425.

[93] de Silva HV, Harmony JA, Stuart WD, Gil CM, Robbins J (1990) Apolipoprotein J: structure and tissue distribution. *Biochemistry* **29**, 5380-5389.

[94] Nuutinen T, Suuronen T, Kauppinen A, Salminen A (2009) Clusterin: a forgotten player in Alzheimer's disease. *Brain Res Rev* **61**, 89-104.

[95] Gelissen IC, Hochgrebe T, Wilson MR, Easterbrook-Smith SB, Jessup W, Dean RT, Brown AJ (1998) Apolipoprotein J (clusterin) induces cholesterol export from macrophage-foam cells: a potential anti-atherogenic function? *Biochem J* **331 (Pt 1)**, 231-237.

[96] Bell RD, Sagare AP, Friedman AE, Bedi GS, Holtzman DM, Deane R, Zlokovic BV (2007) Transport pathways for clearance of human Alzheimer's amyloid beta-peptide and apolipoproteins E and J in the mouse central nervous system. *J Cereb Blood Flow Metab* **27**, 909-918.

[97] Oksman M, Iivonen H, Hogyes E, Amtul Z, Penke B, Leenders I, Broersen L, Lutjohann D, Hartmann T, Tanila H (2006) Impact of different saturated fatty acid, polyunsaturated fatty acid and cholesterol containing diets on beta-amyloid accumulation in APP/PS1 transgenic mice. *Neurobiol Dis* **23**, 563-572.

[98] Refolo LM, Malester B, LaFrancois J, Bryant-Thomas T, Wang R, Tint GS, Sambamurti K, Duff K, Pappolla MA (2000) Hypercholesterolemia accelerates the Alzheimer's amyloid pathology in a transgenic mouse model. *Neurobiol Dis* **7**, 321-331.

[99] Shie FS, Jin LW, Cook DG, Leverenz JB, LeBoeuf RC (2002) Diet-induced hypercholesterolemia enhances brain A beta accumulation in transgenic mice. *Neuroreport* **13**, 455-459.

[100] Sparks DL, Scheff SW, Hunsaker JC, 3rd, Liu H, Landers T, Gross DR (1994) Induction of Alzheimer-like beta-amyloid immunoreactivity in the brains of rabbits with dietary cholesterol. *Exp Neurol* **126**, 88-94.

[101] Thirumangalakudi L, Prakasam A, Zhang R, Bimonte-Nelson H, Sambamurti K, Kindy MS, Bhat NR (2008) High cholesterol-induced neuroinflammation and

amyloid precursor protein processing correlate with loss of working memory in mice. *J Neurochem* **106**, 475-485.

[102] Anstey KJ, Lipnicki DM, Low LF (2008) Cholesterol as a risk factor for dementia and cognitive decline: a systematic review of prospective studies with meta-analysis. *Am J Geriatr Psychiatry* **16**, 343-354.

[103] Kuo YM, Emmerling MR, Bisgaier CL, Essenburg AD, Lampert HC, Drumm D, Roher AE (1998) Elevated low-density lipoprotein in Alzheimer's disease correlates with brain abeta 1-42 levels. *Biochem Biophys Res Commun* **252**, 711-715.

[104] Pfrieger FW (2003) Cholesterol homeostasis and function in neurons of the central nervous system. *Cell Mol Life Sci* **60**, 1158-1171.

[105] Merched A, Xia Y, Visvikis S, Serot JM, Siest G (2000) Decreased high-density lipoprotein cholesterol and serum apolipoprotein AI concentrations are highly correlated with the severity of Alzheimer's disease. *Neurobiol Aging* **21**, 27-30.

[106] Saczynski JS, White L, Peila RL, Rodriguez BL, Launer LJ (2007) The relation between apolipoprotein A-I and dementia: the Honolulu-Asia aging study. *Am J Epidemiol* **165**, 985-992.

[107] Ledesma MD, Dotti CG (2006) Amyloid excess in Alzheimer's disease: what is cholesterol to be blamed for? *FEBS Lett* **580**, 5525-5532.

[108] DeKosky ST (2005) Statin therapy in the treatment of Alzheimer disease: what is the rationale? *Am J Med* **118 Suppl 12A**, 48-53.

[109] Buxbaum JD, Cullen EI, Friedhoff LT (2002) Pharmacological concentrations of the HMG-CoA reductase inhibitor lovastatin decrease the formation of the Alzheimer beta-amyloid peptide in vitro and in patients. *Front Biosci* **7**, a50-59.

[110] Wolozin B (2004) Cholesterol and the biology of Alzheimer's disease. *Neuron* **41**, 7-10.

[111] Fassbender K, Simons M, Bergmann C, Stroick M, Lutjohann D, Keller P, Runz H, Kuhl S, Bertsch T, von Bergmann K, Hennerici M, Beyreuther K, Hartmann T (2001) Simvastatin strongly reduces levels of Alzheimer's disease beta -amyloid peptides Abeta 42 and Abeta 40 in vitro and in vivo. *Proc Natl Acad Sci U S A* **98**, 5856-5861.

[112] Refolo LM, Pappolla MA, LaFrancois J, Malester B, Schmidt SD, Thomas-Bryant T, Tint GS, Wang R, Mercken M, Petanceska SS, Duff KE (2001) A cholesterol-lowering drug reduces beta-amyloid pathology in a transgenic mouse model of Alzheimer's disease. *Neurobiol Dis* **8**, 890-899.

[113] Sparks DL, Kuo YM, Roher A, Martin T, Lukas RJ (2000) Alterations of Alzheimer's disease in the cholesterol-fed rabbit, including vascular inflammation. Preliminary observations. *Ann N Y Acad Sci* **903**, 335-344.

[114] Sparks DL, Lopez J, Connor D, Sabbagh M, Seward J, Browne P (2003) A position paper: based on observational data indicating an increased rate of altered blood chemistry requiring withdrawal from the Alzheimer's Disease Cholesterol-Lowering Treatment Trial (ADCLT). *J Mol Neurosci* **20**, 407-410.

[115] Sparks DL, Sabbagh MN, Connor DJ, Lopez J, Launer LJ, Browne P, Wasser D, Johnson-Traver S, Lochhead J, Ziolwolski C (2005) Atorvastatin for the

treatment of mild to moderate Alzheimer disease: preliminary results. *Arch Neurol* **62**, 753-757.

[116] Sparks DL, Sabbagh MN, Connor DJ, Lopez J, Launer LJ, Petanceska S, Browne P, Wassar D, Johnson-Traver S, Lochhead J, Ziolkowski C (2005) Atorvastatin therapy lowers circulating cholesterol but not free radical activity in advance of identifiable clinical benefit in the treatment of mild-to-moderate AD. *Curr Alzheimer Res* **2**, 343-353.

[117] Wolozin B, Wang SW, Li NC, Lee A, Lee TA, Kazis LE (2007) Simvastatin is associated with a reduced incidence of dementia and Parkinson's disease. *BMC Med* **5**, 20.

[118] Bodovitz S, Klein WL (1996) Cholesterol modulates alpha-secretase cleavage of amyloid precursor protein. *J Biol Chem* **271**, 4436-4440.

[119] Ehehalt R, Keller P, Haass C, Thiele C, Simons K (2003) Amyloidogenic processing of the Alzheimer beta-amyloid precursor protein depends on lipid rafts. *J Cell Biol* **160**, 113-123.

[120] Hartmann T, Bieger SC, Bruhl B, Tienari PJ, Ida N, Allsop D, Roberts GW, Masters CL, Dotti CG, Unsicker K, Beyreuther K (1997) Distinct sites of intracellular production for Alzheimer's disease A beta40/42 amyloid peptides. *Nat Med* **3**, 1016-1020.

[121] Vetrivel KS, Cheng H, Lin W, Sakurai T, Li T, Nukina N, Wong PC, Xu H, Thinakaran G (2004) Association of gamma-secretase with lipid rafts in post-Golgi and endosome membranes. *J Biol Chem* **279**, 44945-44954.

[122] Kirsch C, Eckert GP, Mueller WE (2003) Statin effects on cholesterol micro-domains in brain plasma membranes. *Biochem Pharmacol* **65**, 843-856.

[123] Simons ER, Marshall DC, Long HJ, Otto K, Billingslea A, Tibbles H, Wells J, Eisenhauer P, Fine RE, Cribbs DH, Davies TA, Abraham CR (1998) Blood brain barrier endothelial cells express candidate amyloid precursor protein-cleaving secretases. *Amyloid* **5**, 153-162.

[124] Cole SL, Grudzien A, Manhart IO, Kelly BL, Oakley H, Vassar R (2005) Statins cause intracellular accumulation of amyloid precursor protein, beta-secretase-cleaved fragments, and amyloid beta-peptide via an isoprenoid-dependent mechanism. *J Biol Chem* **280**, 18755-18770.

[125] Kojro E, Gimpl G, Lammich S, Marz W, Fahrenholz F (2001) Low cholesterol stimulates the nonamyloidogenic pathway by its effect on the alpha -secretase ADAM 10. *Proc Natl Acad Sci U S A* **98**, 5815-5820.

[126] Ostrowski SM, Wilkinson BL, Golde TE, Landreth G (2007) Statins reduce amyloid-beta production through inhibition of protein isoprenylation. *J Biol Chem* **282**, 26832-26844.

[127] Hutter-Paier B, Huttunen HJ, Puglielli L, Eckman CB, Kim DY, Hofmeister A, Moir RD, Domnitz SB, Frosch MP, Windisch M, Kovacs DM (2004) The ACAT inhibitor CP-113,818 markedly reduces amyloid pathology in a mouse model of Alzheimer's disease. *Neuron* **44**, 227-238.

[128] Huttunen HJ, Greco C, Kovacs DM (2007) Knockdown of ACAT-1 reduces amyloidogenic processing of APP. *FEBS Lett* **581**, 1688-1692.

[129] Puglielli L, Ellis BC, Ingano LA, Kovacs DM (2004) Role of acyl-coenzyme a: cholesterol acyltransferase activity in the processing of the amyloid precursor protein. *J Mol Neurosci* **24**, 93-96.
[130] Sun Y, Yao J, Kim TW, Tall AR (2003) Expression of liver X receptor target genes decreases cellular amyloid beta peptide secretion. *J Biol Chem* **278**, 27688-27694.
[131] Hirsch-Reinshagen V, Maia LF, Burgess BL, Blain JF, Naus KE, McIsaac SA, Parkinson PF, Chan JY, Tansley GH, Hayden MR, Poirier J, Van Nostrand W, Wellington CL (2005) The absence of ABCA1 decreases soluble ApoE levels but does not diminish amyloid deposition in two murine models of Alzheimer disease. *J Biol Chem* **280**, 43243-43256.
[132] Koldamova RP, Lefterov IM, Staufenbiel M, Wolfe D, Huang S, Glorioso JC, Walter M, Roth MG, Lazo JS (2005) The liver X receptor ligand T0901317 decreases amyloid beta production in vitro and in a mouse model of Alzheimer's disease. *J Biol Chem* **280**, 4079-4088.
[133] Wahrle SE, Jiang H, Parsadanian M, Hartman RE, Bales KR, Paul SM, Holtzman DM (2005) Deletion of Abca1 increases Abeta deposition in the PDAPP transgenic mouse model of Alzheimer disease. *J Biol Chem* **280**, 43236-43242.
[134] Ikeda K, Akiyama H, Arai T, Matsushita M, Tsuchiya K, Miyazaki H (2000) Clinical aspects of argyrophilic grain disease. *Clin Neuropathol* **19**, 278-284.
[135] Chandrakasan S, Ye CJ, Chitlur M, Mohamed AN, Rabah R, Konski A, Heng HH, Savasan S (2011) Malignant fibrous histiocytoma two years after autologous stem cell transplant for Hodgkin lymphoma: Evidence for genomic instability. *Pediatr Blood Cancer* **56**, 1143-1145.
[136] Liao H, Langmann T, Schmitz G, Zhu Y (2002) Native LDL upregulation of ATP-binding cassette transporter-1 in human vascular endothelial cells. *Arterioscler Thromb Vasc Biol* **22**, 127-132.
[137] Noguchi H, Yoshida H, Takamatsu H, Akiyama H (2000) Immunohistochemical studies on tenascin in extrahepatic bile duct remnants of biliary atresia. *In Vivo* **14**, 715-720.
[138] Kolsch H, Heun R, Kerksiek A, Bergmann KV, Maier W, Lutjohann D (2004) Altered levels of plasma 24S- and 27-hydroxycholesterol in demented patients. *Neurosci Lett* **368**, 303-308.
[139] Heverin M, Bogdanovic N, Lutjohann D, Bayer T, Pikuleva I, Bretillon L, Diczfalusy U, Winblad B, Bjorkhem I (2004) Changes in the levels of cerebral and extracerebral sterols in the brain of patients with Alzheimer's disease. *J Lipid Res* **45**, 186-193.
[140] Claudio L (1996) Ultrastructural features of the blood-brain barrier in biopsy tissue from Alzheimer's disease patients. *Acta Neuropathol* **91**, 6-14.
[141] Kalaria RN (1996) Cerebral vessels in ageing and Alzheimer's disease. *Pharmacol Ther* **72**, 193-214.
[142] Kalaria RN (2002) Small vessel disease and Alzheimer's dementia: pathological considerations. *Cerebrovasc Dis* **13 Suppl 2**, 48-52.
[143] Lutjohann D, Papassotiropoulos A, Bjorkhem I, Locatelli S, Bagli M, Oehring RD, Schlegel U, Jessen F, Rao ML, von Bergmann K, Heun R (2000) Plasma 24S-

hydroxycholesterol (cerebrosterol) is increased in Alzheimer and vascular demented patients. *J Lipid Res* **41**, 195-198.

[144] Lutjohann D, von Bergmann K (2003) 24S-hydroxycholesterol: a marker of brain cholesterol metabolism. *Pharmacopsychiatry* **36 Suppl 2**, S102-106.

[145] Papassotiropoulos A, Lutjohann D, Bagli M, Locatelli S, Jessen F, Rao ML, Maier W, Bjorkhem I, von Bergmann K, Heun R (2000) Plasma 24S-hydroxycholesterol: a peripheral indicator of neuronal degeneration and potential state marker for Alzheimer's disease. *Neuroreport* **11**, 1959-1962.

[146] Bjorkhem I, Heverin M, Leoni V, Meaney S, Diczfalusy U (2006) Oxysterols and Alzheimer's disease. *Acta Neurol Scand Suppl* **185**, 43-49.

[147] Meaney S, Heverin M, Panzenboeck U, Ekstrom L, Axelsson M, Andersson U, Diczfalusy U, Pikuleva I, Wahren J, Sattler W, Bjorkhem I (2007) Novel route for elimination of brain oxysterols across the blood-brain barrier: conversion into 7alpha-hydroxy-3-oxo-4-cholestenoic acid. *J Lipid Res* **48**, 944-951.

[148] Belloir B, Kovari E, Surini-Demiri M, Savioz A (2001) Altered apolipoprotein D expression in the brain of patients with Alzheimer disease. *J Neurosci Res* **64**, 61-69.

[149] Lidstrom AM, Bogdanovic N, Hesse C, Volkman I, Davidsson P, Blennow K (1998) Clusterin (apolipoprotein J) protein levels are increased in hippocampus and in frontal cortex in Alzheimer's disease. *Exp Neurol* **154**, 511-521.

[150] Yamagata K, Urakami K, Ikeda K, Ji Y, Adachi Y, Arai H, Sasaki H, Sato K, Nakashima K (2001) High expression of apolipoprotein E mRNA in the brains with sporadic Alzheimer's disease. *Dement Geriatr Cogn Disord* **12**, 57-62.

[151] Calero M, Rostagno A, Matsubara E, Zlokovic B, Frangione B, Ghiso J (2000) Apolipoprotein J (clusterin) and Alzheimer's disease. *Microsc Res Tech* **50**, 305-315.

[152] Gearing M, Schneider JA, Robbins RS, Hollister RD, Mori H, Games D, Hyman BT, Mirra SS (1995) Regional variation in the distribution of apolipoprotein E and A beta in Alzheimer's disease. *J Neuropathol Exp Neurol* **54**, 833-841.

[153] Harr SD, Uint L, Hollister R, Hyman BT, Mendez AJ (1996) Brain expression of apolipoproteins E, J, and A-I in Alzheimer's disease. *J Neurochem* **66**, 2429-2435.

[154] Mufson EJ, Benzing WC, Cole GM, Wang H, Emerich DF, Sladek JR, Jr., Morrison JH, Kordower JH (1994) Apolipoprotein E-immunoreactivity in aged rhesus monkey cortex: colocalization with amyloid plaques. *Neurobiol Aging* **15**, 621-627.

[155] Namba Y, Tsuchiya H, Ikeda K (1992) Apolipoprotein B immunoreactivity in senile plaque and vascular amyloids and neurofibrillary tangles in the brains of patients with Alzheimer's disease. *Neurosci Lett* **134**, 264-266.

[156] Rosenberg ME, Dvergsten J, Correa-Rotter R (1993) Clusterin: an enigmatic protein recruited by diverse stimuli. *J Lab Clin Med* **121**, 205-214.

[157] Zlokovic BV, Martel CL, Mackic JB, Matsubara E, Wisniewski T, McComb JG, Frangione B, Ghiso J (1994) Brain uptake of circulating apolipoproteins J and E complexed to Alzheimer's amyloid beta. *Biochem Biophys Res Commun* **205**, 1431-1437.

[158] Yerbury JJ, Poon S, Meehan S, Thompson B, Kumita JR, Dobson CM, Wilson MR (2007) The extracellular chaperone clusterin influences amyloid formation and toxicity by interacting with prefibrillar structures. *FASEB J* **21**, 2312-2322.

[159] Harold D, Abraham R, Hollingworth P, Sims R, Gerrish A, Hamshere ML, Pahwa JS, Moskvina V, Dowzell K, Williams A, Jones N, Thomas C, Stretton A, Morgan AR, Lovestone S, Powell J, Proitsi P, Lupton MK, Brayne C, Rubinsztein DC, Gill M, Lawlor B, Lynch A, Morgan K, Brown KS, Passmore PA, Craig D, McGuinness B, Todd S, Holmes C, Mann D, Smith AD, Love S, Kehoe PG, Hardy J, Mead S, Fox N, Rossor M, Collinge J, Maier W, Jessen F, Schurmann B, van den Bussche H, Heuser I, Kornhuber J, Wiltfang J, Dichgans M, Frolich L, Hampel H, Hull M, Rujescu D, Goate AM, Kauwe JS, Cruchaga C, Nowotny P, Morris JC, Mayo K, Sleegers K, Bettens K, Engelborghs S, De Deyn PP, Van Broeckhoven C, Livingston G, Bass NJ, Gurling H, McQuillin A, Gwilliam R, Deloukas P, Al-Chalabi A, Shaw CE, Tsolaki M, Singleton AB, Guerreiro R, Muhleisen TW, Nothen MM, Moebus S, Jockel KH, Klopp N, Wichmann HE, Carrasquillo MM, Pankratz VS, Younkin SG, Holmans PA, O'Donovan M, Owen MJ, Williams J (2009) Genome-wide association study identifies variants at CLU and PICALM associated with Alzheimer's disease. *Nat Genet* **41**, 1088-1093.

[160] Lambert JC, Heath S, Even G, Campion D, Sleegers K, Hiltunen M, Combarros O, Zelenika D, Bullido MJ, Tavernier B, Letenneur L, Bettens K, Berr C, Pasquier F, Fievet N, Barberger-Gateau P, Engelborghs S, De Deyn P, Mateo I, Franck A, Helisalmi S, Porcellini E, Hanon O, de Pancorbo MM, Lendon C, Dufouil C, Jaillard C, Leveillard T, Alvarez V, Bosco P, Mancuso M, Panza F, Nacmias B, Bossu P, Piccardi P, Annoni G, Seripa D, Galimberti D, Hannequin D, Licastro F, Soininen H, Ritchie K, Blanche H, Dartigues JF, Tzourio C, Gut I, Van Broeckhoven C, Alperovitch A, Lathrop M, Amouyel P (2009) Genome-wide association study identifies variants at CLU and CR1 associated with Alzheimer's disease. *Nat Genet* **41**, 1094-1099.

[161] Wahrle SE, Jiang H, Parsadanian M, Kim J, Li A, Knoten A, Jain S, Hirsch-Reinshagen V, Wellington CL, Bales KR, Paul SM, Holtzman DM (2008) Overexpression of ABCA1 reduces amyloid deposition in the PDAPP mouse model of Alzheimer disease. *J Clin Invest* **118**, 671-682.

[162] Olesen OF, Dago L (2000) High density lipoprotein inhibits assembly of amyloid beta-peptides into fibrils. *Biochem Biophys Res Commun* **270**, 62-66.

[163] Kontush A (2004) Apolipoprotein Abeta: black sheep in a good family. *Brain Pathol* **14**, 433-447.

[164] Larionov A, Krause A, Miller W (2005) A standard curve based method for relative real time PCR data processing. *BMC Bioinformatics* **6**, 62.

[165] Pussinen PJ, Lindner H, Glatter O, Reicher H, Kostner GM, Wintersperger A, Malle E, Sattler W (2000) Lipoprotein-associated alpha-tocopheryl-succinate inhibits cell growth and induces apoptosis in human MCF-7 and HBL-100 breast cancer cells. *Biochim Biophys Acta* **1485**, 129-144.

[166] Sinn HJ, Schrenk HH, Friedrich EA, Via DP, Dresel HA (1988) Radioiodination of proteins and lipoproteins using N-bromosuccinimide as oxidizing agent. *Anal Biochem* **170**, 186-192.

[167] Bradford MM (1976) A rapid and sensitive method for the quantitation of microgram quantities of protein utilizing the principle of protein-dye binding. *Anal Biochem* **72**, 248-254.

[168] Candela P, Gosselet F, Saint-Pol J, Sevin E, Boucau MC, Boulanger E, Cecchelli R, Fenart L (2010) Apical-to-Basolateral Transport of Amyloid-beta Peptides through Blood-Brain Barrier Cells is Mediated by the Receptor for Advanced Glycation End-Products and is Restricted by P-Glycoprotein. *J Alzheimers Dis* **22**, 849-859.

[169] Schweinzer C, Kober A, Lang I, Etschmaier K, Scholler M, Kresse A, Sattler W, Panzenboeck U (2011) Processing of Endogenous AbetaPP in Blood-Brain Barrier Endothelial Cells is Modulated by Liver-X Receptor Agonists and Altered Cellular Cholesterol Homeostasis. *J Alzheimers Dis* Aug **2**. [Epub Ahead of print]

[170] Horton JD, Shimomura I, Brown MS, Hammer RE, Goldstein JL, Shimano H (1998) Activation of cholesterol synthesis in preference to fatty acid synthesis in liver and adipose tissue of transgenic mice overproducing sterol regulatory element-binding protein-2. *J Clin Invest* **101**, 2331-2339.

[171] Wong J, Quinn CM, Brown AJ (2006) SREBP-2 positively regulates transcription of the cholesterol efflux gene, ABCA1, by generating oxysterol ligands for LXR. *Biochem J* **400**, 485-491.

[172] Zeng L, Liao H, Liu Y, Lee TS, Zhu M, Wang X, Stemerman MB, Zhu Y, Shyy JY (2004) Sterol-responsive element-binding protein (SREBP) 2 down-regulates ATP-binding cassette transporter A1 in vascular endothelial cells: a novel role of SREBP in regulating cholesterol metabolism. *J Biol Chem* **279**, 48801-48807.

[173] Mason JC (2003) Statins and their role in vascular protection. *Clin Sci (Lond)* **105**, 251-266.

[174] Werner N, Nickenig G, Laufs U (2002) Pleiotropic effects of HMG-CoA reductase inhibitors. *Basic Res Cardiol* **97**, 105-116.

[175] Zelcer N, Khanlou N, Clare R, Jiang Q, Reed-Geaghan EG, Landreth GE, Vinters HV, Tontonoz P (2007) Attenuation of neuroinflammation and Alzheimer's disease pathology by liver x receptors. *Proc Natl Acad Sci U S A* **104**, 10601-10606.

[176] Brown J, 3rd, Theisler C, Silberman S, Magnuson D, Gottardi-Littell N, Lee JM, Yager D, Crowley J, Sambamurti K, Rahman MM, Reiss AB, Eckman CB, Wolozin B (2004) Differential expression of cholesterol hydroxylases in Alzheimer's disease. *J Biol Chem* **279**, 34674-34681.

[177] Lefterov I, Fitz NF, Cronican AA, Fogg A, Lefterov P, Kodali R, Wetzel R, Koldamova R (2010) Apolipoprotein A-I deficiency increases cerebral amyloid angiopathy and cognitive deficits in APP/PS1DeltaE9 mice. *J Biol Chem* **285**, 36945-36957.

[178] Corrigan F, Pham CL, Vink R, Blumbergs PC, Masters CL, van den Heuvel C, Cappai R (2011) The neuroprotective domains of the amyloid precursor protein, in traumatic brain injury, are located in the two growth factor domains. *Brain Res* **1378**, 137-143.

[179] Selkoe DJ (1996) Amyloid beta-protein and the genetics of Alzheimer's disease. *J Biol Chem* **271**, 18295-18298.

[180] Vincent B (2004) ADAM proteases: protective role in Alzheimer's and prion diseases? *Curr Alzheimer Res* **1**, 165-174.
[181] Martin M, Dotti CG, Ledesma MD (2010) Brain cholesterol in normal and pathological aging. *Biochim Biophys Acta* **1801**, 934-944.
[182] Zlokovic BV (2010) Neurodegeneration and the neurovascular unit. *Nat Med* **16**, 1370-1371.
[183] Crossgrove JS, Smith EL, Zheng W (2007) Macromolecules involved in production and metabolism of beta-amyloid at the brain barriers. *Brain Res* **1138**, 187-195.
[184] Forloni G, Demicheli F, Giorgi S, Bendotti C, Angeretti N (1992) Expression of amyloid precursor protein mRNAs in endothelial, neuronal and glial cells: modulation by interleukin-1. *Brain Res Mol Brain Res* **16**, 128-134.
[185] Kim WS, Chan SL, Hill AF, Guillemin GJ, Garner B (2009) Impact of 27-hydroxycholesterol on amyloid-beta peptide production and ATP-binding cassette transporter expression in primary human neurons. *J Alzheimers Dis* **16**, 121-131.
[186] Prasanthi JR, Huls A, Thomasson S, Thompson A, Schommer E, Ghribi O (2009) Differential effects of 24-hydroxycholesterol and 27-hydroxycholesterol on beta-amyloid precursor protein levels and processing in human neuroblastoma SH-SY5Y cells. *Mol Neurodegener* **4**, 1.
[187] Famer D, Meaney S, Mousavi M, Nordberg A, Bjorkhem I, Crisby M (2007) Regulation of alpha- and beta-secretase activity by oxysterols: cerebrosterol stimulates processing of APP via the alpha-secretase pathway. *Biochem Biophys Res Commun* **359**, 46-50.
[188] Riddell DR, Zhou H, Comery TA, Kouranova E, Lo CF, Warwick HK, Ring RH, Kirksey Y, Aschmies S, Xu J, Kubek K, Hirst WD, Gonzales C, Chen Y, Murphy E, Leonard S, Vasylyev D, Oganesian A, Martone RL, Pangalos MN, Reinhart PH, Jacobsen JS (2007) The LXR agonist TO901317 selectively lowers hippocampal Abeta42 and improves memory in the Tg2576 mouse model of Alzheimer's disease. *Mol Cell Neurosci* **34**, 621-628.
[189] Wang Y, Rogers PM, Su C, Varga G, Stayrook KR, Burris TP (2008) Regulation of cholesterologenesis by the oxysterol receptor, LXRalpha. *J Biol Chem* **283**, 26332-26339.
[190] Sato R, Inoue J, Kawabe Y, Kodama T, Takano T, Maeda M (1996) Sterol-dependent transcriptional regulation of sterol regulatory element-binding protein-2. *J Biol Chem* **271**, 26461-26464.
[191] Cartagena CM, Burns MP, Rebeck GW (2010) 24S-hydroxycholesterol effects on lipid metabolism genes are modeled in traumatic brain injury. *Brain Res* **1319**, 1-12.
[192] Kojro E, Fuger P, Prinzen C, Kanarek AM, Rat D, Endres K, Fahrenholz F, Postina R (2010) Statins and the squalene synthase inhibitor zaragozic acid stimulate the non-amyloidogenic pathway of amyloid-beta protein precursor processing by suppression of cholesterol synthesis. *J Alzheimers Dis* **20**, 1215-1231.
[193] Nelson TJ, Alkon DL (2005) Insulin and cholesterol pathways in neuronal function, memory and neurodegeneration. *Biochem Soc Trans* **33**, 1033-1036.

[194] Puglielli L, Konopka G, Pack-Chung E, Ingano LA, Berezovska O, Hyman BT, Chang TY, Tanzi RE, Kovacs DM (2001) Acyl-coenzyme A: cholesterol acyltransferase modulates the generation of the amyloid beta-peptide. *Nat Cell Biol* **3**, 905-912.

[195] Huttunen HJ, Havas D, Peach C, Barren C, Duller S, Xia W, Frosch MP, Hutter-Paier B, Windisch M, Kovacs DM (2010) The acyl-coenzyme A: cholesterol acyltransferase inhibitor CI-1011 reverses diffuse brain amyloid pathology in aged amyloid precursor protein transgenic mice. *J Neuropathol Exp Neurol* **69**, 777-788.

[196] Koldamova R, Fitz NF, Lefterov I (2010) The role of ATP-binding cassette transporter A1 in Alzheimer's disease and neurodegeneration. *Biochim Biophys Acta* **1801**, 824-830.

[197] Koldamova R, Staufenbiel M, Lefterov I (2005) Lack of ABCA1 considerably decreases brain ApoE level and increases amyloid deposition in APP23 mice. *J Biol Chem* **280**, 43224-43235.

[198] Buxbaum JD, Gandy SE, Cicchetti P, Ehrlich ME, Czernik AJ, Fracasso RP, Ramabhadran TV, Unterbeck AJ, Greengard P (1990) Processing of Alzheimer beta/A4 amyloid precursor protein: modulation by agents that regulate protein phosphorylation. *Proc Natl Acad Sci U S A* **87**, 6003-6006.

[199] Lane RF, Gatson JW, Small SA, Ehrlich ME, Gandy S (2010) Protein kinase C and rho activated coiled coil protein kinase 2 (ROCK2) modulate Alzheimer's APP metabolism and phosphorylation of the Vps10-domain protein, SorL1. *Mol Neurodegener* **5**, 62.

[200] Pangrsic T, Potokar M, Stenovec M, Kreft M, Fabbretti E, Nistri A, Pryazhnikov E, Khiroug L, Giniatullin R, Zorec R (2007) Exocytotic release of ATP from cultured astrocytes. *J Biol Chem* **282**, 28749-28758.

[201] Koldamova RP, Lefterov IM, Lefterova MI, Lazo JS (2001) Apolipoprotein A-I directly interacts with amyloid precursor protein and inhibits A beta aggregation and toxicity. *Biochemistry* **40**, 3553-3560.

[202] Mulay V, Wood P, Rentero C, Enrich C, Grewal T (2011) Signal Transduction Pathways Provide Opportunities to Enhance HDL and apoAI-Dependent Reverse Cholesterol Transport. *Curr Pharm Biotechnol*.

[203] Yamauchi Y, Hayashi M, Abe-Dohmae S, Yokoyama S (2003) Apolipoprotein A-I activates protein kinase C alpha signaling to phosphorylate and stabilize ATP binding cassette transporter A1 for the high density lipoprotein assembly. *J Biol Chem* **278**, 47890-47897.

[204] Lewis TL, Cao D, Lu H, Mans RA, Su YR, Jungbauer L, Linton MF, Fazio S, LaDu MJ, Li L (2010) Overexpression of human apolipoprotein A-I preserves cognitive function and attenuates neuroinflammation and cerebral amyloid angiopathy in a mouse model of Alzheimer disease. *J Biol Chem* **285**, 36958-36968.

[205] Stuart WD, Krol B, Jenkins SH, Harmony JA (1992) Structure and stability of apolipoprotein J-containing high-density lipoproteins. *Biochemistry* **31**, 8552-8559.

[206] de Silva HV, Stuart WD, Duvic CR, Wetterau JR, Ray MJ, Ferguson DG, Albers HW, Smith WR, Harmony JA (1990) A 70-kDa apolipoprotein designated ApoJ is

a marker for subclasses of human plasma high density lipoproteins. *J Biol Chem* **265**, 13240-13247.

[207] de Silva HV, Stuart WD, Park YB, Mao SJ, Gil CM, Wetterau JR, Busch SJ, Harmony JA (1990) Purification and characterization of apolipoprotein J. *J Biol Chem* **265**, 14292-14297.

[208] Kirszbaum L, Bozas SE, Walker ID (1992) SP-40,40, a protein involved in the control of the complement pathway, possesses a unique array of disulphide bridges. *FEBS Lett* **297**, 70-76.

[209] Ghiso J, Matsubara E, Koudinov A, Choi-Miura NH, Tomita M, Wisniewski T, Frangione B (1993) The cerebrospinal-fluid soluble form of Alzheimer's amyloid beta is complexed to SP-40,40 (apolipoprotein J), an inhibitor of the complement membrane-attack complex. *Biochem J* **293 (Pt 1)**, 27-30.

[210] Strittmatter WJ, Saunders AM, Schmechel D, Pericak-Vance M, Enghild J, Salvesen GS, Roses AD (1993) Apolipoprotein E: high-avidity binding to beta-amyloid and increased frequency of type 4 allele in late-onset familial Alzheimer disease. *Proc Natl Acad Sci U S A* **90**, 1977-1981.

[211] Koudinov AR, Koudinova NV, Kumar A, Beavis RC, Ghiso J (1996) Biochemical characterization of Alzheimer's soluble amyloid beta protein in human cerebrospinal fluid: association with high density lipoproteins. *Biochem Biophys Res Commun* **223**, 592-597.

[212] Tokuda T, Calero M, Matsubara E, Vidal R, Kumar A, Permanne B, Zlokovic B, Smith JD, Ladu MJ, Rostagno A, Frangione B, Ghiso J (2000) Lipidation of apolipoprotein E influences its isoform-specific interaction with Alzheimer's amyloid beta peptides. *Biochem J* **348 Pt 2**, 359-365.

[213] Pflanzner T, Kuhlmann CR, Pietrzik CU (2010) Blood-brain-barrier models for the investigation of transporter- and receptor-mediated amyloid-beta clearance in Alzheimer's disease. *Curr Alzheimer Res* **7**, 578-590.

[214] Deane R, Bell RD, Sagare A, Zlokovic BV (2009) Clearance of amyloid-beta peptide across the blood-brain barrier: implication for therapies in Alzheimer's disease. *CNS Neurol Disord Drug Targets* **8**, 16-30.